Abstract of "Cluster Polylogarithms and Scattering Amplitudes" by John K. Golden, Ph.D., Brown University, May 2015.

Scattering amplitudes have undergone considerable study in the last few years. Much of the progress has come from abandoning Feynman diagram techniques and instead exploring and exploiting the physical constraints and mathematical structures underlying amplitudes. In this thesis, we present a new, unexpected structure underlying certain amplitudes: cluster algebras. Harnessing the power of cluster algebras allows us to calculate previously unknown amplitudes and points the way towards a deeper mathematical understanding of quantum field theory.

We begin by introducing *motivic amplitudes*, which contain all of the essential mathematical content of scattering amplitudes in planar $\mathcal{N} = 4$ supersymmetric Yang-Mills theory. We then establish, through explicit calculations of the two-loop, seven-particle motivic amplitude as well as n-particle two-loop differential, that the amplitude only "depends on" on certain preferred coordinates known in the mathematics literature as *cluster $\mathcal{X}$-coordinates* on $\mathrm{Conf}_n(\mathbb{P}^3)$.

The connection between scattering amplitudes and cluster algebras prompts us to define *cluster polylogarithm functions*, objects which elegantly (and uniquely) contain beautiful motivic and cluster algebraic structure. In particular, cluster polylogarithms allow us to associate specific polylogarithm functions to faces of generalized associahedrons, to which cluster algebras have a natural combinatoric connection. These functions form a sufficient basis to express two-loop amplitudes, and we present an analytic formula for the two-loop seven-particle amplitude as an example. Furthermore, we find intriguing connections between motivic amplitudes and the geometry of associahedrons. For example, we show that the obstruction to the two-loop motivic amplitude being expressible in terms of classical polylogarithms is most naturally represented by certain quadrilateral faces of the appropriate associahedron.

CLUSTER POLYLOGARITHMS AND SCATTERING AMPLITUDES

by

John K. Golden

Submitted in partial fulfillment of the requirements
for the Degree of Doctor of Philosophy in the
Department of Physics at Brown University

Providence, Rhode Island

May 2015

This dissertation by John K. Golden is accepted in its present form by the Department of Physics as satisfying the dissertation requirement for the degree of Doctor of Philosophy.

Date ______________ ______________________________
Marcus Spradlin, Director

Recommended to the Graduate Council

Date ______________ ______________________________
Antal Jevicki, Reader

Date ______________ ______________________________
Chung-I Tan, Reader

Approved by the Graduate Council

Date ______________ ______________________________
Peter M. Weber
Dean of the Graduate School

Curriculum Vitæ

EDUCATION

Brown University

Ph.D., Physics, 2015

University of Rochester

B.Sc., Physics and Mathematics, *magna cum laude*, 2010

AWARDS & HONORS

Galkin Graduate Fellowship	2014
NSF Graduate Research Fellowship Honorable Mention	2011
Barry M. Goldwater Scholarship	2008

PUBLICATONS

"(No) Bootstrap for the Fractal Ising Model,"
with M. Paulos, [arXiv:1411.7932]

"A Cluster Bootstrap for Two-Loop MHV Amplitudes,"
with M. Spradlin, [arXiv:1411.3289]

"Analytic result for the two-loop seven-point MHV amplitude in $\mathcal{N} = 4$ Yang-Mills,"
with M. Spradlin, JHEP **1408**, 154 (2014)

“Cluster Polylogarithms for Scattering Amplitudes,”

with M. Paulos, M. Spradlin, A. Volovich, J. Phys. A **47**, 474005 (2014)

“Motivic Amplitudes and Cluster Coordinates,”

with A. Goncharov, M. Spradlin, C. Vergu, A. Volovich, JHEP **1401**, 091 (2014)

“The Differential of All Two-Loop MHV Amplitudes in $\mathcal{N} = 4$ Yang-Mills,”

with M. Spradlin, JHEP **1309**, 111 (2013)

“Collinear and Soft Limits of Multi-Loop Integrands in $\mathcal{N} = 4$ Yang-Mills,”

with M. Spradlin, JHEP **1205**, 027 (2012)

INVITED TALKS

Great Lakes Strings Conference, University of Michigan, 3/2015

Seminar, University of Michigan, 9/2014

Seminar, Perimeter Institute, 2/2014

Amplitudes Workshop, Caltech, 2/2014

The Geometry and Physics of Scattering Amplitudes,

Simons Center for Geometry and Physics, 12/2013

CONFERENCES & SCHOOLS ATTENDED

Great Lakes Strings Conference, University of Michigan, 3/2015

Strings 2014, Princeton University, 6/2014

PiTP, Institute for Advanced Study, 6/2014

Amplitudes Workshop, Caltech, 2/2014

The Geometry and Physics of Scattering Amplitudes,
Simons Center for Geometry and Physics, 12/2013

Winter School, CERN, 2/2013

Amplitudes and Motives, IHES, 12/2012

Amplitudes, University of Michigan, 11/2011

Acknowledgements

Thanks first and foremost to my advisor Marcus Spradlin for his tireless guidance in all areas (except Mathematica keybindings, which I had to learn on my own). Mark's deep but unassuming knowledge of physics and mathematics in general, and quantum field theory in particular, was stimulating and encouraging. It was always a pleasure to work together, regardless of whether our research was guided by the light of Eärendil or an untamed ornithoid.

None of this would have been possible without the inspiring efforts of my collaborators, Anastasia Volovich, Alexander Goncharov, Cristian Vergu, and Miguel Paulos. Anastasia in particular was like a second advisor to me, providing invaluable advice and support on matters both professional and research-related.

Antal Jevicki and Chung-I Tan have graciously agreed to read this thesis, one more in a long line of kind acts they have done for me over the years. The entire faculty and staff of the Brown Physics Department, especially the High Energy Theory group, have been nothing but helpful and enthusiastic during my time in Providence, and for that I am extremely grateful.

To my friends and family – you have played an integral role in my life during grad school, one that it would be difficult to fully articulate here. Let's have dinner soon, and I'll tell you all about it.

In memory of Gerry Guralnik

Contents

List of Figures x

1 Introduction 1

2 Motivic Amplitudes and Cluster Coordinates 9

2.1 Introduction 10

2.2 The Kinematic Configuration Space $\mathrm{Conf}_n(\mathbb{P}^3)$ 14

2.3 Review of the Two-Loop $n = 6$ MHV Amplitude 23

2.4 Polylogarithms and Motivic Lie Algebras 26

2.5 The Coproducts of Two-Loop MHV Motivic Amplitudes 31

2.6 Cluster Coordinates and Cluster Algebras 35

2.7 Cluster Coordinates and Motivic Analysis for $n = 6, 7$ 53

2.8 Conclusion 65

3 Calculating $dR_n^{(2)}$ 69

3.1 Introduction 70

3.2 Motivation and Review 71

3.3 Tools and Techniques 74

3.4 Results 76

4 Cluster Polylogarithms 82

4.1 Cluster polylogarithm functions 86

4.2 The A_2 function 89

4.3 The A_3 function 93

4.4 Cluster polylogarithms for Gr(4, 7) and the amplitude $R_7^{(2)}$ 99

4.5 Conclusion 103

5 Calculating $R_7^{(2)}$ **107**

5.1 Background 109

5.2 The Problem of Integrating Symbols 112

5.3 The Algorithm for $R_n^{(2)}$ 116

5.4 The Construction of $R_7^{(2)}$ 117

5.5 The Function $R_7^{(2)}$ 121

5.6 Conclusion 124

6 Calculating $\delta\left(R_n^{(2)}\right)|_{\Lambda^2 B_2}$ **126**

6.1 Cluster Coordinates and Coproducts 128

6.2 Elements of the Cluster Bootstrap 130

6.3 Applying the bootstrap 134

6.4 Discussion 136

A Functional Representatives **138**

Bibliography **141**

List of Figures

2.1 The initial quiver for the $\mathrm{Gr}(k,n)$ cluster algebra. 41

2.2 The initial quiver for $\mathrm{Gr}(4,6)$ and its parity conjugate. 50

2.3 The initial quiver for $\mathrm{Gr}(4,7)$ and its parity conjugate 51

2.4 A triangulation T of the hexagon. 55

2.5 A sequence of mutations for five points. 56

2.6 The polytope obtained by gluing together the triangles associated to clusters of the $\mathrm{Gr}(2,6)$ cluster algebra. 58

2.7 The cross-ratios ($\mathcal{X}$-coordinates) around a valence 4 vertex and a valence 5 vertex of the polytope associated to the $\mathrm{Gr}(2,6)$ cluster algebra. 59

2.8 The Stasheff polytope for the $\mathrm{Gr}(2,6)$ cluster algebra, also known as the K_5 associahedron. 61

4.1 The A_2 cluster algebra. 90

4.2 The Stasheff polytope for the A_3 cluster algebra. 94

5.1 Numerical evaluation of the MHV remainder function $R_7^{(2)}$ 123

Chapter 1

Introduction

The development of quantum field theory and the mathematics of Feynman diagrams in many ways recalls the formation of mechanics and calculus by Newton. In both cases novel mathematics were invented principally to give language to an inchoate understanding of the natural world. In the case of Newton, calculus quickly proved far richer than was suggested by his initial work. In particular, the maturation of the calculus of variations lead Euler, Lagrange, and Hamilton to discover the underlying role of the principal of least action in classical mechanics. This principle existed in the original Newtonian framework but was entirely hidden and unknown. The computational power inherent in this deeper formulation of classical mechanics allowed for a much wider range of problems to be solved than was previously possible. Furthermore, this work presaged our current understanding of the quantum world, where again the principle of least action plays a critical role.

Just as Lagrange and Hamilton were able to reformulate mechanics in a more fundamental and computationally powerful way, the same effort is now being applied to quantum field theory. Many exciting new discoveries made over the last few years clearly point towards an intrinsically new understanding of quantum field theory, with important theoretical and practical implications.

One of the most basic calculations in a quantum field theory is that of the scattering amplitude. The technique for calculating these amplitudes with Feynman diagrams is well understood. However, these computations are quite lengthy, even for simple cases. For example, the tree-level contribution to the scattering amplitude for two incoming gluons to produce four outgoing gluons involves thousands of diagrams. This amplitude was first evaluated by Parke and Taylor in 1985 with the aid of a supercomputer, and their result was over 8 pages long [1]. Amazingly, they soon found an expression that was mathematically equivalent to their previous answer but only a single line long [2]. Even more impressive was that they had generalized their result to involve *any* number of gluons. In modern notation, their result was:

$$\mathcal{A}(1^+, 2^+, \ldots, i^-, \ldots, j^-, \ldots, n^+) = \frac{\langle ij \rangle^4}{\langle 12 \rangle \langle 23 \rangle \cdots \langle n1 \rangle}. \tag{1.1}$$

Clearly, the final answer betrays a deep, underlying simplicity which was completely hidden by the way it had originally been calculated.

Since Parke and Taylor's discovery, there have been many leaps forward in our understanding of perturbative quantum field theory. Much of the progress has come from abandoning Feynman diagram techniques and instead exploring and exploiting the physical constraints and mathematical structures underlying amplitudes. This approach has led to many interesting discoveries and new methods for calculating amplitudes, such as BCFW recursion relations at tree [3] and loop [4] levels, the duality between color and kinematics [5], the duality between amplitudes and Wilson loops [6–9], the dual conformal $\to$ Yangian symmetry [10], and the amplituhedron [11].

In this thesis we will focus on pure gluon amplitudes in planar $\mathcal{N} = 4$ supersymmetric Yang-Mills theory. We will further restrict ourselves to the maximally helicity violating (MHV) amplitudes, where two gluons have positive helicity and the rest have negative helicity, which is the simplest non-trivial case available. The all-loop MHV amplitude is conventionally written by factoring out the tree amplitude,

$$\mathcal{A}_n^{\text{MHV}}(\epsilon) = \mathcal{A}_n^{(0);\text{MHV}} \; \mathcal{P}_n^{\text{MHV}}(\epsilon) \tag{1.2}$$

where $\mathcal{A}_n^{(0);\text{MHV}}$ is just the Parke-Taylor formula, eq. (1.1). The regulator ϵ controls the IR-divergence of the amplitude. The function $\mathcal{P}_n^{\text{MHV}}(\epsilon)$ can then be expanded in loop order as

$$\mathcal{P}_n(\epsilon) = \mathcal{P}_n^{(0)}(\epsilon) + \lambda \mathcal{P}_n^{(1)}(\epsilon) + \lambda^2 \mathcal{P}_n^{(2)}(\epsilon) + \ldots, \tag{1.3}$$

where $\mathcal{P}_n^{(0)}(\epsilon) = 1$, and we've dropped the MHV superscript for notational clarity. The form of $\mathcal{P}_n^{(1)}(\epsilon)$ is also well-understood [12] thanks to unitarity cuts. At two loops, Anastasiou, Bern, Dixon, and Kosower [13] showed that the 4-particle amplitude could be expressed in terms of the one-loop amplitude as

$$\mathcal{P}_4^{(2)}(\epsilon) = \frac{1}{2}\left[\mathcal{P}_4^{(1)}(\epsilon)\right]^2 + \mathcal{P}_4^{(1)}(2\epsilon) f^{(2)}(\epsilon) + C^{(2)} + \mathcal{O}(\epsilon) \tag{1.4}$$

where $f^{(2)}(\epsilon)$ and $C^{(2)}$ are known numerical constants and independent of the number of particles. The iterative structure continues at three-loops, which motivated Bern, Dixon, and Smirnov (BDS) [14] to conjecture the general form

$$\mathcal{P}_n^{\text{BDS}}(\epsilon) = \exp\left[\sum_{L=1}^{\infty} \lambda^L \Big(f^{(L)}(\epsilon)\mathcal{P}_n^{(1)}(L\epsilon) + C^{(L)} + \mathcal{O}(\epsilon)\Big)\right]. \tag{1.5}$$

This function, known as the BDS ansatz, matches the known one-loop amplitudes as well as the 4- and 5-particle two-loop amplitudes [15, 16]. Furthermore, it is believed that eq. (1.5) in fact captures the full IR-divergence of the n-particle MHV amplitude. However, for $n > 5$, the remainder function

$$R_n^{(L)} \equiv \mathcal{P}_n(\epsilon) - \mathcal{P}_n^{\text{BDS}}(\epsilon). \tag{1.6}$$

is non-zero. Still, not all hope is lost: $R_n^{(L)}$ is a fascinating quantity to study, and not only because of it's IR-finiteness. First, $R_n^{(L)}$ is a function of uniform transcendentality $2L$. Secondly, and perhaps most importantly, $R_n^{(L)}$ satisfies not only the standard conformal invariance but also a dual conformal invariance in terms of the variables $x_i = p_{i+1} - p_i$. These properties, along with many others (some of which will be proposed in this thesis), combine to create a beautiful function which continues to mystify and entrance physicists and mathematicians alike.

$R_6^{(2)}$ was initially calculated by Del Duca, Duhr, and Smirnov in 2010 [17, 18]. Their 17-page result was simplified to a single line by Goncharov, Spradlin, Vergu, and

Volovich shortly thereafter [19] by use of powerful mathematical machinery, including the *symbol* (explained in sec. 2.4). The concise form of the final result for $R_6^{(2)}$ gave hope that higher-n results, and perhaps a general n-particle two-loop MHV amplitude, might be arrived at swiftly, as was the case at tree-level with the Parke-Taylor formula.

The first understanding of the n-particle structure of $R_n^{(2)}$ was given by Caron-Huot in 2011 [20]. By exploiting the connection between Wilson loops, as well as a conjectured extended supersymmetry, Caron-Huot was able to calculate the symbol of $R_n^{(2)}$, which in this context can be thought of as essentially the differential $dR_n^{(2)}$. With this breakthrough, combined with a surprising simplicty of $R_6^{(2)}$, it seemed inevitable that a closed-form analytic expression for $R_n^{(2)}$ would soon be found. However, it was quickly discovered that there were no sufficiently powerful mathematical tools that could elevate the $dR_n^{(2)}$ to a full function.

Progress in physics often relies on having some understanding of what the answer is going to look like. The principle obstacle faced in the evaluation of $R_n^{(2)}$ is that the constituent functions, *polylogarithms*, are enormously complicated and satisfy numerous identities. Before progress could be made on $R_n^{(2)}$, it was necessary to discover some underlying principles that would remove this redundancy and provide a clearer path towards the answer.

The essential result of this thesis is the discovery of hidden, unexpected mathematical structure in $R_n^{(2)}$. In order to uncover this structure, we introduce *motivic amplitudes*—objects which contain all of the essential mathematical content of scattering amplitudes in planar SYM theory in a completely canonical way, free from the ambiguities inherent in any attempt to choose particular functional representatives. Studying motivic amplitudes allows us to uncover a striking connection between amplitudes and cluster algebras, a relatively new and exciting field of mathematics. We expose deep connections between polylogarithms, cluster algebras, and scattering amplitudes that are as surprising as they are useful. In particular, with cluster algebras as a guide, we are able to describe an algorithm which essentially solves the problem of calculating $R_n^{(2)}$.

In chapter 2 we introduce motivic amplitudes. We find that the cluster structure on the kinematic configuration space $\mathrm{Conf}_n(\mathbb{P}^3)$ underlies the structure of motivic amplitudes. Specifically, we compute explicitly the coproduct of the two-loop seven-particle MHV motivic amplitude $\mathcal{A}_{7,2}^{\mathcal{M}}$ and find that like the previously known six-particle amplitude, it depends only on certain preferred coordinates known in the mathematics literature as *cluster $\mathcal{X}$-coordinates* on $\mathrm{Conf}_n(\mathbb{P}^3)$. We also find intriguing relations between motivic amplitudes and the geometry of generalized associahedrons, to which cluster coordinates have a natural combinatoric connection. For example, the obstruction to $\mathcal{A}_{7,2}^{\mathcal{M}}$ being expressible in terms of classical polylogarithms is most naturally represented by certain quadrilateral faces of the appropriate associahedron.

In chapter 3 we calculate the differential of the planar n-particle, two-loop MHV scattering amplitude in $\mathcal{N} = 4$ super Yang-Mills theory. The result is expressed only in terms of the polylogarithm functions $\mathrm{Li}_k(-x)$, for $k = 1, 2, 3$, with arguments x belonging to the special class of dual conformal cross-ratios known as cluster $\mathcal{X}$-coordinates. The surprising fact that these amplitudes may be expressed in this way provides a striking example of the manner in which the cluster structure on the kinematic configuration space underlies the structure of amplitudes in SYM theory.

In chapter 4 we establish a surprising connection between cluster algebras and polylogarithms, which we term *cluster polylogarithm functions.* We find that all such functions of weight 4 are made up of a single simple building block associated to the A_2 cluster algebra. Adding the requirement of locality on generalized Stasheff polytopes, we find that these A_2 building blocks arrange themselves to form a unique function associated to the A_3 cluster algebra. This A_3 function manifests all of the cluster algebraic structure of the two-loop n-particle MHV amplitudes for all n, and we use it to provide an explicit representation for the most complicated part of the

$n = 7$ amplitude as an example.

In chapter 5 we complete the calculation started in chapter 4, namely, that of $R_7^{(2)}$. Moreover, we describe a general algorithm which can construct explicit analytic formulas for two-loop MHV amplitudes for any number of particles. The non-classical part of an amplitude is built from A_3 cluster polylogarithm functions; classical polylogarithms with (negative) cluster $\mathcal{X}$-coordinate arguments are added to complete the symbol of the amplitude; beyond-the-symbol terms proportional to π^2 are determined by comparison with the differential of the amplitude; and the overall additive constant is fixed by the collinear limit.

The algorithm described in chapter 5 essentially "solves" the problem of calculating two-loop MHV amplitudes, but only algorithmicially, and with much redundancy still in place. In chapter 6 we present a concise, closed-form expression for the mathematically most complicated part (the $\Lambda^2 B_2$ coproduct component) of the n-particle amplitude. This expressions makes manifest several striking features, including a form of "locality" in cluster algebra space. These cluster features remain unexplained, and it is yet unknown how far they can lead us to a closed-form representation of the complete $R_n^{(2)}$.

Broadly construed, the results of this thesis suggest a novel paradigm for the calculation of scattering amplitudes. It remains to see how far these techniques may be generalized to cases beyond the very specific class of amplitudes considered here. However, based on the approach described in this thesis, we can at least provide a rough outline of how to possibly extend these methods for a general scattering amplitude $\mathcal{A}$.

1. precisely characterize the *kinematic space* upon which $\mathcal{A}$ depends,
2. identify a cluster algebra associated with this kinematic space,
3. map the cluster algebra to a space of functions which manifests the cluster

algebraic structure,

4. appropriately sum up these functions to determine $\mathcal{A}$.

The essential idea underlying this scheme is that the kinematics of scattering heavily constrains the functional form of amplitudes.

Chapter 2

Motivic Amplitudes and Cluster Coordinates

2.1 Introduction

The overarching aim of this chapter is to show that SYM theory is an ideal setting in which to study *motivic amplitudes*, as proposed a decade ago in [21] (see in particular sec. 7). Why motivic amplitudes? It remains an important outstanding problem in physics to determine explicit effective constructions for general amplitudes. However the abundance of functional identities amongst generalized polylogarithms precludes the existence of any particular preferred or canonical functional representation or 'formula' for general multi-loop amplitudes (the only exception is reviewed in section 2.3). Our goal is to investigate, following [21], their motivic avatars—motivic amplitudes—which are mathematically more sophisticated, but at the same time much more structured and canonical objects. In particular they are elements of a Hopf algebra. This Hopf algebra is the algebra of functions on the so-called motivic Galois group. The group structure of the latter is encoded in the coproduct of the Hopf algebra. So by studying the coproduct of motivic amplitudes—a structure totally invisible if we remain on the level of functions—we uncover their hidden motivic Galois symmetries. One cannot resist to think that these new symmetries will eventually play an essential role in physics.

A similar upgrading, from multi-zeta values to motivic multi-zeta values, has recently played a crucial role in unlocking the structure of tree-level superstring amplitudes in the α' expansion [22–25]. In SYM theory we expect the motivic approach to be even more powerful since the amplitudes we deal with are not merely numbers but highly nontrivial functions on the $3(n-5)$-dimensional kinematic configuration space $\mathrm{Conf}_n(\mathbb{P}^3)$, the space of collections of n points in the projective space $\mathbb{P}^3$, considered modulo the action of the projective linear group PGL_4.

The one-sentence slogan of this chapter is that *we find that the cluster structure of the space* $\mathrm{Conf}_n(\mathbb{P}^3)$ *underlies the structure of amplitudes in SYM theory.* The technical aspects of our work which support this conclusion can be divided into two parts, which one can think of very roughly as *kinematics* and *dynamics*.

We can phrase the 'kinematic' question we are interested in roughly as: *which variables do motivic amplitudes in SYM theory depend on?* Thanks to dual conformal symmetry [6, 7, 26–31] it is known that appropriately defined n-particle SYM scattering amplitudes depend on $3(n-5)$ algebraically independent dual conformal cross-ratios. However, all experience to date indicates that the functional dependence of amplitudes on these variables always takes very special forms. For example, in the case of the two-loop MHV amplitude for $n=6$ (reviewed in section 2.3), which can be completely expressed in terms of the classical polylogarithm functions Li_m [19], only very particular algebraic functions of the three independent cross-ratios appear as arguments of the Li_m's. It is natural to wonder why these particular arguments appear, and not others, and to ask about the arguments appearing in more general amplitudes (including $n > 6$, higher loops, and non-MHV).

There is a more specific purely mathematical reason to concentrate on the study of the motivic two-loop MHV amplitudes. These amplitudes are polylogarithm-like functions of weight (also known as transcendentality) four. Any such function of weight one on a space X is necessarily of the form $\log F(x)$, the logarithm of a rational function on X. Next, any weight two function can be expressed as a sum of Li_2's and products of two logarithms of rational functions. Similarly, any weight three function is a linear combination of Li_3 's and products of lower weight polylogs of rational functions. So the question 'which variables these functions depend on' is well-defined, up to the functional equations satisfied by Li_2 and Li_3—a beautiful subject on its own. However this is no longer true for functions of weight four [32]. There is an invariant associated to any weight four function, with values in an Abelian group $\Lambda^2 \mathrm{B}_2$, reviewed in sec. 2.4, which is the obstruction for the function to be expressible as a sum of products of classical polylogarithms Li_m. This makes the above question ill-defined. However, upgrading weight four functions to their motivic avatars one sees that their coproducts are expressible via classical motivic polylogs of weights ≤ 3, and so the question makes sense again. Finally, the coproduct preserves all information about motivic amplitudes but an additive constant. So to understand two-loop amplitudes we want first to find explicit formulas for the coproduct of their motivic avatars. On the other hand, the two-loop amplitudes are natural weight four functions, and so one can hope that their detailed analysis might shed a new light on the fundamental unsolved mathematical problems which we face starting at weight four. Therefore, although the level of precision one can reach studying the two-loop motivic MHV amplitudes is unsustainable for higher loops, one can hope to discover general features by looking at the simplest case.

In this chapter we propose that the variables which appear in the study of the MHV amplitudes in SYM theory belong to a class known in the mathematics literature as *cluster $\mathcal{X}$-coordinates* [33] on the configuration space $\mathrm{Conf}_n(\mathbb{P}^3)$.

Cluster $\mathcal{X}$-coordinates in general describe Poisson spaces which are in duality with cluster algebras, originally discovered in [34, 35]. In particular, the space $\mathrm{Conf}_n(\mathbb{P}^3)$ is equipped with a natural Poisson structure, invariant under cyclic shift of the points. This Poisson structure looks especially simple in the cluster $\mathcal{X}$-coordinates: the logarithms of the latter provide collections of canonical Darboux coordinates. It seems remarkable that the arguments of the amplitudes have such special Poisson properties, although at the moment we do not know how to fully exploit this connection (see Chapter 6 for one application).

An immediate consequence of the cluster structure of the space $\mathrm{Conf}_n(\mathbb{P}^3)$ is that its real part $\mathrm{Conf}_n(\mathbb{RP}^3)$ contains a domain $\mathrm{Conf}_n^+(\mathbb{RP}^3)$ of positive configurations of n points in $\mathbb{RP}^3$. This positive domain is evidently a part of the Euclidean domain in $\mathrm{Conf}_n(\mathbb{CP}^3)$, the domain where the amplitudes are well behaved.

The configuration space $\mathrm{Conf}_n(\mathbb{P}^3)$ can be realized as a quotient of the Grassmannian $\mathrm{Gr}(4, \mathbb{C}^n)$ by the action of the group $(\mathbb{C}^*)^{n-1}$. This Grassmannian, describing the external kinematic data of an amplitude, may look unrelated to those which star in [4, 36–40] and involve also 'internal' data related to loop integration variables. However the cluster structure and in particular the positivity play a key role in the Grassmannian approach to amplitudes [40], and we have no doubt that a tight connection between these objects will soon emerge.

Once one accepts the important role played by cluster coordinates as the kinematic variables which, in particular, the coproduct of the two-loop motivic MHV amplitudes are 'allowed' to depend on, it is natural to ask the 'dynamic' question: *what exactly is the dependence on these coordinates*? For example, what explains the precise linear combination of Li_4 functions appearing in the two-loop MHV amplitude for $n = 6$? There is a vast and rich mathematical literature on cluster algebras, which are naturally connected [41] to beautiful combinatorial structures known as cluster complexes and, more specifically, generalized associahedrons (or generalized Stasheff polytopes) [42]. We defer most of the dynamic question to subsequent chapters but report here the first example of a connection between these mathematical structures and motivic amplitudes: we find that the 'distance' between a two-loop amplitude and the classical Li_4 functions, expressed in the $\Lambda^2 \mathrm{B}_2$-obstruction, is naturally formulated in terms of certain two-dimensional quadrilateral faces of the associahedron for $\mathrm{Conf}_n(\mathbb{P}^3)$. Equivalently, the pairs of functions entering the Stasheff polytope $\Lambda^2 \mathrm{B}_2$-obstruction for the two-loop MHV amplitudes Poisson commute.

The outline of this chapter is as follows. In section 2.2 we briefly review various notations for configurations of points in $\mathbb{P}^{k-1}$ and the appearance of the $3(n-5)$-dimensional space $\mathrm{Conf}_n(\mathbb{P}^3)$ as the space on which n-particle scattering amplitudes in SYM theory are defined. We also review the relationship with the Grassmannian $\mathrm{Gr}(4, \mathbb{C}^n)$. In section 2.3 we call attention to the very special arguments appearing inside the Li_4 functions in the two-loop MHV amplitude for $n = 6$. Section 2.4 reviews the mathematics necessary for the motivic amplitudes calculus. We present our result for the coproduct of the two-loop $n = 7$ MHV motivic amplitude in section 2.5 (results for all higher n will be given in chapter 6). In section 2.6 we turn to cluster algebras related to $\mathrm{Gr}(4, n)$, the construction of cluster coordinates, and the Stasheff polytope and cluster $\mathcal{X}$-coordinates for $\mathrm{Conf}_n(\mathbb{P}^3)$. Finally section 2.7 exhibits these concepts for $n = 6, 7$ in detail and contains some analysis of the structure of the two-loop $n = 7$ MHV motivic amplitude and its relation to the Stasheff polytope. While the $n = 6$ case is well known in the mathematical literature, the geometry of the cluster $\mathcal{X}$-coordinates in the $n = 7$ case is more intricate.

2.2 The Kinematic Configuration Space $\mathrm{Conf}_n(\mathbb{P}^3)$

Having argued that scattering amplitudes are a collection of very interesting functions, we begin by addressing a seemingly simple-minded question: what variables do these functions depend on? Despite initial appearances this is far from a trivial question, and somewhat surprisingly a completely satisfactory understanding has only emerged rather recently.

2.2.1 Momentum twistors

The basic problem is essentially this: a scattering amplitude of n massless particles depends on n four-momenta p_i (which we can take to be complex), but these are constrained variables. First of all each one should be light-like, $p_i^2 = 0$ with respect to the Minkowski metric for all i, and secondly energy-momentum conservation requires that $p_1 + \cdots + p_n = 0$. These constraints carve out a non-trivial subvariety of $\mathbb{C}^{4n}$. It is desirable to employ a set of unconstrained variables which parametrize precisely this subvariety. A solution to the problem is provided by momentum twistors, whose construction we now describe.

In the planar limit of SYM theory we have an additional, and crucial, piece of structure: the n particles come together with a specified cyclic ordering. This arises because each particle lives in the adjoint representation of a gauge group and each amplitude is multiplied by some invariant constructed from the gauge group generators of the participating particles. In the planar limit we take the gauge group to be $\mathrm{U}(N)$ with $N \to \infty$, in which case only amplitudes multiplying a single trace $\mathrm{Tr}[T^{a_1} \cdots T^{a_n}]$ of gauge group generators are nonvanishing.

Armed with a specified cyclic ordering of the particles, the conservation constraint is solved trivially by parameterizing each $p_i = x_{i-1} - x_i$ in terms of n dual coordinates x_i. The x_i specify the vertices, in $\mathbb{C}^4$, of an n-sided polygon whose edges are the vectors p_i, each of which is null. A very special feature of SYM theory in the planar limit is that all amplitudes are invariant under conformal transformations in this dual space-time [6, 7, 26–31]

It is often useful, especially when one is interested in discussing aspects of conformal symmetry, to compactify the space-time. For example, in Euclidean signature, a single point at infinity has to be included in order for conformal inversion to make sense. It is also convenient to complexify space-time. Different real sections of this complexified space correspond to different signatures of the space-time metric. The complexified compactification $\widetilde{M}_4$ of four-dimensional space-time is the Grassmannian manifold $\mathrm{Gr}(2, 4, \mathbb{C})$ of 2-dimensional vector spaces in a four dimensional complex vector space V_4; in other words, there is a one-to-one correspondence between points in $\widetilde{M}_4$ and 2-dimensional vector subspaces in V_4. We can projectivize this picture to say that the correspondence is between points in complexified compactified space-time and lines in $\mathbb{P}^3$.

In the Grassmannian picture two points are light-like separated if their corresponding 2-planes intersect. So after projectivization, a pair of light-like separated points in $\widetilde{M}_4$ corresponds to a pair of intersecting lines in $\mathbb{P}^3$. Conformal transformations in space-time correspond to PGL_4 transformations on $\mathbb{P}^3$.

This $\mathbb{P}^3$ space is called twistor space in the physics literature. The importance of this space was first noted in the work of Penrose [43, 44] and more recently emphasized by Witten [45] in the context of Yang-Mills theory scattering amplitudes. However the twistors we need here are not the ones associated to the space-time in which the scattering takes place, but rather the ones associated to the dual space mentioned above, where the x_i live and on which dual conformal symmetry acts. These were called 'momentum twistors' in ref. [46], where they were first introduced. Momentum twistor space has both a chiral supersymmetric version (see ref. [47]) and a non-chiral supersymmetric version (see refs. [48–50]), but we will not make use of these extensions in this chapter.

To summarize: a scattering amplitude depends on a cyclically ordered collection of points x_i in the complexified momentum space $\mathbb{C}^4$, each of which corresponds to a projective line in momentum twistor space. Since each x_i is null separated from its neighbors x_{i-1} and x_{i+1}, their corresponding lines in momentum twistor space intersect. We denote by $Z_i \in \mathbb{P}^3$ the intersection of the lines corresponding to the points x_{i-1} and x_i. Conversely, an ordered sequence of points $Z_1, \ldots, Z_n \in \mathbb{P}^3$ determines a collection of n lines which intersect pairwise and therefore correspond to n light-light separated points x_i in the dual Minkowski space.

2.2.2 Bracket notation

The space we have just described—the collection of n ordered points in $\mathbb{P}^3$ modulo the action of PGL_4—defines $\mathrm{Conf}_n(\mathbb{P}^3)$, read as 'configurations of n points in $\mathbb{P}^3$'. Scattering amplitudes of n particles in SYM theory are functions on this $3(n-5)$-dimensional kinematic domain. This space can be essentially realized as the quotient $\mathrm{Gr}(4, \mathbb{C}^n)/(\mathbb{C}^*)^{n-1}$ of the Grassmannian by considering the space of $4 \times n$ matrices (being the homogeneous coordinates of the n points in $\mathbb{P}^3$) modulo the left-action of PGL_4 as well as independent rescaling of the n columns. In this presentation the natural dual conformal covariant objects are four-brackets of the form $\langle ijkl\rangle := \det(Z_iZ_jZ_kZ_l)$, which is just the $\mathbb{C}^4$ volume of the parallelepiped built on the vectors (Z_i, Z_j, Z_k, Z_l).

More precisely, emphasizing the structures involved, given a volume form ω_4 in a four dimensional vector space V_4, we can define the bracket $\langle v_1, v_2, v_3, v_4\rangle := \omega_4(v_1, v_2, v_3, v_4)$.

These four-brackets are key players in the rest of our story, so we list here a few of their important features. The Grassmannian duality $\mathrm{Gr}(k, n) = \mathrm{Gr}(n-k, n)$ means that configurations of n points in $\mathbb{P}^k$ are dual to configurations of n points in $\mathbb{P}^{n-k-2}$. Explicitly, at six points the relationship between four-brackets in $\mathbb{P}^3$ and two-brackets in $\mathbb{P}^1$ given by

$$\langle ijkl\rangle = \frac{1}{2!}\epsilon_{ijklmn}\langle mn\rangle, \qquad \langle ij\rangle = \frac{1}{4!}\epsilon_{ijklmn}\langle klmn\rangle, \tag{2.1}$$

while the relationship at seven points between four-brackets in $\mathbb{P}^3$ and three-brackets in $\mathbb{P}^2$ is clearly

$$\langle ijkl\rangle = \frac{1}{3!}\epsilon_{ijklmnp}\langle mnp\rangle, \quad \langle ijk\rangle = \frac{1}{4!}\epsilon_{ijklmnp}\langle lmnp\rangle. \tag{2.2}$$

We find it useful to exploit this duality for six and seven points when doing so leads to additional clarity. An invariant treatment of this duality is given below in sec. 2.2.3.

More complicated PGL_4 covariant objects can be formed naturally by using projective geometry inside four-brackets. Such objects will appear later in sec. 2.6, so we review the standard notation for them here. Following the $\cap$ notation introduced in ref. [4] we define the four-brackets with an intersection to be

$$\langle ab(cde) \cap (fgh)\rangle \equiv \langle acde\rangle\langle bfgh\rangle - \langle bcde\rangle\langle afgh\rangle. \tag{2.3}$$

This composite four-bracket vanishes when the line (ab) and the intersection of planes $(cde) \cap (fgh)$ lie in a common hyperplane.

Here is a slightly different way to think about (2.3). Consider a pair of vectors v_1, v_2 in a four dimensional vector space V_4, and a pair of covectors $f_1, f_2 \in V_4^*$. Then we set

$$\langle v_1, v_2; f_1, f_2 \rangle \equiv f_1(v_1)f_2(v_2) - f_1(v_2)f_2(v_1). \tag{2.4}$$

To get (2.3) we just take the covectors $f_1(*) := \langle c, d, e, * \rangle$ and $f_2(*) := \langle f, g, h, * \rangle$.

If we pick a vector c in the intersection of the two hyperplanes, writing them as (ca_2b_2) and (ca_3b_3), then we can rewrite it in a slightly different notation, making more symmetries manifest:

$$\langle a_1 b_1 (ca_2b_2) \cap (ca_3b_3) \rangle = -\langle c | a_1 \times b_1, a_2 \times b_2, a_3 \times b_3 \rangle, \tag{2.5}$$

Precisely, consider the three dimensional quotient $V_4/\langle c \rangle$ of the space V_4 along the subspace generated by the vector c. The volume form ω_4 in V_4 induces a volume form $\omega_4(c, *, *, *)$ in $V_4/\langle c \rangle$, and therefore in the dual space $(V_4/\langle c \rangle)^*$. So we can define three-brackets $\langle *, *, * \rangle_c$ in $(V_4/\langle c \rangle)^*$.

The other six vectors project to the quotient. Taking the cross-products $\times$ of consecutive pairs of these vectors, we get three covectors in $(V_4/\langle c \rangle)^*$. Their volume $-\langle a_1 \times b_1, a_2 \times b_2, a_3 \times b_3 \rangle_c$ equals the invariant (2.4). So we get formula (2.5).

Notice the expansions, where we use $\epsilon_{\alpha\beta\gamma}\epsilon^{\alpha}(\cdot, a, b) = a_\beta b_\gamma - a_\gamma b_\beta$:

$$\begin{aligned}
\langle a_1 \times b_1, a_2 \times b_2, a_3 \times b_3 \rangle &= \epsilon_{\alpha\beta\gamma}\epsilon^{\alpha}(\cdot, a_1, b_1)\epsilon^{\beta}(\cdot, a_2, b_2)\epsilon^{\gamma}(\cdot, a_3, b_3) && (2.6)\\
&= \langle a_1 a_2 b_2 \rangle \langle b_1 a_3 b_3 \rangle - \langle b_1 a_2 b_2 \rangle \langle a_1 a_3 b_3 \rangle && (2.7)\\
&= -\langle a_2 a_1 b_1 \rangle \langle b_2 a_3 b_3 \rangle + \langle a_2 a_3 b_3 \rangle \langle b_2 a_1 b_1 \rangle && (2.8)\\
&= \langle a_3 a_1 b_1 \rangle \langle b_3 a_2 b_2 \rangle - \langle a_3 a_2 b_2 \rangle \langle b_3 a_1 b_1 \rangle. && (2.9)
\end{aligned}$$

2.2.3 Configurations and Grassmannians

Let us formulate now the relationship between the Grassmannians $\mathrm{Gr}(k, \mathbb{C}^n)$ and the configuration spaces more accurately. We start with the notion of configurations.

Let V_k be a vector space of dimension k. Denote by $\mathrm{Conf}_n(k)$ the space of orbits of the group GL_k acting on the space of n-tuples of vectors in V_k. We call it the space of *configurations of n vectors in V_k*. It is important to notice that the sets of configurations of vectors in two different vector spaces of the same dimension are canonically isomorphic. Denote by $\mathrm{Conf}_n(\mathbb{P}^{k-1})$ the space of PGL_k-orbits on the space of n-tuples of points in $\mathbb{P}^{k-1}$, called *configurations of n points in $\mathbb{P}^{k-1}$*.

We consider an n-dimensional 'particle vector space' $\mathbb{C}^n$ with a given basis $(e_1, \ldots, e_n)$. Then a generic k-dimensional subspace h in $\mathbb{C}^n$ determines a configuration of n vectors $(f_1, \ldots, f_n)$ in the dual space h^*: these are the restrictions to h of the coordinate linear functionals in $\mathbb{C}^n$ dual to the basis $(e_1, \ldots, e_n)$. This way we get a well-defined bijection only for generic h, referred to mathematically as a birational isomorphism,

$$\mathrm{Gr}(k, \mathbb{C}^n) \xrightarrow{\sim} \mathrm{Conf}_n(k). \tag{2.10}$$

The group $(\mathbb{C}^*)^n$ acts by rescaling in the directions of the coordinate axes in $\mathbb{C}^k$. This action transforms into rescaling of the vectors of the configuration space $\mathrm{Conf}_n(k)$. The diagonal subgroup $\mathbb{C}^*_{\mathrm{diag}} \subset (\mathbb{C}^*)^n$ acts trivially. So the quotient group $(\mathbb{C}^*)^{n-1} = (\mathbb{C}^*)^n/\mathbb{C}^*_{\mathrm{diag}}$ acts effectively. Passing to the quotients we get a birational isomorphism

$$\mathrm{Gr}(k, \mathbb{C}^n)/(\mathbb{C}^*)^{n-1} \xrightarrow{\sim} \mathrm{Conf}_n(\mathbb{P}^{k-1}). \tag{2.11}$$

The dualities

$$\mathrm{Conf}_n(k) \xrightarrow{=} \mathrm{Conf}_n(n-k), \qquad \mathrm{Conf}_n(\mathbb{P}^k) \xrightarrow{=} \mathrm{Conf}_n(\mathbb{P}^{n-k-2}) \tag{2.12}$$

are best understood via the identification with the Grassmannian (2.10), followed by the obvious isomorphism $\mathrm{Gr}(k, \mathbb{C}^n) = \mathrm{Gr}(n-k, \mathbb{C}^n)$, obtained by taking the orthogonal planes.

2.2.4 The Euclidean region

Scattering amplitudes in field theory have a complicated singularity structure, including poles and branch cut singularities. However, we can find regions in the kinematic space where such singularities are absent. In particular, amplitudes are expected on physical grounds to be real-valued and singularity-free everywhere in the *Euclidean region*, reviewed in this section. It was discussed in ref. [51] in connection with MHV amplitudes in SYM theory.

The Euclidean region is defined most directly in the dual space parametrized by the x_i. We impose that the coordinates of the vectors x_i are real and

$$(x_i - x_{i+1})^2 = 0, \qquad (x_i - x_j)^2 < 0, \text{ otherwise}, \tag{2.13}$$

where the distance is computed with a metric of signature $(+,-,-,-)$ or $(+,+,-,-)$. These constraints define the Euclidean region in terms of the x_i coordinates.

When transformed to twistor coordinates the first constraint in eq. (2.13) is always satisfied. However, the constraint that the components of the vectors x_i should be real is harder to impose. We can think about twistors as being spinor representations of the complexified dual conformal group. This complexified dual conformal group has several real sections: $SU(4)$ which corresponds to Euclidean signature, $SL(4, \mathbb{R})$ which corresponds to split signature $(+,+,-,-)$ and $SU(2,2)$ which corresponds to $(+,-,-,-)$ signature.

In fact, there are two kinds of spinor representations which we call twistors (denoted by Z) and conjugate twistors (denoted by W). There is a Z and a W for every particle in a scattering process, which we denote by Z_i, W_i. Under the dual conformal group the Z and W twistors and transform in the opposite way. That is, if M is a dual conformal transformation,

$$W \to W' = WM^{-1}, \qquad Z \to Z' = MZ. \tag{2.14}$$

This implies that there is an invariant product $W \cdot Z$.

Now we can study the reality conditions. We will not discuss the Euclidean signature $(+,+,+,+)$ any further since it does not allow light-like separation. For split signature, the twistors transform under $SL(4,\mathbb{R})$ so they can be taken to be real and independent. For Lorentzian signature $(+,-,-,-)$ the symmetry group is $SU(2,2)$. If $M \in SU(2,2)$, then $M^\dagger \mathcal{C} M = \mathcal{C}$, where $\mathcal{C}$ is a $(2,2)$ signature matrix which we will take to be real and symmetric. Then $\mathcal{C}Z$ transforms in the same way as $W^\dagger$ so we can consistently impose a reality condition $W^\dagger = \mathcal{C}Z$. This implies that $(W_i \cdot Z_j)^* = W_j \cdot Z_i$. The light-like conditions imply that $W_i = Z_{i-1} \wedge Z_i \wedge Z_{i+1}$, so the previous reality condition can be written in terms of the Z twistors only as $\langle i-1 i i+1 j\rangle^* = \langle j-1 j j+1 i\rangle$.

Finally, let us translate the second condition in eq. (2.13) into twistor language. Space-time distances $(x_i - x_j)^2$ cannot be expressed in twistor variables without first making an arbitrary choice of 'infinity twistor'. However this choice cancels in conformal ratios, and for these the dictionary between space-time and momentum twistor space then implies that

$$\frac{\langle i i+1 j j+1\rangle \langle k k+1 l l+1\rangle}{\langle i i+1 l l+1\rangle \langle j j+1 k k+1\rangle} > 0, \tag{2.15}$$

for all i, j, k, l for which none of the four-brackets vanishes. This condition is certainly guaranteed if $\langle i i+1 j j+1\rangle > 0$ for all nonvanishing four-brackets of this type.

We therefore define the Euclidean region in momentum twistor space by the condition that $\langle ii+1jj+1\rangle > 0$. It has two sub-regions

$$(2,2)\text{ signature:}\qquad \langle ijkl\rangle \in \mathbb{R}, \tag{2.16}$$

$$(3,1)\text{ signature:}\qquad \langle i-1ii+1j\rangle^* = \langle j-1jj+1i\rangle. \tag{2.17}$$

Note that the $(2,2)$ signature region contains the positive Grassmannian which is well-studied mathematically. In contrast, the $(3,1)$ region does not seem to have been studied in the mathematical literature.

2.2.5 Parity

In this section we give a brief introduction to the action of parity on the configuration spaces discussed above. For a more thorough description, see Appendix A of [52]. In this context, parity amounts to replacing the twistors Z_i with their dual twistors W_i. Writing the dual twistors in terms of twistors as[1] $W_i = Z_{i-1}\wedge Z_i \wedge Z_{i+1}$, we see that the effect of parity on four-brackets is

$$\langle i, i{+}1, j, k\rangle \to \langle i{-}1, i, i{+}1, i{+}2\rangle\langle i, i{+}1, (j{-}1, j, j{+}1)\cap(k{-}1, k, k{+}1)\rangle. \tag{2.18}$$

In effect, this amounts to replacing the volume form ω with the dual volume form $*\omega$ where lines have been swapped with points and vice versa.

[1]This is often written as $W_i = \frac{Z_{i-1}\wedge Z_i\wedge Z_{i+1}}{\langle i-1i\rangle\langle ii+1\rangle}$ such that W_i and Z_i scale with opposite weight. The two-brackets $\langle ij\rangle$ are defined by choosing an arbitrary line I (also called 'infinity twistor') and setting $\langle ij\rangle = \langle Iij\rangle$. When constructing cross-ratios these two-brackets cancel out so in the following we will not keep track of them.

2.3 Review of the Two-Loop $n = 6$ MHV Amplitude

In the previous section we reviewed that n-particle scattering amplitudes in SYM theory are functions on the $3(n-5)$-dimensional space $\mathrm{Conf}_n(\mathbb{P}^3)$. It is further believed [40] that any MHV or next-to-MHV (NMHV) amplitude, at any loop order L in perturbation theory, can be expressed in terms of functions of uniform transcendentality weight $2L$. A goal of this chapter is to make a sharper statement about the mathematical structure of these functions. Specifically: that their structure is described by a certain preferred collection of functions on $\mathrm{Conf}_n(\mathbb{P}^3)$ which are known in the mathematics literature as cluster $\mathcal{X}$-coordinates. In this section we provide a simple but illustrative example of this phenomenon.

The simplest nontrivial multi-loop scattering amplitude is the two-loop MHV amplitude for $n = 6$ particles. This was originally computed numerically in [51, 53], then analytically in [17, 18] in terms of generalized polylogarithm functions, and finally in a vastly simplified form in terms of only the classical Li_m functions in [19]. We present it here very mildly reexpressed as

$$R_6^{(2)} = \sum_{i=1}^{3}\left(L_i - \frac{1}{2}\,\mathrm{Li}_4(-v_i)\right) - \frac{1}{8}\left(\sum_{i=1}^{3}\mathrm{Li}_2(-v_i)\right)^2 + \frac{1}{24}J^4 + \frac{\pi^2}{12}J^2 + \frac{\pi^4}{72}, \tag{2.19}$$

in terms of the functions

$$\begin{aligned} L_i &= \frac{1}{384}P_i^4 + \sum_{m=0}^{3}\frac{(-1)^m}{(2m)!!}P_i^m(\ell_{4-m}(x_i^+) + \ell_{4-m}(x_i^-)),\\ P_i &= 2\,\mathrm{Li}_1(-v_i) - \sum_{i=1}^{3}\mathrm{Li}_1(-v_i), \end{aligned} \tag{2.20}$$

and

$$J = \frac{1}{2}\sum_{i=1}^{3} \ell_1(x_i^+) - \ell_1(x_i^-),$$
$$\ell_n(x) = \frac{1}{2}(\mathrm{Li}_n(-x) - (-1)^n \mathrm{Li}_n(-1/x)). \tag{2.21}$$

Our aim in reproducing this formula here is to highlight two rather astonishing facts. The first is that the argument of each Li_n function is the negative of one of the simple cross-ratios

$$\begin{aligned} v_1 &= \frac{\langle 35\rangle\langle 26\rangle}{\langle 23\rangle\langle 56\rangle}, & v_2 &= \frac{\langle 13\rangle\langle 46\rangle}{\langle 16\rangle\langle 34\rangle}, & v_3 &= \frac{\langle 15\rangle\langle 24\rangle}{\langle 45\rangle\langle 12\rangle}, \\ x_1^+ &= \frac{\langle 14\rangle\langle 23\rangle}{\langle 12\rangle\langle 34\rangle}, & x_2^+ &= \frac{\langle 25\rangle\langle 16\rangle}{\langle 56\rangle\langle 12\rangle}, & x_3^+ &= \frac{\langle 36\rangle\langle 45\rangle}{\langle 34\rangle\langle 56\rangle}, \\ x_1^- &= \frac{\langle 14\rangle\langle 56\rangle}{\langle 45\rangle\langle 16\rangle}, & x_2^- &= \frac{\langle 25\rangle\langle 34\rangle}{\langle 23\rangle\langle 45\rangle}, & x_3^- &= \frac{\langle 36\rangle\langle 12\rangle}{\langle 16\rangle\langle 23\rangle} \end{aligned} \tag{2.22}$$

(or their inverses). We caution the reader that the $x_i^\pm$ here are the *negative* of the $x_i^\pm$ used in [19], while the v_i used here are related to the three u_i cross-ratios most commonly seen in the literature by $v_i = (1 - u_i)/u_i$. Of course, these 9 variables are not independent—the dimension of $\mathrm{Conf}_6(\mathbb{P}^3)$ is only three—so one could choose any three of them in terms of which to express all of the others algebraically. It is striking that the argument of each Li_m function in (2.19) is expressible as one of these simple cross-ratios rather than, as might have been the case, some arbitrary algebraic function of cross-ratios.

The second striking fact about (2.19) is that out of the 45 distinct cross-ratios of the form

$$r(i,j,k,l) = \frac{\langle ij\rangle\langle kl\rangle}{\langle jk\rangle\langle il\rangle} \tag{2.23}$$

only the 9 shown in (2.22) actually appear. Note that here, as throughout the chapter, we shall never count both x and $1/x$ separately.

The presentation of (2.19) we have given here also highlights another theme which will pervade this chapter: positivity. The cross-ratios defined in eq. (2.22) all have the manifest property that they are positive whenever each ordered bracket is positive, i.e. whenever $\langle ij \rangle > 0 \;\forall\; i < j$. As this example and others to be discussed below suggest, we expect all MHV amplitudes will have particularly rich structure on the positive subset of the domain $\mathrm{Conf}_n(\mathbb{P}^3)$. The formula (2.19) is expressed in terms of the natural polylogarithm function on the domain of positive real-valued x:

$$\mathrm{Li}_n(-x) = \int_{\Delta_x} \log(1+t_1)\, d\log t_2 \wedge \cdots \wedge d\log t_n := L_n(x) \tag{2.24}$$

where $\Delta_x = \{(t_1, \ldots, t_n) : 0 < t_1 < t_2 < \cdots < t_n < x\}$. The proper continuation of eq. (2.19) to the part of the Euclidean region outside the positive domain was discussed in [19].

In the rest of this chapter we will work almost exclusively not with amplitudes but with coproducts of motivic amplitudes, reviewed in the next section. For such purposes it is sufficient to highlight in $R_6^{(2)}$ only the leading terms

$$R_6^{(2)} = \sum_{i=1}^{3} L_4(x_i^+) + L_4(x_i^-) - \frac{1}{2} L_4(v_i) + \cdots\,, \tag{2.25}$$

where the dots stand for products of functions of lower weight, which are killed by the coproduct δ.

In a certain sense this example is too simple, as this amplitude is likely unique in SYM theory in being expressible in terms of classical polylogarithm functions Li_m only. We do not aim to write explicit formulas for more general amplitudes as there would be no particular preferred or canonical functional form, so the question of *what variables the function depends on* requires a more precise definition involving the more sophisticated mathematics to which we turn our attention in the next section.

2.4 Polylogarithms and Motivic Lie Algebras

In this section we review some of the necessary mathematical preliminaries on transcendental functions and explain ways of distilling the essential motivic content of such functions. The precise mathematical definitions of motivic avatars of polylogarithm-like functions is given in [21]. Taking for granted that such avatars exist, our goal is to provide the elements of motivic calculus necessary to describe their basic properties.

We begin by recalling some elementary mathematical facts about polylogarithm functions from [32, 54] (see [52, 55–57] for recent reviews written for physicists). To each such transcendental function of weight k is associated an element of the k-fold tensor product of the multiplicative group of rational functions modulo constants called its *symbol*. For example, the classical polylogarithm function $\mathrm{Li}_k(x)$ has symbol

$$-(1-x) \otimes \underbrace{x \otimes \cdots \otimes x}_{k-1 \text{ times}}. \tag{2.26}$$

A trivial way to make a function of weight k is to multiply two functions of lower weights k_1, k_2 with $k = k_1 + k_2$. It is often useful to exclude such products from consideration and to focus on the most complicated, intrinsically weight k, part of a function. This may be accomplished via a projection operator ρ which annihilates all products of functions of lower weight. It is defined recursively by

$$\rho(a_1 \otimes \cdots \otimes a_k) = \frac{k-1}{k} \left[\rho(a_1 \otimes \cdots \otimes a_{k-1}) \otimes a_k - \rho(a_2 \otimes \cdots \otimes a_k) \otimes a_1\right] \tag{2.27}$$

beginning with $\rho(a_1) = a_1$. Here, in a slight abuse of notation which we will perpetuate throughout this section, we display for simplicity not how ρ acts on a general weight-k function but rather how it acts on the symbol of such a function.

We use $\mathcal{L}_\bullet$ to denote the algebra of polylogarithm functions modulo products of functions of lower weight. It is a commutative graded Hopf algebra with a coproduct

$\delta : \mathcal{L}_\bullet \mapsto \Lambda^2 \mathcal{L}_\bullet$ which satisfies $\delta^2 = 0$, giving it the structure of a Lie coalgebra. Explicitly, δ may be computed (again, at the level of symbols) by

$$\delta(a_1 \otimes \cdots \otimes a_k) = \sum_{n=1}^{k-1} (a_1 \otimes \cdots \otimes a_n) \bigwedge (a_{n+1} \otimes \cdots \otimes a_k). \tag{2.28}$$

We let B_k denote the Bloch group [58, 59] defined as the quotient of $\mathcal{L}_k$ by the subspace of functional equations for the classical logarithm function Li_k. The case $k = 1$ is trivial (any linear combination of logarithm functions can be combined into a single logarithm) so we simply write "x" to denote the function $\log x$ and therefore denote $\mathcal{L}_1 = \mathbb{C}^*$, the multiplicative group of nonzero complex numbers. For $k > 1$ elements of B_k are finite linear combinations of objects denoted by $\{x\}_k$, which can be read as shorthand for the function $-\mathrm{Li}_k(-x)$. These satisfy[2]

$$\delta\{x\}_k = \begin{cases} (1+x) \bigwedge x & k = 2, \\ \{x\}_{k-1} \bigotimes x & k > 2. \end{cases} \tag{2.29}$$

For $k = 2, 3$ it is a theorem that $\mathcal{L}_k = \mathrm{B}_k$. At weight 4, for the first time, the coproduct has two separate components[3]

$$\delta(a_1 \otimes a_2 \otimes a_3 \otimes a_4)|_{\Lambda^2 \mathrm{B}_2} = \rho(a_1 \otimes a_2) \bigwedge \rho(a_3 \otimes a_4), \tag{2.30}$$

$$\delta(a_1 \otimes a_2 \otimes a_3 \otimes a_4)|_{\mathrm{B}_3 \otimes \mathbb{C}^*} = \rho(a_1 \otimes a_2 \otimes a_3) \bigotimes a_4 - \rho(a_2 \otimes a_3 \otimes a_4) \bigotimes a_1. \tag{2.31}$$

[2] The top line is an element of $\Lambda^2 \mathcal{L}_1$, while the bottom is the element of the summand in $\Lambda^2(\mathcal{L}_{k-1} \oplus \mathcal{L}_1)$ given by vectors of the form $f_{k-1} \otimes f_1 - f_1 \otimes f_{k-1}$, and we use the standard notation of denoting such an element simply by $f_{k-1} \otimes f_1 \in \mathcal{L}_{k-1} \otimes \mathcal{L}_1$.

[3] These expressions are simply transcriptions of the components of eq. (2.28). Specifically, eq. (2.30) is the $n = 2$ term in eq. (2.28), while eq. (2.31) is the sum of the $n = 1$ and $n = 3$ terms in eq. (2.28), with the $n = 1$ term receiving a minus sign when put into the order shown in eq. (2.31) as implied by the $\bigwedge$ in eq. (2.28). We have chosen to write some ρ's explicitly in eqs. (2.30) and (2.31) but they are not necessary since $\rho(x)$ and x represent the same element in $\mathcal{L}_k$. For the same reason, we could have acted on both sides of the $\bigwedge$ in eq. (2.28) with the ρ operator without changing the meaning of that definition.

The classical function $\mathrm{Li}_4(x)$ has coproduct components

$$\delta\,\mathrm{Li}_4(x)|_{\Lambda^2\,\mathrm{B}_2} = 0, \tag{2.32}$$

$$\delta\,\mathrm{Li}_4(x)|_{\mathrm{B}_3\,\otimes\mathbb{C}^*} = -\{-x\}_3 \otimes x, \tag{2.33}$$

so it is clear that any polylogarithm function of weight 4 which has a nonzero $\Lambda^2\,\mathrm{B}_2$ content cannot possibly be written in terms of classical functions. It is moreover conjectured that the converse is true [32][4]. In this sense we can say that it is the $\Lambda^2\,\mathrm{B}_2$ coproduct component which measures the "non-trivial part" of a weight-four polylogarithm function.

2.4.1 Integrability

Next we discuss the integrability condition which plays the crucial role in the following two sections. A second application of δ at weight 4 maps each of the two components to $\mathrm{B}_2 \otimes \Lambda^2\mathbb{C}^*$, as indicated in the diagram[5]:

$$\begin{tikzcd} & \mathcal{L}_4 \arrow[dl] \arrow[dr] & \\ \Lambda^2\,\mathrm{B}_2 \arrow[dr] & & \mathrm{B}_3 \otimes \mathbb{C}^* \arrow[dl] \;, \\ & \mathrm{B}_2 \otimes \Lambda^2\mathbb{C}^* & \end{tikzcd}$$

[4]More generally, it is conjectured that a weight-k function f_k can be written in terms of the classical polylogarithm Li_k if and only if all components of δf_k vanish except possibly $\mathcal{L}_{k-1} \otimes \mathbb{C}^*$.

[5]Note that this is not a commutative diagram; indeed according to eq (2.36) it is better thought of as an *anti*commutative diagram.

where the bottom two arrows are given explicitly by

$$\delta(\{x\}_2 \wedge \{y\}_2) = \{y\}_2 \otimes (1+x) \wedge x - \{x\}_2 \otimes (1+y) \wedge y, \tag{2.34}$$

$$\delta(\{x\}_3 \otimes y) = \{x\}_2 \otimes x \wedge y. \tag{2.35}$$

Given arbitrary elements $b_{22} \in \Lambda^2 \mathrm{B}_2$ and $b_{31} \in \mathrm{B}_3 \otimes \mathbb{C}^*$, there does not necessarily exist any function $f_4 \in \mathcal{L}_4$ whose coproduct components are b_{22} and b_{31}. A necessary and sufficient condition for such a function to exist is that the integrability condition

$$0 = \delta^2 f_4 = \delta(b_{22}) + \delta(b_{31}) \tag{2.36}$$

is satisfied. Equivalently, we can say that *a pair b_{22}, b_{31} satisfying (2.36) uniquely determines a weight-four polylogarithm function (modulo products of functions of lower weight).*

It is important to note that given any element $b_{22} \in \Lambda^2 \mathrm{B}_2$ there does exist some function f_4 with b_{22} as its coproduct component (indeed Goncharov has written down [60] an explicit map $\kappa : \Lambda^2 \mathrm{B}_2 \to \mathrm{B}_3 \otimes \mathbb{C}^*$ such that the pair $b_{22}, \kappa(b_{22})$ satisfies (2.36) for any $b_{22} \in \Lambda^2 \mathrm{B}_2$), but for generic b_{22} the $\mathrm{B}_3 \otimes \mathbb{C}^*$ component $\kappa(b_{22})$ of that function will not have any cluster algebra structure of the type we study below.

2.4.2 Motivic scattering amplitudes

The L-loop n-particle MHV motivic amplitudes in SYM theory, considered modulo products, are elements $\mathcal{A}^{\mathcal{M}}_{n,L} \in \mathcal{L}_{2L}$. The two-loop motivic amplitudes are therefore elements

$$\mathcal{A}^{\mathcal{M}}_{n,2}(Z_1, \ldots, Z_n) \in \mathcal{L}_4(F), \quad F = \mathbb{Q}(Z_1, \ldots, Z_n) \tag{2.37}$$

defined by a generic configuration of n points $(Z_1, \ldots, Z_n)$ in $\mathbb{P}^3$. Therefore, as was explained above, they can be expressed via $\mathrm{Li}_4(z)$ if and only if the $\Lambda^2 \mathrm{B}_2$ obstruction vanishes. This is exactly what happened in [19] where the two-loop $n = 6$ MHV amplitude was calculated as a sum of classical 4-logarithms. The problem set out for us here and in subsequent work is therefore:

Problem. Calculate the motivic n-particle two-loop MHV amplitudes for $n > 6$. More specifically, this amounts to computing the coproduct

$$\delta_{\mathcal{M}}(\mathcal{A}_{n,2}^{\mathcal{M}}(Z_1, \ldots, Z_n)) \in \Lambda^2\mathrm{B}_2 \bigoplus \mathrm{B}_3 \otimes \mathbb{C}^*. \tag{2.38}$$

The coproduct determines the amplitude as a function up to a constant and products of similar functions of lower weight. The coproduct is given in terms of the groups B_n, $n = 1, 2, 3$, and so its calculation is a precise problem. Let us emphasize that due to the 'one-variable' nature of the groups B_n, to write an element in $\Lambda^2\mathrm{B}_2 \bigoplus \mathrm{B}_3 \otimes \mathbb{C}^*$ we need a collection of functions on the configuration space $\mathrm{Conf}_n(\mathbb{P}^3)$—the arguments of the dilogarithms and trilogarithms. The only ambiguity of such a presentation results from the functional equations they satisfy.

As we show below, these functions for the 2-loop n-particle MHV motivic amplitudes, where $n = 6, 7$, are cluster $\mathcal{X}$-coordinates on the space $\mathrm{Conf}_n(\mathbb{P}^3)$. Moreover, although functional equations do come into the picture, the ones we see for the two-loop amplitudes are also of cluster nature, and discussed in Appendix B of [52]

We would like to stress that without the motivic approach one cannot even formulate Problem 2.4.2—there is no way to define the coproduct just on the level of functions.

2.5 The Coproducts of Two-Loop MHV Motivic Amplitudes

Using the symbol of the two-loop n-point MHV amplitude, as computed in [20], one can calculate the coproduct $\delta(\mathcal{A}^{\mathcal{M}}_{n,2})$ of the corresponding motivic amplitude as defined in the previous section and summarized in eq. (2.38). For $n = 6$ the $\Lambda^2\,\mathrm{B}_2$ component is trivial, as was noted already in [19], while the $\mathrm{B}_3 \otimes \mathbb{C}^*$ part of the coproduct may be read off immediately from (2.25):

$$\delta(\mathcal{A}^{\mathcal{M}}_{6,2})|_{\mathrm{B}_3 \otimes \mathbb{C}^*} = \sum_{i=1}^{3} \{x_i^+\}_3 \otimes x_i^+ + \{x_i^-\}_3 \otimes x_i^- - \frac{1}{2}\{v_i\}_3 \otimes v_i. \tag{2.39}$$

We defer results for general n to a subsequent chapter and present here explicit results only for $n = 7$, since our main goal at the moment is to call the reader's attention to the same two non-trivial features that we emphasized in section 2.3. The first feature is that the entry z appearing inside each $\{z\}_2$ or $\{z\}_3$ is a single cross-ratio (rather than, as might have been the case, some arbitrary algebraic function of cross-ratios); the second feature is that of the thousands of such cross-ratios one can form at $n = 7$, only a small handful actually appear in the motivic amplitudes. The structure of the results presented here will be extensively discussed in subsequent sections.

2.5.1 The $\Lambda^2\,\mathrm{B}_2$ component for $n=7$

We find that the $\Lambda^2\,\mathrm{B}_2$ component of $\delta(\mathcal{A}^{\mathcal{M}}_{7,2})$ can be expressed as

$$\sum_{\text{dihedral}}\Bigg(\left\{\frac{\langle 7\times 1, 2\times 3, 4\times 5\rangle}{\langle 127\rangle\langle 345\rangle}\right\}_2 \wedge \left\{\frac{\langle 2\times 3, 4\times 6, 7\times 1\rangle}{\langle 167\rangle\langle 234\rangle}\right\}_2$$
$$+\left\{\frac{\langle 614\rangle\langle 675\rangle}{\langle 671\rangle\langle 645\rangle}\right\}_2 \wedge \left\{\frac{\langle 2\times 3, 4\times 6, 7\times 1\rangle}{\langle 167\rangle\langle 234\rangle}\right\}_2 + \left\{\frac{\langle 312\rangle\langle 347\rangle}{\langle 371\rangle\langle 342\rangle}\right\}_2 \wedge \left\{\frac{\langle 713\rangle\langle 746\rangle}{\langle 716\rangle\langle 734\rangle}\right\}_2\Bigg), \tag{2.40}$$

where the sum indicates that one should sum over the dihedral group Dih_7 acting on the particle labels, resulting in a total of $3\times 14 = 42$ terms.

It is important to note that this expression is of course not unique. There are two kinds of ambiguities: first of all, there are dilogarithm identities which hold at the level of B_2 and are a consequence of Abel's pentagon relation

$$\sum_{i=1}^{5}\mathcal{L}_2(r(x_i, x_{i+1}, x_{i+2}, x_{i+3})) = 0, \tag{2.41}$$

where $\mathcal{L}_2$ is the Bloch-Wigner dilogarithm

$$\mathcal{L}_2(z) := \Im(\mathrm{Li}_2(-z) + \arg(1+z)\log|z|), \quad z\in\mathbb{C} \tag{2.42}$$

and the cross-ratio r is defined as

$$r(x_1,x_2,x_3,x_4) = \frac{(x_1-x_2)(x_3-x_4)}{(x_2-x_3)(x_1-x_4)}. \tag{2.43}$$

One slightly non-trivial, but easily checked, example is

$$0 = -\left\{\frac{\langle 127\rangle\langle 156\rangle\langle 345\rangle}{\langle 157\rangle\langle 1\times 2, 3\times 4, 5\times 6\rangle}\right\}_2 + \left\{\frac{\langle 127\rangle\langle 256\rangle\langle 345\rangle}{\langle 257\rangle\langle 1\times 2, 3\times 4, 5\times 6\rangle}\right\}_2$$
$$+\left\{-\frac{\langle 567\rangle\langle 1\times 2, 3\times 4, 5\times 6\rangle}{\langle 256\rangle\langle 1\times 7, 3\times 4, 5\times 6\rangle}\right\}_2 - \left\{-\frac{\langle 127\rangle\langle 345\rangle\langle 567\rangle}{\langle 157\rangle\langle 2\times 7, 3\times 4, 5\times 6\rangle}\right\}_2 - \left\{\frac{\langle 571\rangle\langle 562\rangle}{\langle 512\rangle\langle 567\rangle}\right\}_2. \tag{2.44}$$

Such identities relate different, but equivalent, expressions for the $\Lambda^2\,\mathrm{B}_2$ component which in general have different numbers of terms.

Secondly there is ambiguity in writing (2.40) due to the trivial identities

$$\{x\}_2 \wedge \{y\}_2 = -\{1/x\}_2 \wedge \{y\}_2 = \{1/x\}_2 \wedge \{1/y\}_2 = -\{x\}_2 \wedge \{1/y\}_2 \tag{2.45}$$

which preserve the number of terms.

Given these ambiguities one may wonder about the value in providing any explicit formula such as (2.40). Is there some invariant way of presenting the $\Lambda^2\,\mathrm{B}_2$ part of the coproduct of this amplitude, without having to commit any particular representation? To phrase this question in language familiar to physicists: if we think about the equations (2.44) and (2.45) as generating some kind of gauge transformations, then what is the gauge-invariant content of the $\Lambda^2\,\mathrm{B}_2$ component of this coproduct?

We pose this question here merely as a teaser; to answer it fully requires the mathematical machinery to be built up in section 2.6. Nevertheless we will also tease the reader here with the answer: the terms in (2.40) are naturally in correspondence with certain quadrilateral faces of the E_6 Stasheff polytope, and there is a unique representative with this property.

2.5.2 The $\mathrm{B}_3 \otimes \mathbb{C}^*$ component for $n = 7$

In order to save space, we will make use of the dihedral symmetry and invariance under rescaling of the MHV amplitude to write only the two independent B_3 components necessary to express the full answer. First, for the $\langle 124\rangle$ component of $\mathbb{C}^*$ we find the B_3 element

$$\begin{aligned}
&\left\{\frac{\langle 127\rangle\langle 256\rangle\langle 345\rangle}{\langle 257\rangle\langle 1\times 2, 3\times 4, 5\times 6\rangle}\right\}_3 + \left\{\frac{\langle 125\rangle\langle 234\rangle\langle 567\rangle}{\langle 257\rangle\langle 1\times 2, 3\times 4, 5\times 6\rangle}\right\}_3 \\
&- \left\{\frac{\langle 127\rangle\langle 234\rangle\langle 345\rangle\langle 567\rangle}{\langle 257\rangle\langle 347\rangle\langle 1\times 2, 3\times 4, 5\times 6\rangle}\right\}_3 + \left\{\frac{\langle 124\rangle\langle 157\rangle}{\langle 127\rangle\langle 145\rangle}\right\}_3 + \left\{-\frac{\langle 127\rangle\langle 254\rangle\langle 516\rangle}{\langle 124\rangle\langle 256\rangle\langle 517\rangle}\right\}_3 \\
&- \left\{\frac{\langle 214\rangle\langle 257\rangle}{\langle 217\rangle\langle 245\rangle}\right\}_3 + \left\{\frac{\langle 412\rangle\langle 435\rangle}{\langle 415\rangle\langle 423\rangle}\right\}_3 - \left\{\frac{\langle 412\rangle\langle 437\rangle}{\langle 417\rangle\langle 423\rangle}\right\}_3 - \left\{-\frac{\langle 147\rangle\langle 452\rangle\langle 516\rangle}{\langle 142\rangle\langle 456\rangle\langle 517\rangle}\right\}_3 \\
&- \left\{-\frac{\langle 247\rangle\langle 453\rangle\langle 526\rangle}{\langle 243\rangle\langle 456\rangle\langle 527\rangle}\right\}_3 + \left\{\frac{\langle 412\rangle\langle 457\rangle}{\langle 417\rangle\langle 425\rangle}\right\}_3 - \left\{\frac{\langle 512\rangle\langle 547\rangle}{\langle 517\rangle\langle 524\rangle}\right\}_3 + \left\{\frac{\langle 712\rangle\langle 745\rangle}{\langle 715\rangle\langle 724\rangle}\right\}_3 \\
&- \left\{\frac{\langle 413\rangle\langle 457\rangle}{\langle 417\rangle\langle 435\rangle}\right\}_3 + \left\{\frac{\langle 423\rangle\langle 457\rangle}{\langle 427\rangle\langle 435\rangle}\right\}_3 - \left\{-\frac{\langle 241\rangle\langle 453\rangle\langle 527\rangle}{\langle 243\rangle\langle 457\rangle\langle 521\rangle}\right\}_3 + \left\{-\frac{\langle 241\rangle\langle 473\rangle\langle 725\rangle}{\langle 243\rangle\langle 475\rangle\langle 721\rangle}\right\}_3 \\
&+ \left\{\frac{\langle 512\rangle\langle 567\rangle}{\langle 517\rangle\langle 526\rangle}\right\}_3 - \left\{-\frac{\langle 254\rangle\langle 576\rangle\langle 721\rangle}{\langle 256\rangle\langle 571\rangle\langle 724\rangle}\right\}_3 - \left\{\frac{\langle 514\rangle\langle 567\rangle}{\langle 517\rangle\langle 546\rangle}\right\}_3 + \left\{-\frac{\langle 452\rangle\langle 576\rangle\langle 741\rangle}{\langle 456\rangle\langle 571\rangle\langle 742\rangle}\right\}_3 \\
&- \left\{\frac{\langle 524\rangle\langle 567\rangle}{\langle 527\rangle\langle 546\rangle}\right\}_3 + \left\{-\frac{\langle 453\rangle\langle 576\rangle\langle 742\rangle}{\langle 456\rangle\langle 572\rangle\langle 743\rangle}\right\}_3 .
\end{aligned} \tag{2.46}$$

Secondly, for $\langle 125\rangle$ (this is symmetric under $1 \leftrightarrow 2, 7 \leftrightarrow 3, 6 \leftrightarrow 4$) we find

$$\begin{aligned}
&-\left\{\frac{\langle 157\rangle\langle 234\rangle}{\langle 1\times 2, 3\times 4, 5\times 7\rangle}\right\}_3 - \left\{\frac{\langle 123\rangle\langle 457\rangle}{\langle 1\times 2, 3\times 4, 5\times 7\rangle}\right\}_3 - \left\{\frac{\langle 127\rangle\langle 134\rangle\langle 567\rangle}{\langle 167\rangle\langle 1\times 2, 3\times 4, 5\times 7\rangle}\right\}_3 \\
&+ \left\{\frac{\langle 127\rangle\langle 234\rangle\langle 567\rangle}{\langle 267\rangle\langle 1\times 2, 3\times 4, 5\times 7\rangle}\right\}_3 + \left\{\frac{\langle 123\rangle\langle 345\rangle\langle 567\rangle}{\langle 356\rangle\langle 1\times 2, 3\times 4, 5\times 7\rangle}\right\}_3 \\
&- \left\{\frac{\langle 124\rangle\langle 345\rangle\langle 567\rangle}{\langle 456\rangle\langle 1\times 2, 3\times 4, 5\times 7\rangle}\right\}_3 - \left\{\frac{\langle 123\rangle\langle 145\rangle}{\langle 125\rangle\langle 134\rangle}\right\}_3 - 2\left\{\frac{\langle 125\rangle\langle 167\rangle}{\langle 127\rangle\langle 156\rangle}\right\}_3 \\
&+ \left\{\frac{\langle 412\rangle\langle 435\rangle}{\langle 415\rangle\langle 423\rangle}\right\}_3 + \left\{\frac{\langle 512\rangle\langle 534\rangle}{\langle 514\rangle\langle 523\rangle}\right\}_3 - \left\{-\frac{\langle 231\rangle\langle 354\rangle\langle 526\rangle}{\langle 234\rangle\langle 356\rangle\langle 521\rangle}\right\}_3 + \left\{-\frac{\langle 241\rangle\langle 453\rangle\langle 526\rangle}{\langle 243\rangle\langle 456\rangle\langle 521\rangle}\right\}_3 \\
&+ \left\{\frac{\langle 523\rangle\langle 546\rangle}{\langle 526\rangle\langle 534\rangle}\right\}_3 + (1 \leftrightarrow 2, 7 \leftrightarrow 3, 6 \leftrightarrow 4).
\end{aligned} \tag{2.47}$$

The full $\mathrm{B}_3 \otimes \mathbb{C}^*$ part of the coproduct of the two-loop $n = 7$ MHV motivic amplitude is assembled in terms of these two building blocks as

$$\sum_{\text{dihedral}} \left[(\text{eq. } 2.46) \otimes \frac{\langle 124 \rangle \langle 567 \rangle}{\langle 127 \rangle \langle 456 \rangle} + \frac{1}{2} (\text{eq. } 2.47) \otimes \frac{\langle 125 \rangle \langle 167 \rangle \langle 234 \rangle}{\langle 123 \rangle \langle 127 \rangle \langle 456 \rangle} \right]. \tag{2.48}$$

Let us comment briefly on the action of parity on eq. (2.48). If we apply parity to the first term in eq. (2.48) and then the permutation $(1, 7, 6, 5, 4, 3, 2)$, the $\mathbb{C}^*$ term is unchanged. The corresponding B_3 terms are identical up to a 40-term Li_3 identity, of the type discussed in Appendix B of [52]. The parity invariance of the second term in eq. (2.48) is easier to prove: applying parity followed by the permutation $(4, 5, 6, 7, 1, 2, 3)$ leaves both the $\mathbb{C}^*$ term and the corresponding B_3 part invariant. Therefore in this case the parity invariance is manifest, without requiring any Li_3 identities. We note with interest that the aforementioned 40-term identity is the *only* nontrivial Li_3 identity which plays a role in elucidating the structure of this amplitude.

2.6 Cluster Coordinates and Cluster Algebras

Having presented concrete results of the calculation of the coproduct for the two-loop $n = 7$ MHV amplitude, we now turn to a second main theme of the chapter: establishing the connection between the coproduct of motivic amplitudes and cluster algebras. We start with a short introduction to cluster algebras, which were discovered and first developed in a series of papers [34, 35] by Fomin and Zelevinsky. The configuration space $\mathrm{Conf}_n(\mathbb{P}^k)$ of n points in $\mathbb{P}^k$ has the structure of a *cluster Poisson variety* [33]—a structure closely related to cluster algebras. This section is aimed primarily at physicists since most of this material is a review of fairly well-known mathematical facts, with a focus on the intended application to $\mathrm{Conf}_n(\mathbb{P}^3)$, the space on which scattering amplitudes live. Our aim in this section is to guide the reader quickly to an understanding of what cluster variables, which we refer to as cluster $\mathcal{A}$-coordinates, are for the Grassmannians, what cluster $\mathcal{X}$-coordinates are for the configuration spaces $\mathrm{Conf}_n(\mathbb{P}^{k-1})$, and how these coordinates may be systematically constructed via a process called mutation.

To guide the reader, let us specify the spaces where different types of cluster coordinates live. Recall (see sec. 2.2) that the Grassmannian $\mathrm{Gr}(k,n)$ is birationally isomorphic to the configuration space of vectors $\mathrm{Conf}_n(k)$. The latter projects onto the space of projective configurations $\mathrm{Conf}_n(\mathbb{P}^{k-1})$:

$$\mathrm{Gr}(k,n) \xrightarrow{\sim} \mathrm{Conf}_n(k) \xrightarrow{\pi} \mathrm{Conf}_n(\mathbb{P}^{k-1}). \tag{2.49}$$

Cluster $\mathcal{A}$-coordinates live naturally on the Plücker cone $\widetilde{\mathrm{Gr}}(k,n)$ over the Grassmannian rather then on the Grassmannian itself. This cone can be identified birationally with the configuration space $\widetilde{\mathrm{Conf}}_n(k)$ of n vectors modulo the action of the group SL_k rather then GL_k. Abusing terminology, one often refers to them as coordinates on the Grassmannian. Cluster $\mathcal{X}$-coordinates live naturally on the smaller space $\mathrm{Conf}_n(\mathbb{P}^{k-1})$—its dimension is n less then that of the $\widetilde{\mathrm{Conf}}_n(k)$. They describe a collection of log-canonical Darboux coordinate systems for the natural cyclic invariant Poisson structure on the space $\mathrm{Conf}_n(\mathbb{P}^{k-1})$. Using the canonical projection

$$\widetilde{\pi} : \widetilde{\mathrm{Gr}}(k,n) \longrightarrow \mathrm{Conf}_n(\mathbb{P}^{k-1})$$

one can lift the cluster $\mathcal{X}$-coordinates on $\mathrm{Conf}_n(\mathbb{P}^{k-1})$, and express them as monomials of the cluster variables in the Grassmannian cluster algebra. One cannot extend, however, the Poisson structure to the cluster algebra without breaking the cyclic invariance. Notice that the cluster algebra structure itself on $\widetilde{\mathrm{Conf}}_n(k)$ is (twisted) cyclic invariant. The cyclic invariance is a crucial feature of the planar scattering amplitudes. So it is important that both Grassmannian cluster algebra and the cluster Poisson structure on $\mathrm{Conf}_n(\mathbb{P}^{k-1})$ are cyclic invariant.

2.6.1 Introduction and definitions

We can informally define cluster algebras as follows: they are commutative algebras constructed from distinguished generators (called *cluster variables*) grouped into non-disjoint sets of constant cardinality (called *clusters*), which are constructed iteratively from an initial cluster by an operation called *mutation*. The number of variables in a cluster is called the rank of the cluster algebra.

A simple example is the A_2 cluster algebra defined by the following data:

- cluster variables: a_m for $m \in \mathbb{Z}$, subject to $a_{m-1}a_{m+1} = 1 + a_m$
- rank: 2
- clusters: $\{a_m, a_{m+1}\}$ for $m \in \mathbb{Z}$
- initial cluster: $\{a_1, a_2\}$
- mutation: $\{a_{m-1}, a_m\} \to \{a_m, a_{m+1}\}$.

Using the exchange relation $a_{m-1}a_{m+1} = 1 + a_m$ one sees that

$$a_3 = \frac{1+a_2}{a_1}, \quad a_4 = \frac{1+a_1+a_2}{a_1 a_2}, \quad a_5 = \frac{1+a_1}{a_2}, \quad a_6 = a_1, \quad a_7 = a_2. \tag{2.50}$$

Therefore, the sequence a_m is periodic with period five and the number of cluster variables is finite.

When expressing the cluster variables a_m in terms of a_1 and a_2, we encounter two interesting features. First, the denominators of the cluster variables are always monomials. In general the structure of an algebra is such that one might expect the cluster variables to be more general rational functions of the initial cluster variables, but in fact the denominator is always a monomial. This is known as the 'Laurent phenomenon' (see [34, 61]). A second feature is that, conjecturally, the numerator of each cluster variable, expressed in terms of the original cluster variables, is always a polynomial with positive integral coefficients.

Some cluster algebras may be defined in terms of another piece of mathematical machinery: quivers. A quiver is an oriented graph, and in the following we restrict to connected, finite quivers without loops (arrows with the same origin and target) and two-cycles (pairs of arrows going in opposite directions between two vertices).

Given a quiver and a choice of some vertex k on that quiver we can define a new quiver obtained by *mutating* at vertex k. The new quiver is obtained by applying the following operations on the initial quiver:

- for each path $i \to k \to j$, add an arrow $i \to j$,
- reverse all arrows on the edges incident with k,
- and remove any two-cycles that may have formed.

The mutation at k is an involution; when applied twice in succession at the same vertex we come back to the original quiver.

Quivers of the special type we restricted to are in one-to-one correspondence with skew-symmetric matrices defined as

$$b_{ij} = (\#\text{arrows } i \to j) - (\#\text{arrows } j \to i). \tag{2.51}$$

Since at most one of the terms above is nonvanishing, $b_{ij} = -b_{ji}$. Under a mutation at vertex k the matrix b transforms to b' given by

$$b'_{ij} = \begin{cases} -b_{ij}, & \text{if } k \in \{i,j\}, \\ b_{ij}, & \text{if } b_{ik}b_{kj} \leq 0, \\ b_{ij} + b_{ik}b_{kj}, & \text{if } b_{ik}, b_{kj} > 0, \\ b_{ij} - b_{ik}b_{kj}, & \text{if } b_{ik}, b_{kj} < 0. \end{cases} \tag{2.52}$$

If we start with a quiver with n vertices and associate to each vertex i a variable a_i, we can use the skew-symmetric matrix b to define a mutation relation at the vertex k by

$$a_k a'_k = \prod_{i|b_{ik}>0} a_i^{b_{ik}} + \prod_{i|b_{ik}<0} a_i^{-b_{ik}}, \tag{2.53}$$

with the understanding that an empty product is set to one. The mutation at k changes a_k to a'_k defined by eq. (2.53) and leaves the other cluster variables unchanged.

To illustrate these ideas we note that the initial cluster of the a_2 cluster algebra can be expressed by the quiver $a_1 \to a_2$. Then, a mutation at a_1 replaces it by $a'_1 = \frac{1+a_2}{a_1} \equiv a_3$ and reverses the arrow. A mutation at a_2 replaces it by $a'_2 = \frac{1+a_1}{a_2} \equiv a_5$ and preserves the direction of the arrow.

Cluster Poisson varieties. These are defined using the same combinatorial skeleton: quivers and mutations of quivers. We assign now to the vertices of the quiver variables $\{x_i\}$ which mutate according to the following rule:

$$x'_i = \begin{cases} x_k^{-1}, & i = k, \\ x_i(1 + x_k^{\operatorname{sgn} b_{ik}})^{b_{ik}}, & i \neq k \end{cases}. \tag{2.54}$$

There is a natural Poisson bracket on the cluster $\mathcal{X}$-coordinates. It is enough to define the Poisson bracket between the $\mathcal{X}$-coordinates in a given cluster, for which it is given in terms of the antisymmetric matrix b_{ij} defined in (2.51) by

$$\{x_i, x_j\} = b_{ij} x_i x_j. \tag{2.55}$$

An important property of this Poisson bracket is that it is invariant under mutations, in the sense that

$$\{x'_i, x'_j\} = b'_{ij} x'_i x'_j \tag{2.56}$$

whenever x'_i and b'_{ij} are obtained from x_i and b_{ij} by a mutation.

Given a quiver described by the matrix b, the cluster $\mathcal{A}$- and $\mathcal{X}$-coordinates can be related as follows:

$$x_i = \prod_j a_j^{b_{ij}}. \tag{2.57}$$

This relation is preserved under mutations (changing, of course, the b_{ij}-matrix).

We would like to stress that the cluster $\mathcal{A}$- and $\mathcal{X}$-coordinates live on different spaces of the same dimension, denoted $\mathcal{A}$ and $\mathcal{X}$. Indeed, the they are parametrized by the same set, the set of vertices of the corresponding quiver. Formula (2.57) is just a coordinate way to express a canonical map of spaces $p : \mathcal{A} \to \mathcal{X}$. The dimension of the fibers of this map is the corank of the matrix b.

A sequence of cluster mutations can result in reproducing the original quiver, while providing a non-trivial transformation of the cluster $\mathcal{A}$- and $\mathcal{X}$-coordinates. Such transformations form a group, introduced in [33] under the name *cluster modular group*.

2.6.2 Grassmannian cluster algebras and cluster Poisson spaces $\mathrm{Conf}_n(\mathbb{P}^{k-1})$

In our application we are interested in a special class of cluster algebras called *cluster algebras of geometric type*. They are also described by quivers, but some of the vertices

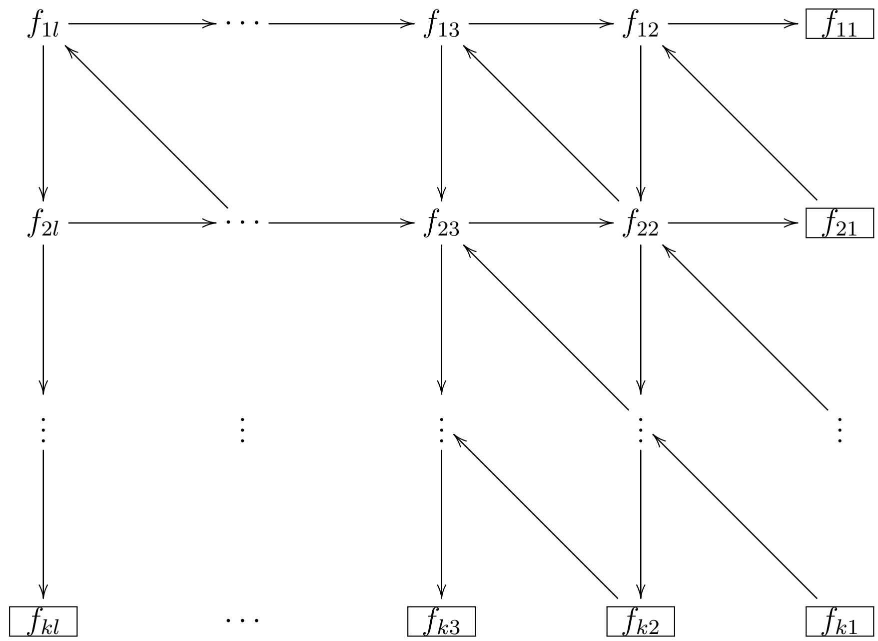

Figure 2.1: The initial quiver for the $\mathrm{Gr}(k,n)$ cluster algebra (see refs. [63, 64]).

are special and called *frozen vertices*. Edges connecting two frozen vertices are not allowed,[6] and we also do not allow mutations on the frozen vertices. The variables associated to the frozen vertices are called *coefficients* instead of *cluster variables* (and the rank of the algebra is equal only to the number of unfrozen vertices). We define the *principal part* of such a quiver to be the quiver obtained by erasing the frozen vertices as well as all edges which connect them to any of the non-frozen vertices. When drawing these special kinds of quivers, we will indicate each frozen node by placing its label inside a box.

We now review the cluster algebras of geometric type which arise from the Grassmannian $\mathrm{Gr}(k,n)$ [62]. The Plücker coordinates $\langle i_1 \dots i_k \rangle$, being the minors obtained by computing the determinant of the indicated columns $i_1 \dots i_k$ of a matrix representative of a point in $\mathrm{Gr}(k,n)$, are examples of $\mathcal{A}$-coordinates.

[6]There is a different approach, advocated in [33], where half-edges between frozen variables not only allowed, but in fact play a crucial role in the amalgamation construction: building bigger cluster structures from the smaller ones.

The Plücker coordinates satisfy the relation

$$\langle i,j,I\rangle\langle k,l,I\rangle = \langle i,k,I\rangle\langle j,l,I\rangle + \langle i,l,I\rangle\langle j,k,I\rangle, \tag{2.58}$$

where I is a multi-index with $k-2$ entries, which bears a resemblance to the exchange relation shown in eq. (2.53). Indeed the cluster algebra for $\mathrm{Gr}(k,n)$ is constructed by starting with an initial cluster whose variables are certain Plücker coordinates. The operation of mutation generates additional Plücker coordinates, as well as other, more complicated, cluster $\mathcal{A}$-coordinates. For general k and n and with $l = n-k$, the appropriate initial quiver is given in ref. [63] (this construction is also reviewed in ref. [64]) and shown in fig. 2.1, where

$$f_{ij} = \begin{cases} \frac{\langle i+1,\ldots,k,k+j,\ldots,i+j+k-1\rangle}{\langle 1,\ldots,k\rangle}, & i \le l-j+1, \\ \frac{\langle 1,\ldots,i+j-l-1,i+1,\ldots,k,k+j,\ldots,n\rangle}{\langle 1,\ldots,k\rangle}, & i > l-j+1 \end{cases}. \tag{2.59}$$

The boxes identify the frozen variables while the rest of the variables are unfrozen.

In order to obtain the quivers we will use below we need to make one last change to the quiver above. We rescale all the coordinates, frozen and unfrozen, by $\langle 1,\ldots,k\rangle$. This produces a frozen variable $\langle 1,\ldots,k\rangle$ which connects to the node labeled by f_{1l} by an ingoing arrow. After this modification all the unfrozen vertices of the initial quiver have an equal number of ingoing and outgoing arrows.

The simplest nontrivial example is that of $\mathrm{Gr}(2,5)$, which is relevant for configurations of five points in $\mathbb{P}^1$. In this case the initial quiver is simply

$$\begin{tikzcd} \boxed{\langle 12\rangle} \arrow[dr] & & & \\ & \langle 13\rangle \arrow[r] \arrow[d] & \langle 14\rangle \arrow[r] \arrow[d] & \boxed{\langle 15\rangle} \\ & \boxed{\langle 23\rangle} & \boxed{\langle 34\rangle} \arrow[ul] & \boxed{\langle 45\rangle} \arrow[ul] \end{tikzcd} \tag{2.60}$$

where each node is labeled by its $\mathcal{A}$-coordinate. In this case it is easy to check that successive mutations on the two unfrozen vertices, in any order, generate only five distinct quivers. The algebra so generated is nothing but the A_2 algebra defined at the beginning of sec. 2.6.1. The name of the algebra comes from the fact that the principal part of this initial quiver is the same as the Dynkin diagram of the A_2 Lie algebra.

Let us use this example to calculate $\mathcal{X}$-coordinates. There is one such coordinate associated to each unfrozen node k, expressed by taking the product of the $\mathcal{A}$-coordinates on the nodes connected to k by an incoming arrow, divided by the product of the $\mathcal{A}$-coordinates on the nodes connected to k by an outgoing arrow. So in the A_2 quiver shown above the $\mathcal{X}$-coordinates associated to the nodes $\langle 13\rangle$ and $\langle 14\rangle$ are $\langle 12\rangle\langle 34\rangle/\langle 23\rangle\langle 14\rangle$ and $\langle 13\rangle\langle 45\rangle/\langle 34\rangle\langle 15\rangle$ respectively. Cluster $\mathcal{A}$-coordinates are not invariant under rescaling of the individual vectors in a $\mathrm{Gr}(k,n)$ matrix, but the $\mathcal{X}$-coordinates are. Therefore only the latter are good coordinates on the quotient $\mathrm{Gr}(k,n)/(\mathbb{C}^*)^{n-1} = \mathrm{Conf}_n(\mathbb{P}^{k-1})$ and are hence appropriate objects to appear in motivic amplitudes.

To connect with the general cluster Poisson varieties and $\mathcal{X}$-coordinates, in this example we use only the unfrozen part of the quiver to build them. This leads to a reduced cluster $\mathcal{X}$-space $\mathcal{X}'$, and the map described coordinately in (2.57) reduces to a surjective map $p' : \mathcal{A} \to \mathcal{X}'$. It describes the projection $\widetilde{\mathrm{Gr}}(k,n) \to \mathrm{Conf}_n(\mathbb{P}^{k-1})$.

The two simplest examples relevant to SYM theory scattering amplitudes are those for 6 or 7 points in $\mathbb{P}^3$ (or, equivalently, in $\mathbb{P}^1$ or $\mathbb{P}^2$, respectively). For the former it is evident from fig. 2.1 that the principal part of the quiver is the same as the A_3 Dynkin diagram. For the latter the initial quiver is slightly more complicated:

$$\begin{tikzcd}
\boxed{\langle 167\rangle} \arrow[dr] & & & & \\
& \langle 267\rangle \arrow[r] \arrow[d] & \langle 367\rangle \arrow[r] \arrow[d] & \langle 467\rangle \arrow[r] \arrow[d] & \boxed{\langle 567\rangle} \\
& \langle 126\rangle \arrow[r] \arrow[d] & \langle 236\rangle \arrow[r] \arrow[d] \arrow[ul] & \langle 346\rangle \arrow[r] \arrow[d] \arrow[ul] & \boxed{\langle 456\rangle} \arrow[ul] \\
& \boxed{\langle 127\rangle} & \boxed{\langle 123\rangle} \arrow[ul] & \boxed{\langle 234\rangle} \arrow[ul] & \boxed{\langle 345\rangle} \arrow[ul]
\end{tikzcd} \quad . \tag{2.61}$$

If we label the vertices occupied initially by $\langle 267\rangle$, $\langle 367\rangle$, $\langle 467\rangle$, $\langle 126\rangle$, $\langle 236\rangle$, $\langle 346\rangle$ by numbers 1 through 6, then after a sequence of mutations at vertices 4, 3, 2, 5, 1, 4, 3, 4, 6, the principal part of the quiver is brought into the form of the E_6 Dynkin diagram[7]

$$\begin{tikzcd}
& & \langle 256\rangle \arrow[d] & & \\
\langle 124\rangle & \langle 247\rangle \arrow[l] \arrow[r] & \langle 5{\times}6,7{\times}2,3{\times}4\rangle & \langle 3{\times}4,5{\times}6,7{\times}1\rangle \arrow[l] \arrow[r] & \langle 157\rangle
\end{tikzcd} \quad . \tag{2.62}$$

Therefore the $\mathrm{Gr}(3,7)$ cluster algebra is also called the E_6 algebra.

In [35] Fomin and Zelevinsky showed that a cluster algebra is of finite type (i.e., it has a finite number of cluster variables) if there exists a sequence of mutations which turns the principal part of its quiver into the Dynkin diagram of some classical Lie algebra. However, if the principal part of the quiver contains a subgraph which is an affine Dynkin diagram, then the cluster algebra is of infinite type.

In ref. [62], Scott classified all the Grassmannian cluster algebras of finite type. As discussed in sec. 2.2, the relevant Grassmannian for scattering amplitudes in SYM

[7]If we order them in the same way as in the initial cluster, the $\mathcal{A}$-coordinates after this sequence of mutations are $\langle 3\times 4, 5\times 6, 7\times 1\rangle$, $\langle 256\rangle$, $\langle 124\rangle$, $\langle 247\rangle$, $\langle 5\times 6, 7\times 2, 3\times 4\rangle$, $\langle 157\rangle$.

theory is $\mathrm{Gr}(4,n)$, for $n \geq 6$. If $n = 6$ we need $\mathrm{Gr}(4,6) = \mathrm{Gr}(2,6)$ which is of finite type A_3. If $n = 7$ we need $\mathrm{Gr}(4,7) = \mathrm{Gr}(3,7)$ which is again of finite type E_6. However, starting at $n = 8$ the relevant cluster algebras are not of finite type anymore. This indicates that there are infinitely many different $\mathcal{A}$-coordinates which could appear in the symbol of these amplitudes, and infinitely many different $\mathcal{X}$-coordinates could appear in their coproduct.

Besides the usual Plücker determinants, mutations also lead in general to more complicated $\mathcal{A}$-coordinates. For example, with $\mathrm{Gr}(4,8)$ one runs in to

$$\langle 12(345) \cap (678) \rangle \equiv \langle 1345 \rangle \langle 2678 \rangle - \langle 2345 \rangle \langle 1678 \rangle. \tag{2.63}$$

As discussed in sec. 2.2, the notation with $\cap$ emphasizes the following geometrical fact: the composite bracket $\langle 12(345) \cap (678) \rangle$ vanishes whenever the points 1 and 2 are coplanar with the projective line $(345) \cap (678)$ obtained by intersecting the two projective planes (345) and (678).

One miraculous feature of the mutations is that the denominator can always be canceled by the numerator, after using Plücker identities. Therefore, the $\mathcal{A}$-coordinates always end up being *polynomials* in the Plücker coordinates. This is an analog of the Laurent phenomenon mentioned above. An example which appears for $\mathrm{Gr}(4,8)$ is

$$\frac{\langle 1237 \rangle \langle 1245 \rangle \langle 1678 \rangle + \langle 1278 \rangle \langle 45(671) \cap (123) \rangle}{\langle 1267 \rangle} = \langle 45(781) \cap (123) \rangle. \tag{2.64}$$

Here the left-hand side is the raw expression obtained for a certain $\mathcal{A}$-coordinate following some mutation, while the right-hand side is a simplified expression where the denominator has been canceled by applying a Plücker relation to the numerator in order to pull out all overall factor of $\langle 1267 \rangle$.

Both of these types of non-Plücker $\mathcal{A}$-coordinates, eqs. (2.64) and (2.63), appear in the symbol of the two-loop $n = 8$ MHV amplitude [20], and the simpler ones of the type in eq. (2.64) appear already for $n = 7$—indeed the long formulas in section 2.5 are littered with these composite brackets (though expressed there in the $\mathbb{P}^2$ language).

However, since the number of $\mathcal{A}$-coordinates is infinite for $\mathrm{Gr}(4, 8)$, mutations must eventually generate even more exotic $\mathcal{A}$-coordinates. A still relatively simple example is

$$-\langle(123) \cap (345), (567) \cap (781)\rangle. \tag{2.65}$$

This quantity vanishes when the lines $(123)\cap(345)$ and $(567)\cap(781)$ intersect, which is equivalent to saying that the lines $(345) \cap (567)$ and $(781) \cap (123)$ intersect. But there are even more complicated $\mathcal{A}$-coordinates such as

$$\begin{aligned}\langle 1246\rangle\langle 1256\rangle\langle 1378\rangle\langle 3457\rangle - \langle 1246\rangle\langle 1257\rangle\langle 1378\rangle\langle 3456\rangle -\\ \langle 1246\rangle\langle 1278\rangle\langle 1356\rangle\langle 3457\rangle + \langle 1278\rangle\langle 1257\rangle\langle 1346\rangle\langle 3456\rangle +\\ \langle 1236\rangle\langle 1278\rangle\langle 1457\rangle\langle 3456\rangle.\end{aligned} \tag{2.66}$$

Neither of these complicated quantities appears as an entry in the symbol of the $n = 8$ MHV amplitude at two loops, but we know of no reason why they can not appear at higher loops. However, it is obvious that only a finite subset of them can appear at any given order in perturbation theory. It would be extremely interesting to understand more about these algebras and their relation to amplitudes.

One final, important comment has to do with cyclic symmetry, which is an exact symmetry of MHV amplitudes (and of all super-amplitudes). Notice that the initial quivers we have been using break the cyclic symmetry of the configuration of points. In order to see that the cyclic symmetry is preserved we need to show that by mutations one can reach another quiver whose labels are permuted by one unit. For the case of $\mathrm{Gr}(3, 7)$ described above, this can not be done in fewer than six mutations, since all the unfrozen $\mathcal{A}$-coordinates need to change. Indeed one can easily show that after mutating in the vertices which are initially labeled by $\langle 126\rangle$, $\langle 267\rangle$, $\langle 236\rangle$, $\langle 367\rangle$, $\langle 346\rangle$ and $\langle 467\rangle$, we obtain the cluster with the vertex labels shifted by one $\langle 123\rangle \to \langle 234\rangle$, etc. This proves the cyclic symmetry for $\mathrm{Gr}(3,7)$. It is not hard to imagine that a similar procedure can be applied in the general $\mathrm{Gr}(k,n)$ case, but we do not provide a complete proof of cyclic symmetry here.

2.6.3 Generalized Stasheff polytopes

In this section we review the connection [41] between cluster algebras and certain polytopes, including the generalized Stasheff polytope or associahedron [42]. Many additional details and examples may also be found in [65].

The unfrozen vertices of a cluster algebra of rank r can be taken to be the vertices of an $r-1$-simplex. A k-simplex is a generalization of the notion of a triangle and can be defined as a convex hull of its $k+1$ vertices. A 0-simplex is a point, a 1-simplex is a line, a 2-simplex is a triangle, a 3-simplex is a tetrahedron, and so on.

If we take a subset of $l+1$ vertices of the $k+1$ vertices of a k-simplex we can form an l-simplex which is called a *face* of the k-simplex. The number of l-faces of a k-simplex is $\binom{k+1}{l+1}$.

When doing a mutation in a cluster algebra of rank r, one of the $\mathcal{A}$-coordinates changes while the other $r-1$ stay unchanged. They define an $r-2$-face of the initial $r-1$-simplex. Therefore, after mutation we obtain a new $r-1$-simplex which shares a $r-2$-face with the initial simplex. We can glue them along this face to form an $r-1$-dimensional polytope. For cluster algebras of finite type, by doing all possible mutations, we can build a polytope out of finitely many simplices.

In this language, the $\mathcal{X}$-coordinates of the cluster algebra correspond to $r-2$-faces of the $r-1$-simplex. The number of such faces is $\binom{r}{r-1} = r$, which equal to the rank of the algebra. Under mutations, one of the $\mathcal{X}$-coordinates transforms to its inverse while the others transform in a more complicated way. So more properly we should associate to each $r-2$-face the pair consisting of an $\mathcal{X}$-coordinate and its inverse.

The dual of the polytope we have described is called the Stasheff polytope (or associahedron, for a reason we will describe in the following section) associated to the cluster algebra. It is a theorem which is deduced from [34], that for any cluster algebras, the faces are always either quadrilaterals or pentagons. For example, the Stasheff polytope associated to $\mathrm{Gr}(2,6)$ has 3 quadrilateral faces and 6 pentagonal faces, while the $\mathrm{Gr}(3,7)$ polytope has 1785 quadrilaterals and 1071 pentagons.

2.6.4 Poisson bracket and generalized Stasheff polytopes

There is a simple connection between the Poisson bracket and the geometry of the Stasheff polytope, which plays an important role in elucidating the structure of motivic amplitudes.

Two $\mathcal{X}$-coordinates x_1, x_2 have zero Poisson bracket if the Stasheff polytope has some quadrilateral face containing both x_1 and x_2 at each vertex in the configuration

$$\begin{array}{ccc} \boxed{\{x_1, x_2, \ldots\}} & \text{———} & \boxed{\{1/x_1, x_2, \ldots\}} \\ | & & | \\ \boxed{\{x_1, 1/x_2, \ldots\}} & \text{———} & \boxed{\{1/x_1, 1/x_2, \ldots\}} \end{array}, \tag{2.67}$$

where the dots stand for other $\mathcal{X}$-coordinates (some of which may overlap between some, but not all, of the four corners). In such a case the variables x_1, x_2 form a closed $A_1 \times A_1$ subalgebra. Moving left-to-right or up-to-down is accomplished by mutating on x_1 or x_2, respectively.

Two $\mathcal{X}$-coordinates x_1, x_2 have Poisson bracket ± 1 if they form a closed A_2 subalgebra. In this case the Stasheff polytope has some pentagonal face containing x_1

and x_2 in the configuration

$$
\begin{tikzcd}[arrows=dash]
 & \boxed{\{x_1 + x_2 + x_1 x_2, \ldots\}} \arrow[dl] \arrow[dr] & \\
\boxed{\{x_2(1+x_1)/x_1, \ldots\}} \arrow[d] & & \boxed{\{x_1(1+x_2)/x_2, \ldots\}} \arrow[d] \\
\boxed{\{x_1, \ldots\}} \arrow[rr] & & \boxed{\{x_2, \ldots\}}
\end{tikzcd}
. \tag{2.68}
$$

2.6.5 Parity invariance

In this section we show that the parity operation is an element of the cluster modular group. Specifically, we verify that the parity transform of any quiver is related by a sequence of mutations to the original quiver. This implies that the set of cluster $\mathcal{X}$-coordinates is closed under parity. It would be very interesting to see if the rest of the cluster modular group plays some role, or has a nice interpretation when acting on motivic amplitudes.

Of course, in simple cases like six points in $\mathbb{P}^3$ the parity invariance of the set of cluster $\mathcal{X}$-coordinates can be explicitly checked by enumerating all of them. However, due to the large number of cluster coordinates, this is much more difficult for seven points and it is impossible for more than seven points since then the cluster algebras are of infinite type.

For six points in $\mathbb{P}^3$ the initial quiver is shown in fig. 2.2a. The parity conjugate is obtained by replacing $\langle ijkl\rangle \to [ijkl]$, and then rewriting the $[ijkl]$ in terms of angle brackets as follows

$$
\begin{aligned}
[1235] &= \langle 6123\rangle\langle 1234\rangle\langle 2456\rangle, \qquad & [1245] &= \langle 6123\rangle\langle 3456\rangle\langle 1245\rangle, \\
[1345] &= \langle 2345\rangle\langle 3456\rangle\langle 6124\rangle, \qquad & [1234] &= \langle 6123\rangle\langle 1234\rangle\langle 2345\rangle,
\end{aligned}
$$
$$
\text{cyclic permutations of } [1234].
$$

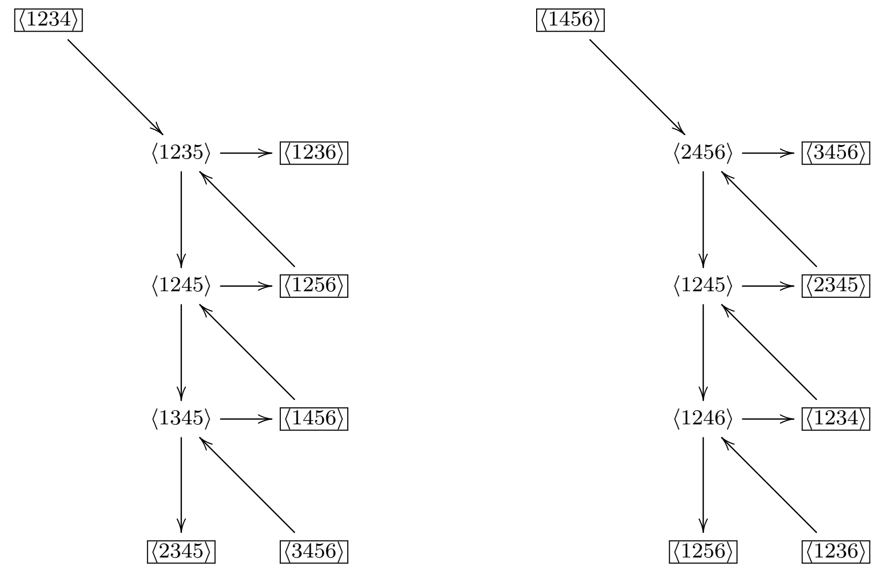

(a) (b)

Figure 2.2: The initial quiver (a) for $\mathrm{Gr}(4,6)$ and its parity conjugate (b).

The $\mathcal{X}$-coordinates of the quiver in fig. 2.2b generate parity conjugates of the $\mathcal{X}$-coordinates of the quiver in fig. 2.2a. This quiver can be obtained from the initial quiver by mutations, but with opposite directions of the arrows. Switching the direction of all arrows replaces all the cross-ratios by their inverses. This does not change the set of cluster coordinates since if a cross-ratio is a cluster $\mathcal{X}$-coordinate then its inverse is also a cluster $\mathcal{X}$-coordinate.

We should note here that the parity transformation is, up to signs, the same as shifting all the points by three. For example, $\langle 1234\rangle \to \langle 1456\rangle$, $\langle 1235\rangle \to \langle 2456\rangle$.

The seven-point case is a bit more complicated. Here also we start with the initial quiver in fig. 2.3a to which we apply parity $\langle ijkl\rangle \to [ijkl]$. Let us focus on the $\mathcal{X}$-coordinate sitting at the vertex labeled by $\langle 1235\rangle$ in fig. 2.3a. It is given by $\frac{\langle 1234\rangle\langle 1256\rangle}{\langle 1236\rangle\langle 1245\rangle}$.

Using equations similar to the ones we used above for six points, we can write the

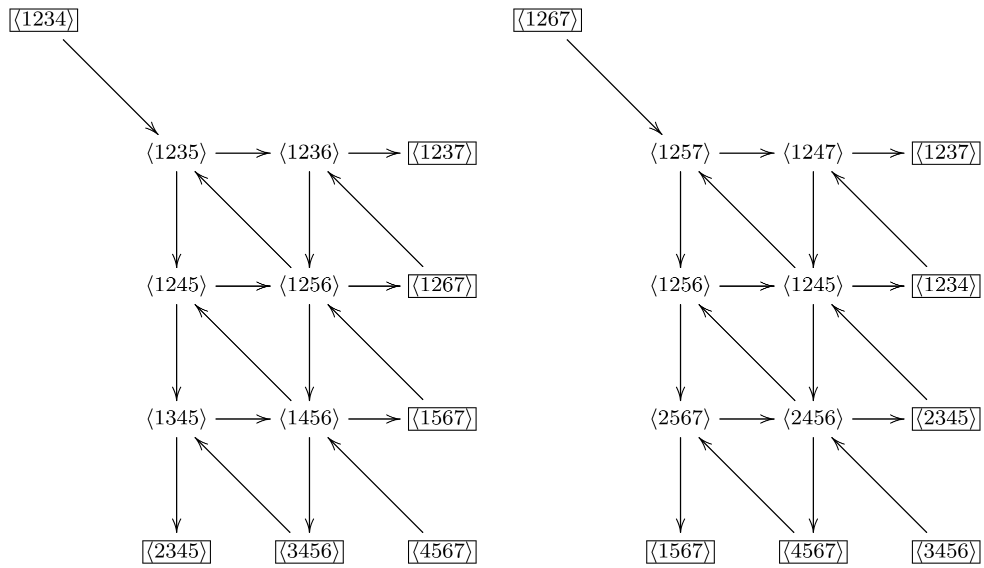

(a) (b)

Figure 2.3: The initial quiver (a) for Gr$(4,7)$ and its partner (b) which makes the parity conjugation property manifest.

parity conjugate of the quiver $\mathcal{X}$-coordinate at vertex $\langle 1235\rangle$ as

$$\frac{\langle 1234\rangle\langle 1256\rangle}{\langle 1236\rangle\langle 1245\rangle} \to \frac{[1234][1256]}{[1236][1245]} = \frac{\langle 1256\rangle\langle 2345\rangle\langle 4567\rangle}{\langle 1245\rangle\langle 2567\rangle\langle 3456\rangle}. \tag{2.69}$$

The parity conjugated cross-ratio is the same as the inverse cross-ratio sitting at the opposite corner, at $\langle 2456\rangle$ in the partner quiver in fig. 2.3b. Each of the unfrozen variables has a correspondent among the unfrozen variables of the partner quiver. The $\mathcal{X}$-coordinates of vertices which are in correspondence are inverse and parity conjugate to one another. The correspondence between vertices is defined as follows: the unfrozen vertices fit in a rectangular pattern. Flip this rectangular pattern along the vertical and the horizontal. After these flips the pattern of unfrozen vertices fits over the pattern of unfrozen vertices of the partner quiver (note that after superposition all the arrows point in the opposite directions after this sequence of operations). For example, the correspondence between the vertices in figs. 2.3a, 2.3b is the following: $\langle 1235\rangle \leftrightarrow \langle 2456\rangle$, $\langle 1245\rangle \leftrightarrow \langle 1245\rangle$, $\langle 1256\rangle \leftrightarrow \langle 1256\rangle$, $\langle 1236\rangle \leftrightarrow \langle 2567\rangle$,

$\langle 1345\rangle \leftrightarrow \langle 1247\rangle$, $\langle 1456\rangle \leftrightarrow \langle 1257\rangle$.

Now we can show that the set of cluster $\mathcal{X}$-coordinates is closed under parity conjugation. First, it is easy to show that the quiver in fig. 2.3b can be obtained from the quiver in fig. 2.3a after four mutations. Another way to show that the two quivers can be obtained from one another by mutations is to notice that the quiver in fig. 2.3a can be transformed to the quiver in fig. 2.3b by a dihedral transformation of external data $1 \leftrightarrow 2$, $3 \leftrightarrow 7$, $4 \leftrightarrow 6$. Then the conclusion follows from the dihedral symmetry of the cluster algebra. So they generate the same cluster algebra. Moreover, for every sequence of mutations in the quiver in fig. 2.3a, we can perform the same sequence of mutations in the corresponding vertices of the partner quiver in fig. 2.3b and we obtain the inverses of parity conjugate $\mathcal{X}$-coordinates. This analysis can be extended without difficulty to the general case of cluster algebras $G(4, n)$.

2.6.6 Cluster algebras and the positive Grassmannian

The positive Grassmannian is defined as the subspace of the real Grassmannian for which the ordered Plücker coordinates are all positive:

$$\mathrm{Gr}^{+}(k, n) = \{(c_1 \cdots c_n) \in \mathrm{Gr}(k, n, \mathbb{R}) : \langle c_{a_1} \cdots c_{a_k}\rangle > 0 \text{ whenever } a_1 < \cdots < a_k\}.$$

The mutation relation (2.53) clearly respects positivity: if the $\mathcal{A}$-coordinates in the initial cluster are all chosen to be positive, then all subsequently generated $\mathcal{A}$-coordinates, in every cluster, will continue to be positive. The same trivially holds for $\mathcal{X}$-coordinates since they are just products of $\mathcal{A}$-coordinates.

It is manifest that set of positive configurations of points on $\mathbb{P}^3$ constitutes a subspace of what physicists call the Euclidean region, in which scattering amplitudes are expected to be smooth, real-valued functions. This is in strong accord with the main slogan of [40], though we are talking here about positivity in the external kinematic data, rather than in the Grassmannian of internal (i.e., loop integration) variables. It seems clear that the full power of positivity has not yet been unleashed.

By construction, any cluster $\mathcal{X}$-coordinate x has the property that $1 + x$ factors into a product of $\mathcal{A}$-coordinates. We have found empirically that positivity allows for a quick criterion to go the other way around: suppose we have identified some cross-ratio r for which $1 + r$ so factors; how do we determine whether or not r is a cluster $\mathcal{X}$-coordinate? The answer is simply to evaluate the triple

$$\{r, -1 - r, -1 - 1/r\} \tag{2.70}$$

at a random point in the positive Grassmannian. In all of our experience to date, one of these three quantities will be positive and the other two negative; the positive one is an $\mathcal{X}$-coordinate and the other two are not. Certainly this criterion is valid for $n = 6, 7$ where we can enumerate all such possibilities, and it has held true at higher n in all cases we have looked at. However in the infinite-dimensional algebras we can not exclude the possibility that there might exist some sufficiently complicated cross-ratio r for which $1 + r$ factorizes, yet no member of the above list is an $\mathcal{X}$-coordinate. Let us note also that for a given cross-ratio r, different elements of the above list may be $\mathcal{X}$-coordinates with respect to different orderings of the external points.

2.7 Cluster Coordinates and Motivic Analysis for $n = 6, 7$

We now have built up all of the machinery we need in order to carry out a full motivic analysis of the two-loop $n = 6, 7$ MHV amplitudes. To that end we begin this section with a detailed discussion of the cluster coordinates and Stasheff polytopes for $\mathrm{Gr}(2, 6)$ and $\mathrm{Gr}(3, 7)$.

2.7.1 Clusters and coordinates for $\mathrm{Gr}(2,6)$

Beginning with the initial quiver for $\mathrm{Gr}(2,6)$, we can generate all of the clusters and their $\mathcal{A}$- and $\mathcal{X}$-coordinates by successively mutating at various vertices. The A_3 cluster algebra generated in this manner has a total of 15 $\mathcal{A}$-coordinates, which are the standard Plücker coordinates $\langle ij\rangle$ on $\mathrm{Gr}(2,6)$. The six coordinates with i and j adjacent (mod 6) are frozen, while the remaining nine are unfrozen.

However, in the special case of $\mathrm{Gr}(2,n)$ cluster algebras the mutations can also be given a simple geometric interpretation which we now describe. The discussion in this section follows ref. [33].

We start with a configuration of n points in $\mathbb{P}^1$ with coordinates z_i, $i = 1,\dots,n$ and we fix a cyclic ordering. To these points we associate a convex polygon, with each vertex of the polygon labeled by one coordinate z_i. Then, consider a complete triangulation T of this polygon, as in fig. 2.4.

A triangulation T and a diagonal E of that triangulation uniquely determine a quadrilateral for which E is a diagonal. The points in $\mathbb{P}^1$ corresponding to the vertices of this quadrilateral have a cross-ratio in $\mathbb{P}^1$. For example, to the diagonal E in fig. 2.4 we associate the cross-ratio

$$r(3,5,1,2) = r(1,2,3,5) \equiv \frac{(z_1-z_2)(z_3-z_5)}{(z_2-z_3)(z_1-z_5)}. \tag{2.71}$$

Note that the vertices of the quadrilateral are read in the same order as the cyclic order of the n points, starting at one of the points incident with the diagonal E. Note that it doesn't matter which of the two points incident with E we start with, due to the identity

$$r(k,l,i,j) = r(i,j,k,l). \tag{2.72}$$

Moreover, if we read the list of vertices in the opposite order, we obtain the inverse

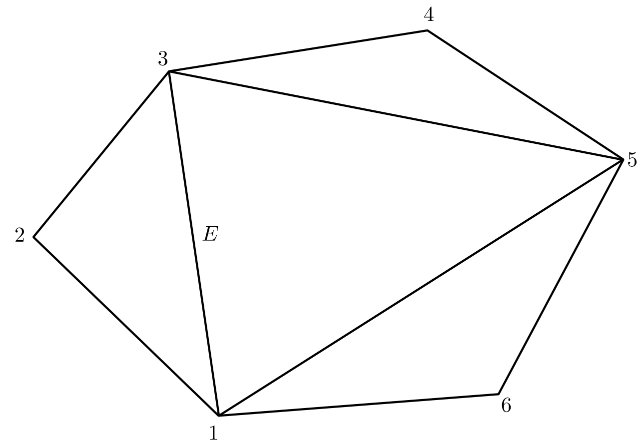

Figure 2.4: A triangulation T of the hexagon. One of the edges of the triangulation is marked by E.

cross-ratio since

$$r(i,l,k,j) = \frac{1}{r(i,j,k,l)}. \tag{2.73}$$

Now we introduce a function b which associates to a pair of diagonals in a triangulation a number which is 0 or ± 1. Two diagonals in a triangulation are called adjacent if they are the sides of one of the triangles of the triangulation. If two diagonals E and F are not adjacent we set $b_{EF} = 0$. If E and F are adjacent we set $b_{EF} = 1$ if E comes before F when listing the diagonals at $E \cap F$ in anticlockwise order. Otherwise we set $b_{EF} = -1$.

Now we can define cluster transformations (or mutations). The starting point is a triangulation, to which we can associate a set of cross-ratios, as described above (one cross-ratio for each diagonal). A cluster transformation is obtained by picking one of the diagonals and replacing it with the other diagonal in the same quadrilateral. A sequence of such mutations is represented in fig. 2.5, where after five steps we reach the original configuration.

It is not hard to show that the effect of a mutation on the diagonal labeled by k

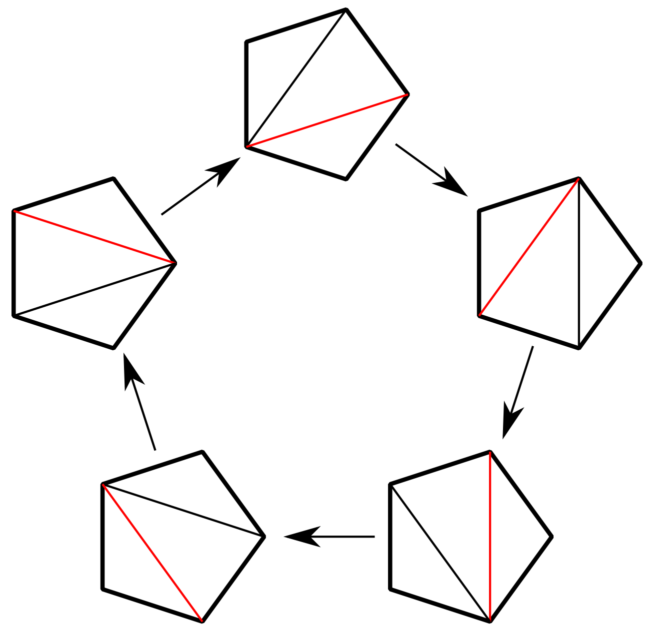

Figure 2.5: A sequence of mutations for five points. At each step the side colored in red gets flipped.

on the cross-ratios X_j corresponding to the other diagonals is given by

$$X_i' = \mu_k X_i = \begin{cases} X_k^{-1}, & i = k, \\ X_i(1 + X_k^{\mathrm{sgn}(b_{ik})})^{b_{ik}}, & i \neq k. \end{cases} \tag{2.74}$$

This is the same as eq. (2.54). As we noted before, flipping the diagonal produces the inverse of the initial cross-ratio. The mutation in eq. (2.74) reproduces this. Also, the cross-ratios corresponding to diagonals non-adjacent to the diagonal being flipped remain unchanged. This is obvious since in this case $b_{ik} = 0$.

Now let us specialize to the case $n = 6$ of interest. A hexagon admits 14 distinct complete triangulations, each having three diagonals. These correspond to the 14 different clusters, each with three $\mathcal{X}$ coordinates. Out of these 42 are 15 distinct coordinates (as mentioned before we never count both x and $1/x$ separately). Nine of these ratios were already displayed in eq. (2.22); the remaining six have not been given a name in previous literature on $n = 6$ scattering amplitudes since they do not appear in the two-loop answer. For completeness let us list here all 15 $\mathcal{X}$-coordinates

$$\begin{aligned}
v_1 &= r(3,5,6,2), & v_2 &= r(1,3,4,6), & v_3 &= r(5,1,2,4), \\
x_1^+ &= r(2,3,4,1), & x_2^+ &= r(6,1,2,5), & x_3^+ &= r(4,5,6,3), \\
x_1^- &= r(1,4,5,6), & x_2^- &= r(5,2,3,4), & x_3^- &= r(3,6,1,2), \\
e_1 &= r(1,2,3,5), & e_2 &= r(2,3,4,6), & e_3 &= r(3,4,5,1), \\
e_4 &= r(4,5,6,2), & e_5 &= r(5,6,1,3), & e_6 &= r(6,1,2,4),
\end{aligned} \tag{2.75}$$

in terms of the $\mathbb{P}^1$ cross-ratio defined in eq. (2.23).

Out of the 45 possible cross-ratios of the form $r(i,j,k,l)$, the 15 $\mathcal{X}$-coordinates are special in that they are precisely those in which the points i,j,k,l come in cyclic order. The three most well-known cross-ratios which are *not* cluster $\mathcal{X}$-coordinates are the ones known in the literature as

$$u_1 = -r(3,6,5,2), \qquad u_2 = -r(1,4,3,6), \qquad u_3 = -r(5,2,1,4). \tag{2.76}$$

These are related to cluster $\mathcal{X}$-coordinates by $u_i = 1/(1+v_i)$.

2.7.2 The generalized Stasheff polytope for $\mathrm{Gr}(2,6)$

Let us now discuss the geometry of the Stasheff polytope for the A_3 cluster algebra detailed in the previous section. In this case each cluster is in correspondence with a 2-simplex, or a triangle. There are 14 clusters, to each of which corresponds a triangle. We can label each triangle by the three $\mathcal{A}$-coordinates which appear on its

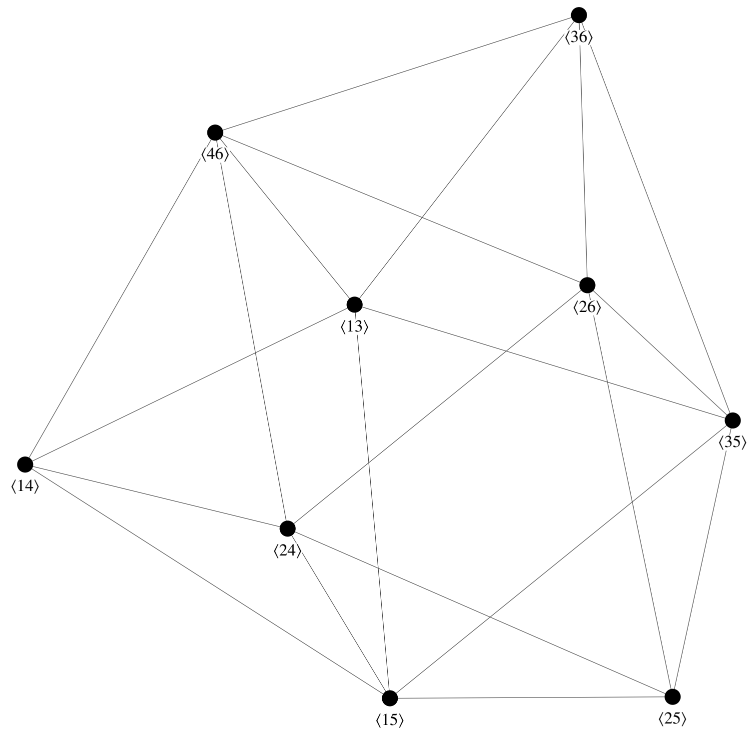

Figure 2.6: The polytope obtained by gluing together the triangles associated to clusters of the $\mathrm{Gr}(2,6)$ (i.e., A_3) cluster algebra.

vertices:

$$\begin{array}{llll}
\langle 13\rangle, \langle 14\rangle, \langle 15\rangle, & \langle 14\rangle, \langle 15\rangle, \langle 24\rangle, & \langle 13\rangle, \langle 15\rangle, \langle 35\rangle, & \langle 13\rangle, \langle 14\rangle, \langle 46\rangle, \\
\langle 15\rangle, \langle 24\rangle, \langle 25\rangle, & \langle 14\rangle, \langle 24\rangle, \langle 46\rangle, & \langle 15\rangle, \langle 25\rangle, \langle 35\rangle, & \langle 13\rangle, \langle 35\rangle, \langle 36\rangle, \\
\langle 13\rangle, \langle 36\rangle, \langle 46\rangle, & \langle 24\rangle, \langle 25\rangle, \langle 26\rangle, & \langle 24\rangle, \langle 26\rangle, \langle 46\rangle, & \langle 25\rangle, \langle 26\rangle, \langle 35\rangle, \\
\langle 26\rangle, \langle 35\rangle, \langle 36\rangle, & \langle 26\rangle, \langle 36\rangle, \langle 46\rangle. & &
\end{array} \tag{2.77}$$

These triangles fit together in a polytope with 14 triangular faces, shown in fig. 2.6. The polytope has 9 vertices given by the non-frozen $\mathcal{A}$-coordinates $\langle 13\rangle$, $\langle 14\rangle$, $\langle 15\rangle$, $\langle 24\rangle$, $\langle 25\rangle$, $\langle 26\rangle$, $\langle 35\rangle$, $\langle 36\rangle$ and $\langle 46\rangle$, and 21 edges.

All faces are triangles, but there are two different types of vertices: $\langle 14\rangle$, $\langle 25\rangle$ and $\langle 36\rangle$ have valence four (they are incident with four edges) while the other six vertices have valence five. The polytope has the topology of a sphere as can be confirmed by computing the Euler characteristic $\chi = V - E + F = 9 - 21 + 14 = 2$.

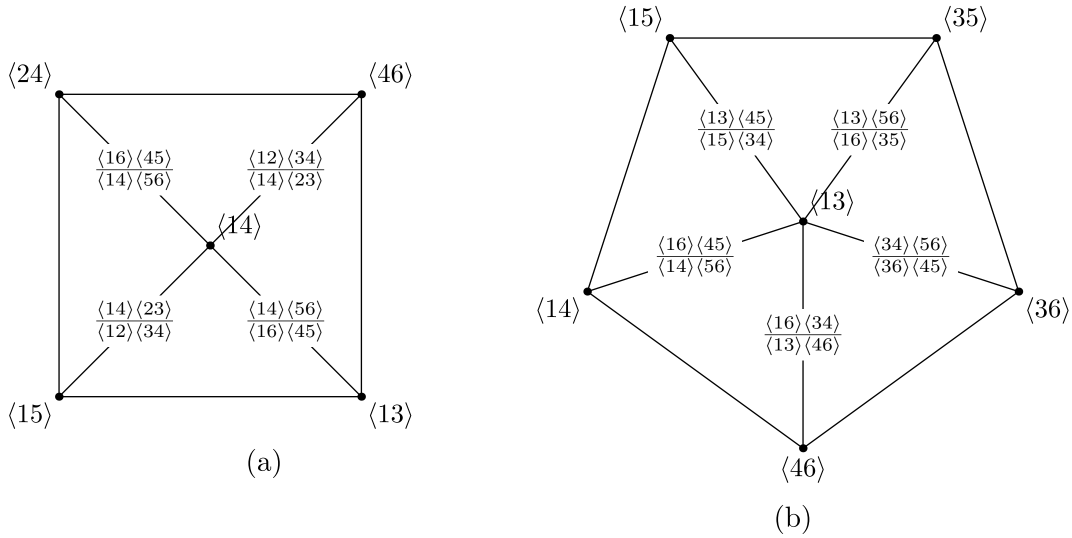

Figure 2.7: The cross-ratios ($\mathcal{X}$-coordinates) around a valence 4 vertex (a) and a valence 5 vertex (b) of the polytope (fig. 2.6) associated to the $\mathrm{Gr}(2,6)$ cluster algebra. For clarity we have omitted the crucial overall minus sign in front of each $\mathcal{X}$-coordinate.

Now recall that to each edge of the polytope we can associate a pair consisting of an $\mathcal{X}$-coordinate and its inverse. Let us take a closer look at the $\mathcal{X}$-coordinates corresponding to the edges incident on the two kinds of vertices. In order for the association between $\mathcal{X}$-coordinates and edges to be one-to-one, we need to pick an orientation. Consider for example the valence 4 vertex shown in fig. (2.7a). As we go around it we encounter the cross-ratios

$$\frac{\langle 14\rangle\langle 23\rangle}{\langle 12\rangle\langle 34\rangle}, \qquad \frac{\langle 14\rangle\langle 56\rangle}{\langle 16\rangle\langle 45\rangle}, \qquad \frac{\langle 12\rangle\langle 34\rangle}{\langle 14\rangle\langle 23\rangle}, \qquad \frac{\langle 16\rangle\langle 45\rangle}{\langle 14\rangle\langle 56\rangle}. \tag{2.78}$$

The third cross-ratio is an inverse of the first while the fourth is an inverse of the second. Therefore, the cluster coordinates are the same as for the $A_1 \times A_1$ cluster algebra. This is the dual of the statement shown in eq. (2.67).

On the other hand, if we consider for example the valence 5 vertex shown in fig. 2.7b, the corresponding list of cross-ratios is

$$\frac{\langle 13\rangle\langle 45\rangle}{\langle 15\rangle\langle 34\rangle}, \qquad \frac{\langle 13\rangle\langle 56\rangle}{\langle 16\rangle\langle 35\rangle}, \qquad \frac{\langle 34\rangle\langle 56\rangle}{\langle 36\rangle\langle 45\rangle}, \qquad \frac{\langle 16\rangle\langle 34\rangle}{\langle 13\rangle\langle 46\rangle}, \qquad \frac{\langle 16\rangle\langle 45\rangle}{\langle 14\rangle\langle 56\rangle}. \tag{2.79}$$

These are the $\mathcal{X}$-coordinates of an A_2 cluster algebra. It can be checked that these are precisely the arguments of dilogarithms in the five-term dilogarithm identity (2.41). This is the dual of the statement shown in eq. (2.68).

The dual polytope, shown in fig. 2.8, has 14 vertices and 9 faces, three of which are quadrilaterals and six of which are pentagons. This is the Stasheff polytope or the K_5 associahedron. The name associahedron comes from the following construction: consider n (in the case of K_5 we take $n = 5$) non-commutative variables and all the ways of inserting parentheses. For example, we have $((ab)(cd))e$, $(((ab)c)d)e$, etc. In total there are C_{n-1} ways of parenthesizing n variables, where C_n is the nth Catalan number. Then, join together two such expressions if one can be obtained from the other by applying the associativity rule once. By joining all these expressions, we build up the Stasheff polytope.

2.7.3 Cluster coordinates for $\mathrm{Gr}(3,7)$

Beginning with the initial quiver for $\mathrm{Gr}(3,7)$, we can similarly generate all of the clusters and their $\mathcal{A}$- and $\mathcal{X}$-coordinates by successive mutations until all possibilities are exhausted. The E_6 algebra generated in this manner has a total of 49 well-known $\mathcal{A}$-coordinates, composed of the 35 Plücker coordinates $\langle ijk\rangle$ on $\mathrm{Gr}(3,7)$ together with 14 composite brackets of the form

$$\langle 1\times 2, 3\times 4, 5\times 6\rangle, \qquad \langle 1\times 2, 3\times 4, 5\times 7\rangle \tag{2.80}$$

and their cyclic images. The seven coordinates $\langle 123\rangle, \ldots, \langle 712\rangle$ are frozen, while the remaining forty-two are unfrozen.

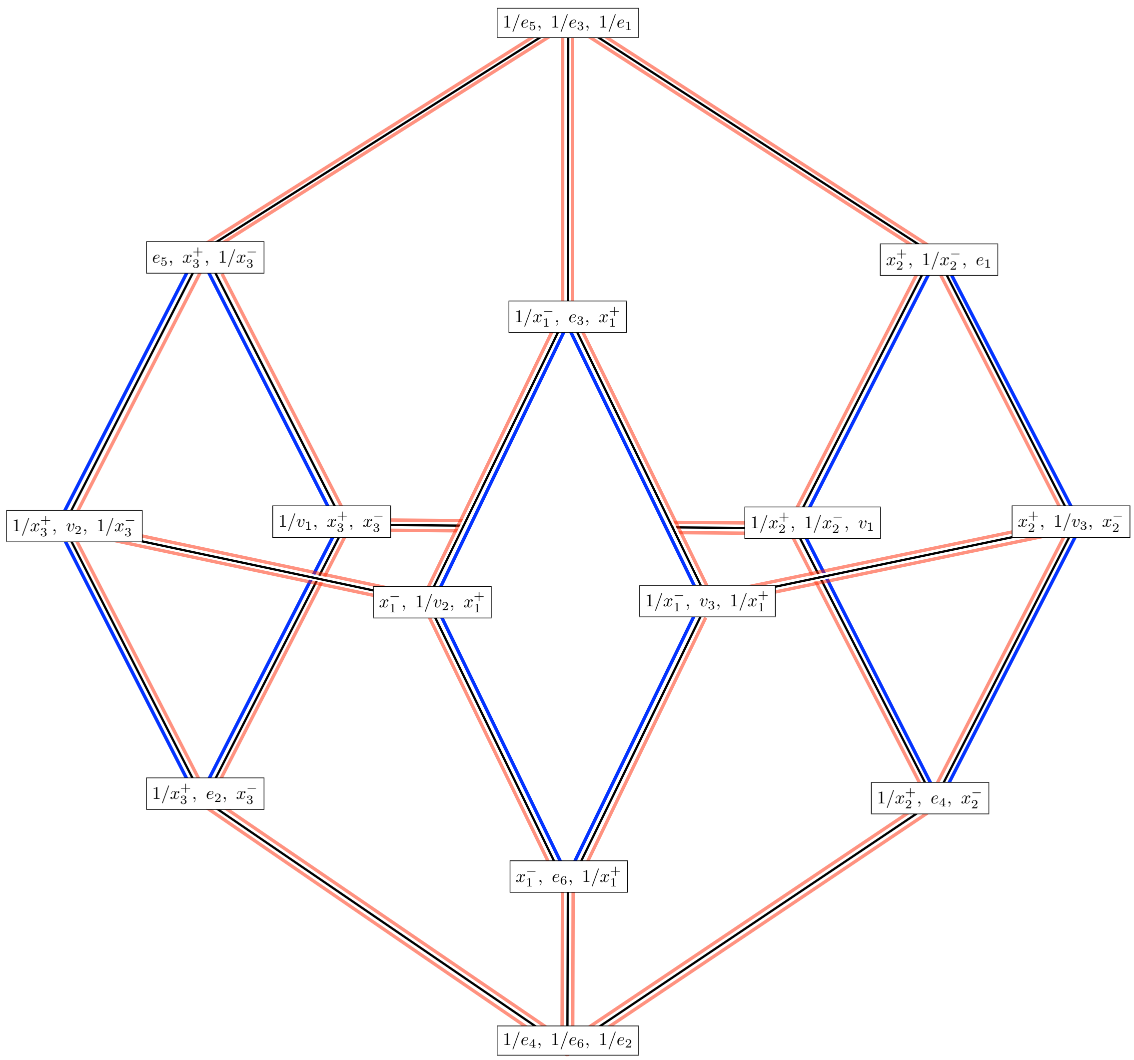

Figure 2.8: The Stasheff polytope for the $\mathrm{Gr}(2,6)$ (or A_3) cluster algebra, also known as the K_5 associahedron. Each of the 14 vertices (clusters) is labeled by its three $\mathcal{X}$-coordinates. The 21 edges connect pairs of clusters which are related to each other by some mutation. The 9 faces comprise three quadrilaterals (shown in blue) and six pentagons (shown in red). These correspond respectively to $A_1 \times A_1$ and A_2 subalgebras.

Mutation generates 833 distinct clusters, which altogether contain a total of 385 $\mathcal{X}$-coordinates. We list all of them here by separating them into four classes, and use the notation

$$r(a|b,c,d,e) = \frac{\langle abc\rangle\langle ade\rangle}{\langle acd\rangle\langle abe\rangle} \tag{2.81}$$

as well as the $\mathbb{P}^2$ cross-ratio defined in eq.(2.43).

First of all there are $3 \times 7 = 21$ coordinates of the form

$$r(2|1,3,5,6), \quad \frac{\langle 231\rangle\langle 456\rangle}{\langle 4\times 5, 6\times 1, 2\times 3\rangle}, \quad \frac{\langle 127\rangle\langle 234\rangle\langle 345\rangle\langle 567\rangle}{\langle 257\rangle\langle 347\rangle\langle 1\times 2, 3\times 4, 5\times 6\rangle} \tag{2.82}$$

together with their cyclic images. Each of these cross-ratios is real (that is, equal to its parity conjugate), and it suffices to take only their cyclic images since a dihedral transformation (i.e., $i \to 8-i$) maps this set back to itself.

Secondly there are a further $2 \times 14 = 28$ real cross-ratios of the form

$$r_3(1,2,5,6,3,4), \quad \frac{\langle 127\rangle\langle 256\rangle\langle 345\rangle}{\langle 257\rangle\langle 1\times 2, 3\times 4, 5\times 6\rangle}, \tag{2.83}$$

together with their dihedral images.

Next come $6 \times 2 \times 7 = 84$ complex (that is, not equal to their parity conjugates) cross-ratios of the form

$$\begin{aligned} &r(2|1,3,4,5), \quad r(1|6,3,4,5), \quad r(3|2,4,5,1), \\ &\qquad r_3(1,5,3,2,6,4), \quad r_3(1,4,6,2,3,5), \quad \frac{\langle 127\rangle\langle 234\rangle\langle 567\rangle}{\langle 267\rangle\langle 3\times 4, 5\times 7, 1\times 2\rangle}, \end{aligned} \tag{2.84}$$

together with their parity conjugates and all cyclic images thereof.

Finally we have the $9 \times 2 \times 14 = 252$ complex cross-ratios

$$\begin{gathered}
r(1|5,2,3,4), \quad r(1|6,2,3,4), \quad r(1|6,2,3,5), \quad r(1|6,2,4,5), \quad r(2|1,3,4,6), \\
r_3(1,2,4,6,3,5), \quad r_3(1,4,3,6,5,2), \quad r_3(1,3,5,6,2,4), \quad \frac{\langle 261\rangle\langle 345\rangle}{\langle 4\times 5, 6\times 1, 2\times 3\rangle},
\end{gathered} \tag{2.85}$$

together with their parity conjugates and all dihedral images thereof.

Note that we have expressed most of the cross-ratios above in a form in which they do not depend explicitly on point number 7. The three most complicated cross-ratios are exceptions to this, and for these three we find it worthwhile to display here the non-trivial factorizations

$$\begin{aligned}
1+\frac{\langle 127\rangle\langle 256\rangle\langle 345\rangle}{\langle 257\rangle\langle 1\times 2, 3\times 4, 5\times 6\rangle} &= \frac{\langle 125\rangle\langle 7\times 2, 3\times 4, 5\times 6\rangle}{\langle 257\rangle\langle 1\times 2, 3\times 4, 5\times 6\rangle}, \\
1+\frac{\langle 127\rangle\langle 234\rangle\langle 567\rangle}{\langle 267\rangle\langle 3\times 4, 5\times 7, 1\times 2\rangle} &= \frac{\langle 257\rangle\langle 1\times 2, 3\times 4, 6\times 7\rangle}{\langle 267\rangle\langle 1\times 2, 3\times 4, 5\times 7\rangle}, \\
1+\frac{\langle 127\rangle\langle 234\rangle\langle 345\rangle\langle 567\rangle}{\langle 257\rangle\langle 347\rangle\langle 1\times 2, 3\times 4, 5\times 6\rangle} &= \frac{\langle 1\times 2, 3\times 4, 5\times 7\rangle\langle 7\times 2, 3\times 4, 5\times 6\rangle}{\langle 257\rangle\langle 347\rangle\langle 1\times 2, 3\times 4, 5\times 6\rangle}.
\end{aligned} \tag{2.86}$$

All three of the cluster $\mathcal{X}$-coordinates on the left-hand side of this equation appear in the $\mathrm{B}_3 \otimes \mathbb{C}^*$ part of the coproduct of the two-loop $n = 7$ MHV amplitude.

2.7.4 Structure of the motivic two-loop $n = 7$ MHV amplitude

Obviously it is impractical for us to display the Stasheff polytope for the $\mathrm{Gr}(3,7)$ cluster algebra, with its 833 vertices, 2499 edges, and 2856 two-dimensional faces (of which 1785 are quadrilaterals and the other 1071 are pentagons). However, we are in a position now to carry out a 'motivic analysis' of the two-loop $n = 7$ MHV amplitude using the information contained in the previous section.

First of all we note the amazing fact that all of the entries of $\{z\}_2$ and $\{z\}_3$ in the results in sec. 2.5 are always cluster $\mathcal{X}$-coordinates of $\mathrm{Conf}_7(\mathbb{P}^2)$. Interestingly, of the 385 such coordinates available, only 231 of them actually appear in the $n = 7$ MHV amplitude at two loops. This might be a two-loop accident, but if it continues to hold at higher loop order it would be important to find some sort of geometric explanation.

Turning our attention now to the expression for the $\Lambda^2 \mathrm{B}_2$ part of the coproduct shown in eq. (2.40), we note first of all the further highly nontrivial fact that for each term $\{x_1\}_2 \wedge \{x_2\}_2$, there is always at least one of the 833 clusters which contains both x_1 and x_2. And more spectacularly, the variables always appear in pairs with Poisson bracket $\{x_1, x_2\} = 0$. Now we understand the geometric meaning of the ambiguity mentioned in eq. (2.45), in light of eq. (2.67)—it is exactly the ambiguity of trying to chose one of the four vertices of a quadrilateral, when there is no reason at all to have to make a choice: each term in $\Lambda^2 \mathrm{B}_2$ corresponds naturally to a certain quadrilateral face.

We conclude that the most canonical, invariant way of expressing the $\Lambda^2 \mathrm{B}_2$ part of the coproduct of the two-loop $n = 7$ MHV amplitude is not by the formula (2.40), but by writing it as a sum of 42 quadrilateral faces of the E_6 Stasheff polytope. It is obviously of paramount importance to understand what makes these 42 special, out of the 1785 such faces available.

An analysis of the $\mathrm{B}_3 \otimes \mathbb{C}^*$ part of the coproduct requires a classification of all of the possible A_3, $A_2 \times A_1$ and $A_1 \times A_1 \times A_1$ subalgebras of E_6. The Stasheff polyhedron has 1547 three-dimensional faces, consisting of 357 cubes ($A_1 \times A_1 \times A_1$), 714 pentaprisms ($A_2 \times A_1$) and 476 of the A_3 polytopes shown in fig. 2.8. We expect these to play a role in unlocking further structure in the two-loop n-point MHV amplitudes, which we will explore in future chapters.

2.8 Conclusion

Appropriately defined scattering amplitudes in maximally supersymmetric Yang-Mills theory are functions on $\mathrm{Conf}_n(\mathbb{P}^3)$ which have a very rich mathematical structure but do not, in general, admit any particular canonical or even preferred functional representation. The one important exception is the two-loop MHV amplitude for $n = 6$ reviewed in section (2.3), which does have a canonical form (up to trivial Li_m identities): that in which it is expressed only in terms of the classical polylogarithm functions, with only (minus) cluster $\mathcal{X}$-coordinates as arguments.

More general amplitudes may be computed numerically if desired (for example all two-loop MHV amplitudes may be evaluated with reasonable efficiency [66]), but we do not strive to find any particular explicit analytic formulas for them. It often happens in physics and in mathematics that when one reaches sufficiently deep into a subject, one realizes that the appropriate objects of study are not what one originally thought, but some suitable generalization or modification thereof. In this vein we have proposed that our focus on the mathematical structure of scattering amplitudes in SYM theory should fall on what we call motivic amplitudes, and in particular on their coproducts, which capture the 'mathematically most complicated part' of an amplitude.

By drawing on our explicit results for the two-loop $n = 6$ and $n = 7$ MHV motivic amplitudes, we have shown that an important role is played by cluster coordinates, which are preferred sets of coordinates on $\mathrm{Conf}_n(\mathbb{P}^3)$ with very rich mathematical structure. Specifically, we conjecture based on the examples presented here, as well as others that we have computed, that for all MHV motivic amplitudes, to all loop order, the following is true: given any iterated coproduct component expressible in terms of the Bloch groups, the corresponding Bloch group elements $\{x\}_k$ are given by cluster $\mathcal{X}$-coordinates x. The algebras relevant for $n = 6, 7$ are of finite type, being the A_3 and E_6 algebras respectively, while for $n > 7$ the relevant algebras are of infinite type.

If one accepts that cluster $\mathcal{X}$-coordinates answer the 'kinematical' question *which variables do motivic amplitudes depend on?*, it is natural to turn attention next to the 'dynamical' question of exactly in which combinations they appear in amplitudes. We have provided a first glimpse by showing that the terms in $\Lambda^2 \mathrm{B}_2$ component of the coproduct of the two-loop $n = 7$ MHV amplitude—the component which measures the obstruction to writing this amplitude in terms of the classical polylogarithm functions only—are in correspondence with quadrilateral faces of the relevant Stasheff polytope (i.e., with $A_1 \times A_1$ subalgebras of the cluster algebra). Again based on other examples which we have analyzed, we conjecture that this statement remains true for all two-loop MHV amplitudes. However a great deal of structure remains to be understood. In particular, only a very small number of all possible quadrilaterals actually make an appearance in $\Lambda^2 \mathrm{B}_2$; what, if anything, is the special geometric significance of these particular quadrilaterals? What is the geometric significance of the cluster $\mathcal{X}$-coordinates appearing in $\mathrm{B}_3 \otimes \mathbb{C}^*$, or in non-MHV amplitudes, or at higher loops? A few of these questions will be addressed in future chapters.

Many other interesting questions are also raised by our work. For example, Dixon, Drummond and Henn have employed with great success the strategy of studying the space of all integrable, conformally invariant symbols whose letters are drawn from the collection of available $\mathcal{A}$-coordinates at $n = 6$. By imposing all physical constraints available to them at the time, they were able to determine the symbol of the two-loop NMHV amplitude exactly [67], and that of the three-loop MHV amplitude up to two parameters [68] which were subsequently determined in [69]. We have proposed that only $\mathcal{X}$-coordinates can appear in the coproduct of MHV amplitudes, which is a stronger condition than that only $\mathcal{A}$-coordinates can appear in their symbols. The functions $\mathrm{Li}_m(1+x)$ and $\mathrm{Li}_m(1+1/x)$ for any $\mathcal{X}$-coordinate x for example satisfy the latter but not the former. Hence in particular we expect to see neither $\mathrm{Li}_m(u_i)$ nor

$\mathrm{Li}_m(1-u_i)$ anywhere in the coproduct of $n=6$ MHV amplitudes, to any loop order. It would be very interesting to investigate in detail how restrictive this condition is in the space of all integrable symbols, in order to see whether our new 'motivic' constraint could aid future computations employing this strategy.

It is also important to point out that in the examples we've looked at, only a fraction of all available $\mathcal{X}$-coordinates actually make an appearance. For example in section 2.3 we emphasized that only the 9 coordinates (2.22) enter the two-loop $n=6$ amplitude, out of the 15 available. Then in section 2.5 we found that only 231 of the 385 available $\mathcal{X}$-coordinates make an appearance in the two-loop $n=7$ motivic amplitude. We do not yet have an understanding of the criterion which selects these particular subsets of $\mathcal{X}$-coordinates, nor whether this phenomenon is just an accident at two loops or continues to hold at higher loop order. If it does, this obviously constrains the space of possible motivic amplitudes even more strongly than just the $\mathcal{X}$-coordinate condition discussed in the previous paragraph. We cannot help but note with amusement the fact that $9/15 = 231/385$, but we certainly have too little data to speculate on whether or not this is just a coincidence.

A number of interesting questions about the connection between motivic amplitudes, cluster coordinates and other recent approaches to scattering amplitudes can now be asked. A fair amount of recent work has considered the behavior of amplitudes in various restricted domains, such as two-dimensional or multi-Regge kinematics (see for example [70–74] or [75–80], respectively), where in either case considerable simplification occurs. Also, it has long been appreciated that the behavior of amplitudes under collinear (and especially multi-collinear) limits strongly constrains their structure, and the operator product expansion (OPE) to the null polygonal Wilson loop [81–84] aims to compute arbitrary amplitudes at finite coupling in a systematic expansion around the collinear limit. It would very nice to have a thorough understanding of these limits and expansions directly at the level of cluster algebras, or even individual quivers.

Finally, we have so far made no explicit reference to the integrability of planar SYM theory (see the review [85]), which clearly plays a crucial but so far not fully exploited part in unlocking the structure of its amplitudes (approaches other than the OPE mentioned above include for example [10, 86–88]). We hope that motivic amplitudes and cluster coordinates will be found to be useful in these and other endeavors, just as general 'motivic' methods based on the symbol calculus of polylogarithm functions are finding ever wider applications to physical computations in quantum field theory, including Feynman integrals, amplitudes, form factors, correlation functions, and Wilson loops [55, 89–95], not just in SYM theory but even QCD [56, 96–98] and string theory [22–25] as well.

Chapter 3

Calculating $dR_n^{(2)}$

3.1 Introduction

Insights gleaned from difficult calculations have driven much of the recent progress in unlocking the structure of $\mathcal{N} = 4$ super Yang-Mills (SYM) theory. The synergy between technical and conceptual advances frequently enables the undertaking of previously impossible calculations; the often surprising results of which in turn fuel a deeper understanding of the theory. Indeed, in SYM theory the search for such insights, rather than the need for busywork, is precisely the motivation for carrying out arduous new calculations.

In this chapter we complete the analytic calculation of the differential $dR_n^{(2)}$ of the planar two-loop n-particle MHV amplitudes (or, more properly, the 'remainder functions'—with infrared divergences subtracted off in a standard way [13, 14]). Reasonably efficient numerical techniques for evaluating $R_n^{(2)}$ have been available for some time [66], and analytic formulas are known in two-dimensional kinematics [71] but a breakthrough towards unlocking the general analytic structure of these amplitudes was made by Caron-Huot in [20]. By considering the dual superconformal symmetry of a certain generalization of scattering amplitudes depending on twice the usual number of Grassmann variables, he was able to express $dR_n^{(2)}$ in terms of a certain combination of one-fold integrals. Here we complete the evaluation of these integrals and present analytic expressions for $dR_n^{(2)}$. We find that they can be expressed completely in terms of the functions $\mathrm{Li}_k(-x)$, for $k = 1, 2, 3$ with arguments x always belonging to the set of cluster $\mathcal{X}$-coordinates on the kinematic configuration space $\mathrm{Conf}_n(\mathbb{P}^3)$. This provides strong support for the claim in chapter 2 that the cluster structure of this space underlies the structure of amplitudes in SYM theory.

While this computation may seem modest in scope, we feel that it is a useful example in which to showcase the power of the two most recent additions to the amplitudeologist's toolkit: positivity and cluster $\mathcal{X}$-coordinates. In particular, the positive domain, a subset of the kinematic domain $\mathrm{Conf}_n(\mathbb{P}^3)$, is evidently the natural habitat for amplitudes in SYM theory, and cluster $\mathcal{X}$-coordinates provide a natural set of arguments for these amplitudes to 'depend on'. It is our hope that other analytic formulae in SYM theory can be unlocked using these or similar approaches. In particular, it would be very interesting to see if the monodromies of $R_n^{(2)}$, which were computed in integral form in [83] (see also [99]), can be similarly expressed only in terms of $\mathrm{Li}_k(-x)$.

Following ample motivation (but minimal review), we present our analytic expression for $dR_n^{(2)}$. For additional introductory material, we refer the reader to chapter 2 and the references therein.

3.2 Motivation and Review

In [20], Caron-Huot expressed the differential of the planar two-loop n-particle MHV amplitude as

$$dR_n^{(2)} = \sum_{i,j} C_{i,j}\; d\log\langle i{-}1\, i\, i{+}1\, j\rangle \tag{3.1}$$

and presented a means of calculating the coefficient functions $C_{i,j}$. Already the fact that the differential may be expressed in the form of eq. (3.1) is a nontrivial all-loop-order prediction of [20].

Thanks to the full dihedral symmetry of the amplitude in the particle labels, it is sufficient to focus on $C_{2,i}$. This was given as a sum of four components $C_{2,i}^{(a)}$, for $a = 1, 2, 3, 4$, two of which were represented analytically as

$$C_{2,i}^{(1)} = \log u \times \sum_{j=2}^{i-1} \sum_{k=i}^{n+1} \left[\mathrm{Li}_2(1 - u_{j,k,k-1,j+1}) + \log \frac{x_{j,k}^2}{x_{j+1,k}^2} \log \frac{x_{j,k}^2}{x_{j,k-1}^2} \right] \tag{3.2}$$

where for our purposes it is sufficient to take $x_{i,j}^2 = \langle i\, i{+}1\, j\, j{+}1\rangle$, and

$$C_{2,i}^{(4)} = -2\,\mathrm{Li}_3(1 - \frac{1}{u}) - \mathrm{Li}_2(1 - \frac{1}{u}) \log u - \frac{1}{6} \log^3 u + \frac{\pi^2}{6} \log u, \tag{3.3}$$

where

$$u_{i,j,k,l} = \frac{\langle i\, i{+}1\, j\, j{+}1\rangle\langle k\, k{+}1\, l\, l{+}1\rangle}{\langle i\, i{+}1\, k\, k{+}1\rangle\langle j\, j{+}1\, l\, l{+}1\rangle} \tag{3.4}$$

and $u \equiv u_{2,i-1,i,1}$. $C_{2,i}^{(2)}$ has the integral representation

$$\begin{aligned}
C_{2,i}^{(2)} \quad = \quad & \sum_{j=4}^{i-2} \int_1^2 d_X \log \frac{\langle X i{-}1 i\rangle}{\langle X i j\rangle} \Big(\mathrm{Li}_2(1-u_{X,i-1,i,j}) - \mathrm{Li}_2(1-u_{X,i-1,i,j-1}) \\
& \qquad + \mathrm{Li}_2(1-u_{i,j-1,j,i-1}) + \mathrm{Li}_2(1-u_{X,j,j-1,i-1}) - \mathrm{Li}_2(1-u_{X,j,j-1,i}) \\
& \qquad + \log u_{X,i-1,i,j} \log u_{X,j,j-1,i-1} \Big) \\
& + \sum_{j=4}^{i-2} \int_1^2 d_X \log \frac{\langle X i{-}1 i\rangle}{\langle X i i{+}1\rangle} \Big(\mathrm{Li}_2(1-u_{i-1,1,X,j}) + \mathrm{Li}_2(1-u_{i,j,j-1,1}) \\
& \qquad + \mathrm{Li}_2(1-u_{1,j,j-1,X}) - \mathrm{Li}_2(1-u_{i-1,1,X,j-1}) - \mathrm{Li}_2(1-u_{i,j,j-1,X}) \\
& \qquad + \log u_{i-1,1,X,j} \log u_{i,j,j-1,1} \Big) \\
& + \int_1^2 d_X \log \frac{\langle X i{-}1 i\rangle}{\langle X 3 4\rangle} \left(\mathrm{Li}_2(1-u_{2,i,i-1,3}) - \mathrm{Li}_2(1-u_{X,i,i-1,3}) \right)
\end{aligned} \tag{3.5}$$

and $C_{2,i}^{(3)}$ may be determined from $C_{2,i}^{(2)}$ by imposing dihedral symmetry on eq. (3.1), which fixes

$$C_{2,i}^{(3)}(1,2,\ldots,n) = C_{2,4+n-i}^{(2)}(3,2,\ldots,4). \tag{3.6}$$

While eqs. (3.2) and (3.3) along with the integral representation in eq. (3.5) were sufficient to compute the symbol of $dR_n^{(2)}$ in [20], any attempt at an analytic expression for $dR_n^{(2)}$ would have encountered two major obstacles:

Choosing a 'Good' Kinematic Domain

First of all, n-particle scattering amplitudes in SYM theory are multi-valued functions on the $3(n-5)$-dimensional kinematic configuration space $\mathrm{Conf}_n(\mathbb{P}^3)$, and in computing scattering amplitudes it is often very difficult to get all of the branch cuts in the right place. In particular, Mathematica's `Integrate[]` function has no *a priori* understanding of $\mathrm{Conf}_n(\mathbb{P}^3)$ and cannot be expected to easily return an analytic formula valid on the whole of this domain—at best it can produce numerical results at specifically inputted kinematic points, or an analytic formula valid on some subdomain of its own choosing. On physical grounds, amplitudes should be real-valued and singularity-free throughout the Euclidean domain, a subset of $\mathrm{Conf}_n(\mathbb{P}^3)$. Even for what is in some sense the simplest non-trivial multi-loop amplitude, $R_6^{(2)}$, finding a formula with these properties was by far the hardest part of [19]. For $n > 6$, where the kinematic configuration space is far more complicated (due to Gram determinant constraints amongst dual conformal cross-ratios), finding explicit formulas valid throughout even just the Euclidean domain seems like a daunting challenge. Instead of giving up all hope, one would be content to find expressions valid even in some subset of the Euclidean domain. But, which subset should one look at? What principle, either mathematical or physical, could make any one subset more worthy of attention than another?

Choosing 'Good' Li_k Arguments

The second complication has to do with the class of iterated integrals of the type which define generalized polylogarithm functions and which appear in the result of [20]. Such functions can be partially characterized by their symbols, but integrating a function of this type can generate a function whose symbol contains entries that are, in general, arbitrary alebgraic functions of the entries in the symbol of the original function. Already Caron-Huot's result for the symbol of $R_n^{(2)}$ contains rather non-trivial algebraic functions on $\mathrm{Conf}_n(\mathbb{P}^3)$, and one might have worried that even more complicated functions could appear after integration. Yet, true believers in SYM theory know well that it only ever produces very special polylogarithmic functions, not 'general' ones. One would therefore have every reason to expect only relatively straightforward expressions to actually appear in amplitudes. Unfortunately, unless one knows in advance what to look out for, the plethora of identities amongst polylogarithm functions makes it difficult to identify any particular set of arguments as preferred over any other set.

3.3 Tools and Techniques

Fortunately, related recent advances have shown how to overcome both obstacles at the same time.

Cluster $\mathcal{X}$-coordinates

We begin by addressing the question of Li_k arguments by noting that in chapter 2 it was shown via examples at $n = 6, 7$, and suggested more generally, that (in a sense made precise in that paper) two-loop MHV amplitudes only 'depend on' certain very special variables. These variables are called cluster $\mathcal{X}$-coordinates on the kinematic configuration space $\mathrm{Conf}_n(\mathbb{P}^3)$, which may be realized as the Grassmannian quotient $\mathrm{Gr}(4, n)/(\mathbb{C}^*)^{n-1}$. For the purpose of this chapter, the notion of 'depending on' only certain variables can be stated very clearly: in support of chapter 2, we find that the differential $dR_n^{(2)}$ of all two-loop MHV amplitudes can be expressed only in terms of the functions $\mathrm{Li}_k(-x)$, for $k = 1, 2, 3$ with arguments x always belonging to the set of cluster $\mathcal{X}$-coordinates on $\mathrm{Conf}_n(\mathbb{P}^3)$.

In fact, we find that (in line with the expectation expressed in the previous section) only relatively tame $\mathcal{X}$-coordinates appear in $dR_n^{(2)}$, for any n. The most complicated of these is the cross-ratio

$$-\frac{\langle 12 i{-}1 i\rangle\langle 123 j\rangle\langle 2 j{-}1 j j{+}1\rangle\langle j{-}1 j i{-}1 i\rangle}{\langle 12 j j{+}1\rangle\langle 2 j i{-}1 i\rangle\langle i{-}1 i (123)\cap(j{-}1 j j{+}1)\rangle} \tag{3.7}$$

which depends on the eight points $\{1, 2, 3, j-1, j, j+1, i-1, i\}$. The fact that the complexity of two-loop MHV amplitudes stabilizes (in this sense) already at $n = 8$ is manifest in the result of [20]. This implies that a full understanding of the cluster structure on $\mathrm{Conf}_8(\mathbb{P}^3)$ is sufficient to understand the structure of all such amplitudes.

The Positive Domain

We now turn to the question of the kinematical domain, where the sole dependence on cluster $\mathcal{X}$-coordinates plays a fortuitous role. A salient feature of cluster $\mathcal{X}$-coordinates is that they are positive-valued everywhere in the positive domain, which is the subset of the Euclidean domain defined by imposing that $\langle abcd \rangle > 0$ whenever $a < b < c < d$. With the differential $dR_n^{(2)}$ expressed completely in terms of the functions $\mathrm{Li}_k(-x)$, it therefore becomes manifestly real-valued and singularity free throughout the positive domain. (Moreover, we believe that $R_n^{(2)}$ itself is also positive-valued throughout the positive domain, but that is another matter.) The importance of positivity for scattering amplitudes was first emphasized in [40], though in a somewhat different context. Their Grassmannian for the integrand involves both 'external' kinematic data as well as 'internal' loop integration variables, but it is now clear that positivity in the 'external' data alone plays a similarly important role for the fully integrated amplitudes which we study here.

Before proceeding let us add one crucial disclaimer. As reviewed in chapter 2, for $n > 7$ the cluster algebra associated to $\mathrm{Conf}_n(\mathbb{P}^3)$ has an infinite number of cluster $\mathcal{X}$-coordinates (although of course only a finite number actually appear in $dR_n^{(2)}$). Moreover there is no known general classification of these coordinates, and given any cross-ratio there does not exist any general algorithm for determining whether or not it actually is a cluster $\mathcal{X}$-coordinate. Therefore, for $n > 7$ we use the empirical criterion discussed in section 2.6.6: we say that a cross-ratio x is a cluster $\mathcal{X}$-coordinate if $1+x$ factors into a product of four-brackets as a consequence of Plücker relations and if $x > 0$ everywhere inside the positive domain.

Given the two advances we have reviewed—the understanding that the natural domain on which to study multi-loop amplitudes in SYM theory is the positive domain, and that the natural set of arguments appearing inside the Li_k functions for two-loop MHV amplitudes are cluster $\mathcal{X}$-coordinates—analytically integrating eq. (3.5) transforms from being merely possible to being inevitable.

3.4 Results

In this section we present the Li_3 and $\mathrm{Li}_2 \times \mathrm{Li}_1$ contributions to $dR_n^{(2)}$. There are, in addition, terms of the form Li_1^3 and $\pi^2 \, \mathrm{Li}_1$ which are too numerous to efficiently display here. For this reason we attach to this submission a Mathematica notebook [100] which contains the necessary expressions and which can construct the full analytic formula for $dR_n^{(2)}$ for any given n.

While the original integral representation of $C_{i,j}$ required the general object $u_{i,j,k,l}$, the integrated result can be written in terms of the slightly smaller class of cross-ratios defined by $u_{i,j,k} = u_{i,j,k,i-1}$. The cluster $\mathcal{X}$-coordinates related to the three-index u's (in the same sense that the v_i and the u_i used in Chapter 2 for $n = 6$ are related to each other) are

$$v_{i,j,k} = \frac{1}{u_{i,j,k}} - 1 = -\frac{\langle i(i{-}1\, i{+}1)(j\, j{+}1)(k\, k{+}1)\rangle}{\langle i{-}1\, i\, k\, k{+}1\rangle\langle i\, i{+}1\, j\, j{+}1\rangle}. \tag{3.8}$$

For any n, $v_{i,j,k}$ is a cluster $\mathcal{X}$-coordinate as long as $i < j < k \pmod{n}$. We also find it useful to define another type of ratio,

$$w_{i,j,k} = \frac{v_{i,k-1,k} u_{i,k-1,k}}{v_{j,k-1,k}} \tag{3.9}$$

which is a cluster $\mathcal{X}$-coordinate when $i = j \pm 1$. Because we are interested only in objects of the form $\mathrm{Li}_k(-x)$, where x is a cluster $\mathcal{X}$-coordinate, we will make one more definition

$$\mathrm{li}_k(x) = \mathrm{Li}_k(-x) \tag{3.10}$$

purely in the interest of cleaning up the notation.

We begin with the essentially semantic task of converting $C^{(1)}$ and $C^{(4)}$ into $\mathcal{X}$-coordinate form. Expressing $C^{(4)}_{2,i}$ in the desired form is trivial:

$$C^{(4)}_{2,i} = -2\,\mathrm{li}_3(v_{2,i-1,i}) - \mathrm{li}_2(v_{2,i-1,i})\,\mathrm{li}_1(v_{2,i-1,i}) + \mathcal{O}(\mathrm{li}_1^3). \tag{3.11}$$

$C^{(1)}$ is slightly more difficult, since it involves non-conformal objects such as $\log \frac{x^2_{j,k}}{x^2_{j,k-1}}$. Of course, the expression as a whole is conformally invariant, but it takes some combinatoric effort to recast things as an explicit sum over conformal cross-ratios. This is only a problem for the $\mathcal{O}(\mathrm{Li}_1^3)$ ratios, our results for this are in the attached Mathematica notebook. For $\mathrm{Li}_2 \times \mathrm{Li}_1$, we find that the ratios appearing are in fact already in cluster $\mathcal{X}$-coordinate form, giving

$$\begin{aligned} C^{(1)}_{2,i} = -\,\mathrm{li}_1(v_{2,i-1,i})\Bigg(& \sum_{j=2}^{i-2}\sum_{k=i}^{n} \mathrm{li}_2(v_{j+1,k,k+1}) \\ & - \sum_{k=i+2}^{n} \mathrm{li}_2(v_{k,2,i-1}) - \sum_{j=4}^{i-2} \mathrm{li}_2(v_{j,i,1})\Bigg) + \mathcal{O}(\mathrm{li}_1^3). \end{aligned} \tag{3.12}$$

This sum looks slightly different than eq. (3.2) because we find it useful to make explicit the behavior of $1 - u_{j,k,k-1,j+1}$ at various upper and lower limits of the j, k summation indices. The double-sum of eq. (3.12) contains some boundary terms which diverge—specifically, when j, k equal $2, n$ or $i-2, i$. However, these divergences cancel when the $\mathcal{O}(\mathrm{Li}_1^3)$ terms are added. The attached Mathematica file identifies and discards these canceling divergent terms.

We now turn to the main focus of this chapter: the evaluation of the remaining integrals in $C^{(2)}_{2,i}$. For fixed i, j, the terms on the first four lines of eq. (3.5) altogether depend on at most nine distinct momentum twistors. We can therefore focus our efforts entirely on evaluating the integrals for the case $n = 9, i = 8, j = 5$, and then replace $\{4, 5, 6, 7, 8, 9\} \to \{j-1, j, j+1, i-1, i, i+1\}$ to recover the summand for arbitrary i, j. One may immediately worry about divergences at boundary terms in the sum, such as $j = i - 2$; while these cases do create individual terms that are divergent, these divergences cancel out in the full function.

In order to present our result for $C_{2,i}^{(2)}$ in a succinct fashion, let us define the following permutation operators acting on the particle labels:

$$\sigma_a = Z_{a-1} \leftrightarrow Z_{a+1} \tag{3.13}$$

$$\sigma_{a,b} = 1 - \sigma_a - \sigma_b + \sigma_a\sigma_b \tag{3.14}$$

$$\sigma_{a,b,c} = 1 - \sigma_a - \sigma_b - \sigma_c + \sigma_a\sigma_b + \sigma_a\sigma_c + \sigma_b\sigma_c - \sigma_a\sigma_b\sigma_c \tag{3.15}$$

as well as the four cross-ratios

$$\begin{aligned}
R_1 &= -\frac{\langle 12j{-}1j\rangle\langle 2ji{-}1i\rangle\langle j{-}1jj{+}1i\rangle}{\langle 2j{-}1jj{+}1\rangle\langle 12ji\rangle\langle j{-}1ji{-}1i\rangle}, \\
R_2 &= -\frac{\langle 2i{-}1ii{+}1\rangle\langle 12ij\rangle\langle i{-}1ij{-}1j\rangle}{\langle 12i{-}1i\rangle\langle 2ij{-}1j\rangle\langle i{-}1ii{+}1j\rangle}, \\
R_3 &= -\frac{\langle 123j\rangle\langle 12i{-}1i\rangle\langle 2j{-}1ji\rangle}{\langle 123i\rangle\langle 12j{-}1j\rangle\langle 2i{-}1ij\rangle}, \\
R_4 &= -\frac{\langle 12i{-}1i\rangle\langle 123j\rangle\langle 2j{-}1jj{+}1\rangle\langle j{-}1ji{-}1i\rangle}{\langle 12jj{+}1\rangle\langle 2ji{-}1i\rangle\langle i{-}1i(123)\cap(j{-}1jj{+}1)\rangle},
\end{aligned} \tag{3.16}$$

which are all cluster $\mathcal{X}$-coordinates. Note that there is additional symmetry present in in the arguments of R_1 and R_2, which are related via $R \to 1/R$ combined with $i \leftrightarrow j$.

Given these definitions, we find that $C_{2,i}^{(2)}$ has the following relatively simple Li_3

contribution:

$$\begin{aligned}
&\mathrm{li}_3(v_{2,i-1,i}) - \mathrm{li}_3\left(w_{3,2,i}\right) + \mathrm{li}_3\left(w_{2,3,i}\right) \\
&\qquad - \sum_{j=4}^{i-2} \sigma_{2,i,j} \Big(\mathrm{li}_3\left(R_1\right) + \mathrm{li}_3\left(R_2\right) + \mathrm{li}_3\left(R_3\right) - \mathrm{li}_3\left(R_4\right) \Big). \qquad (3.17)
\end{aligned}$$

The three symmetries lead to 32 distinct Li_3's in each term in the j sum. This presentation has discarded all terms which cancel telescopically in the sum. One can alternatively incorporate the non-summand terms into the summand by including some telescopic cancellations, thus increasing the total number of Li_3 terms (still all with cluster $\mathcal{X}$-coordinates as arguments) in the summand to 48.

While there are no remaining telescopic cancellations in eq (3.17), the full 32 Li_3 terms do not appear for all values of i and j[1]. For example, six of the Li_3 terms go to zero at the upper limit of the sum, $j = i - 2$.

It is interesting to note that the evaluation of the integrals in eq. (3.5), for the general case $n = 9, i = 8, j = 5$, necessarily produces Li_3's with *non*-cluster arguments. However, these terms cancel telescopically in the j sum and are zero at the $j = 4$ and $j = i - 2$ boundaries.

[1]The exact counting is: for $n > 6$ the total number of Li_3 terms in $C^{(2)}_{2,i}$ is given by $32i - 172$ for $5 < i < n$ and $26n - 142$ for $i = n$. For $n = 6$, $C^{(2)}_{2,6}$ has 12 Li_3 terms. $C^{(2)}_{2,i} = 0$ for $i < 5$.

Next we turn to the $\text{Li}_2 \times \text{Li}_1$ contribution to $C_{2,i}^{(2)}$, which we represent here as

$$
\begin{aligned}
&\text{li}_1\left(v_{2,i-1,i}\right)\left(\text{li}_2(v_{i,1,3}) - \text{li}_2\left(v_{3,i-1,i}\right)\right) - \left(\text{li}_1\left(v_{2,i-1,i}\right) + \text{li}_1\left(v_{3,i-1,i}\right)\right)\text{li}_2\left(w_{2,3,i}\right) \\
&-\sum_{j=4}^{i-2}\Bigg(\sigma_{2,j}\Bigg(\left(\text{li}_1\left(v_{i,2,j-1}\right) + \text{li}_1\left(v_{2,i-1,i}\right)\sigma_i\right)\left(\text{li}_2\left(R_1\right) - \text{li}_2\left(R_2\right)\right) \\
&\qquad +\frac{1}{2}\left(\text{li}_1\left(v_{i,2,j-1}\right) + \text{li}_1\left(v_{i,2,j}\right)\right)\left(\text{li}_2\left(R_1\right) - \text{li}_2\left(R_3\right)\right) \\
&\qquad +\frac{1}{2}\left(\text{li}_1\left(v_{2,j,i-1}\right) - \text{li}_1\left(v_{j,i-1,1}\right) - 2\,\text{li}_1\left(v_{i,2,j-1}\right) + \frac{1}{2}\,\text{li}_1\left(v_{2,j-1,j}\right)\right) \\
&\qquad\qquad\qquad\qquad\qquad\qquad\qquad\qquad \times\left(1-\sigma_i\right)\left(\text{li}_2\left(R_1\right) - \text{li}_2\left(R_3\right)\right)\Bigg) \\
&\qquad +\left(1-\sigma_j\right)\Bigg(\left(\text{li}_1\left(v_{2,j,i-1}\right) + \text{li}_1\left(v_{2,j-1,j}\right)\right)\left(1-\sigma_2\right)\sigma_i\,\text{li}_2\left(R_4\right) \\
&\qquad +\frac{1}{2}\left(3\,\text{li}_1\left(v_{i,2,j-1}\right) + \text{li}_1\left(v_{i,2,j}\right)\right)\left(1-\sigma_i\right)\sigma_2\left(\text{li}_2\left(R_4\right)\right) - \text{li}_1\left(v_{2,i-1,i}\right)\sigma_2\sigma_i\,\text{li}_2\left(R_4\right) \\
&\qquad +\frac{1}{2}\left(\text{li}_1\left(v_{2,j,i-1}\right) - \text{li}_1\left(v_{j,i-1,1}\right) + \text{li}_1\left(v_{i,2,j-1}\right) + \text{li}_1\left(v_{i,2,j}\right) + \frac{1}{2}\,\text{li}_1\left(v_{2,j-1,j}\right)\right) \\
&\qquad\qquad\qquad\qquad\qquad\qquad\qquad\qquad\qquad\qquad \times\sigma_{2,i}\left(\text{li}_2\left(R_4\right)\right)\Bigg) \\
&\qquad +\text{li}_1\left(v_{2,i-1,i}\right)\sigma_{i,j}\sigma_2\left(\text{li}_2\left(R_1\right) + \text{li}_2\left(R_2\right)\right)\Bigg).
\end{aligned}
\tag{3.18}
$$

It is important to emphasize that our particular expression for eq. (3.18) is far from being unique. Some additional symmetry can be introduced by adding terms that telescopically cancel, as was the case with the Li_3 sum. Furthermore, there exist numerous non-trivial identities amongst the Li_2 terms in eq. (3.18), introducing additional redundancy. This particular representation was chosen simply because it was the most typographically concise presentation we could deduce.

We conclude this chapter with a brief discussion of parity (see Appendix A for a thorough introduction). The parity invariance of $dR_n^{(2)}$ follows from the fact that $*C_{i,j} = C_{j,i}$ and $\sum_i C_{i,j} = 0$. These properties can be made manifest at the level of the symbol, as was done in [20], but our integrated results sacrifice explicit parity invariance for brevity. Of course, parity invariance in our functional representation can be confirmed through the application of (numerous) polylogarithm identities.

Chapter 4

Cluster Polylogarithms

There exists a vast mathematical literature on cluster algebras (see for example [101]), and also a large literature on the mathematical structure of generalized polylogarithm functions. One of the general themes to emerge this work so far has been the observation that the perturbative scattering amplitudes in $\mathcal{N} = 4$ supersymmetric Yang-Mills (SYM) theory, which have also been the object of intense study in recent years, tie these two topics intimately together[1].

In this chapter we take a few steps towards a systematic investigation of the intersection between these fields of mathematics. To that end we define and study the simplest examples of *cluster polylogarithm functions*—pure transcendental functions which "depend on" (in a way to be made precise below) only the cluster coordinates of some cluster algebra. Even the mere existence of non-trivial examples of such functions is not a priori obvious—for example, we will see that the Gr(3,5) cluster algebra admits only a single non-trivial cluster function of weight four. Special functions of this kind are apparently not known in the mathematical literature, but we know they exist and are likely to have remarkable properties since SYM theory evidently provides (in addition to numerous other generous mathematical gifts) at least one infinite class of such functions: the two-loop n-particle MHV amplitudes.

In addition to the purely mathematical motivation for exploring this new class of special functions, our work also has a practical application for physicists. The symbol of all two-loop n-particle MHV amplitudes has been known for almost three years from the work of Caron-Huot [20], but it remains an interesting outstanding problem to write explicit analytic formulas for these amplitudes[2]. So far this has been accomplished [17, 18] only for the very special case of $n = 6$, where the result surprisingly can be written entirely in terms of the classical polylogarithm functions

[1] See also [40] for a different relation between cluster algebras and scattering amplitudes.

[2] Considerable analytic progress has been made both at two loops and (in some cases) far beyond for special kinematic configurations, including for example multi-Regge kinematics [75, 76, 79, 80, 102], the near-collinear limit [84, 103, 104], and 2d kinematics [71–73, 105] (see also [106] for comments on cluster structure in 2d kinematics). Fully analytic formulas for the *differential* of the two-loop MHV amplitude for all n were computed in chapter 3.

Li_k [19] (a curiosity which we "explain" below). To write analytic results for generic scattering amplitudes, even in SYM theory, requires giving up the crutch of working with only the relatively tame classical functions and entering the much larger and wilder world of generalized polylogarithm functions. Several impressive analytic results of this type have been achieved for higher-loop or non-MHV $n = 6$ amplitudes in SYM theory by Dixon and collaborators [67, 107]. Applying similar technology at higher n looks challenging because the required computer power grows rapidly with n. Ultimately this is due to the fact that absent other guidance, one would run the risk of being forced to work with a vastly overcomplete basis of functions not specifically tailored to the problem at hand.

When studying $n > 6$ amplitudes in SYM theory it is desirable, for both practical as well as aesthetic reasons, to seek out functional representations which manifest (to the extent possible) all of the important properties of an amplitude. For example, the GSVV formula [19], unlike the previously known DDS formula, makes three important properties of the two-loop $n = 6$ MHV amplitude trivially manifest: it is classical, dihedral invariant, and real-valued everywhere inside the Euclidean domain. (There is also one interesting property which the GSVV formula does not make manifest: the fact that it is positive-valued everywhere inside the positive domain.) Working with functional representatives which manifest as many properties as possible has enormous practical advantages over working with a generic basis of functions, and also helps to elucidate the deeper mathematical structure of the amplitudes. Of course as time passes we may discover new, previously unnoticed properties, allowing us the opportunity to further upgrade the class of functions we work with.

Suppose we were to commission some very special custom non-classical polylogarithm function (or collection of functions) specifically suited for the purpose of expressing the two-loop n-point MHV amplitudes. Based on what we know about these amplitudes today, what properties should we demand these special functions manifest? The most basic property we should impose is that the symbol alphabet should consist of the cluster $\mathcal{A}$-coordinates of the $\mathrm{Gr}(4, n)$ cluster algebra, a property of the amplitudes which is manifest in the result of [20]. We call such functions "cluster $\mathcal{A}$-functions". For the special case of the $\mathrm{Gr}(4, 6)$ algebra, relevant to $n = 6$ particle amplitudes, functions of this type (and satisfying also various other physical constraints) were extensively studied, and fully classified through weight 6 in [67, 68, 107].

Taking inspiration from this program of classifying allowed functions, we consider here two additional properties of the two-loop MHV amplitudes which were introduced in chapter 2: (1) the coproduct of these amplitudes can be expressed entirely in terms of $\mathcal{X}$-coordinates [33] on the cluster Poisson variety $\mathrm{Conf}_n(\mathbb{P}^3)$ (or equivalently, the $\mathrm{Gr}(4, n)$ cluster algebra), and moreover (2) that the $\Lambda^2\,\mathrm{B}_2$ component of the coproduct can be expressed entirely in terms of pairs of variables which Poisson commute.

Remarkably we find that the two simplest non-trivial cluster polylogarithm functions exactly fit the bill. Specifically, we find at transcendentality weight four that the $\mathrm{Gr}(3, 5)$ cluster algebra (also called A_2) admits a unique non-trivial function satisfying property (1), and the $\mathrm{Gr}(4, 6)$ (or A_3) cluster algebra admits a unique non-trivial function (itself a linear combination of A_2 functions) which in addition satisfies property (2). We have checked explicitly for a small handful of cluster algebras that the functions associated with all A_2 and A_3 subalgebras provide a complete basis for *all* weight-four functions satisfying these properties. It is certainly an interesting mathematical problem to explore the universe of cluster functions for general algebras, but for the more limited purpose of expressing two-loop MHV amplitudes it seems that the six-particle A_3 function is all we need. Although the structure of the n-point amplitude stabilizes at relatively small n (that means that higher n amplitudes can be written in terms of building blocks involving smaller values of n), it is rather surprising that the basic two-loop building block seems to involve only six particles.

In section 4.1 we briefly review some mathematical background necessary for formulating our definition of cluster functions. In sections 4.2 and 4.3 respectively we discuss the A_2 and A_3 functions, and in section 4.4 we comment on the problem of expressing two-loop n-point MHV amplitudes in terms of A_3 functions, providing an explicit result for $n = 7$ as an example.

4.1 Cluster polylogarithm functions

Let us begin by providing a lightning review of (see Chapter 2 for details) of the types of variables which make an appearance in the study of scattering amplitudes in SYM theory: cluster $\mathcal{A}$- and cluster $\mathcal{X}$-coordinates. Much of what we have to say about cluster polylogarithm functions may be interesting to investigate in the context of general algebras, but we restrict our attention here largely to Grassmannian cluster algebras, and in particular to the $\mathrm{Gr}(4, n)$ algebra relevant to the kinematic configuration space $\mathrm{Conf}_n(\mathbb{P}^3)$ of n-particle scattering in SYM theory.

Examples of $\mathcal{A}$-coordinates on $\mathrm{Gr}(4, n)$ include the ordinary Plücker coordinates $\langle ijkl\rangle$ as well as certain particular homogeneous polynomials in them such as

$$\begin{aligned} \langle a(bc)(de)(fg)\rangle &\equiv \langle abde\rangle\langle acfg\rangle - \langle abfg\rangle\langle acde\rangle, \\ \langle ab(cde) \cap (fgh)\rangle &\equiv \langle acde\rangle\langle bfgh\rangle - \langle bcde\rangle\langle afgh\rangle, \end{aligned} \tag{4.1}$$

while the $\mathcal{X}$-coordinates are certain cross-ratios which can be built from $\mathcal{A}$-coordinates.

For $n > 7$ there exist arbitrarily more complicated $\mathcal{A}$-coordinates on $\mathrm{Gr}(4, n)$. These appear to play no role at two loops (they likely do appear at higher loop order) since the symbol of the n-point two-loop MHV amplitude was computed in [20] and nothing more exotic than the examples shown in eq. (4.1) occurs.

We emphasize that not every homogeneous polynomial of Plücker coordinates is an $\mathcal{A}$-coordinate, nor is every cross-ratio one can write down an $\mathcal{X}$-coordinate. The only surefire algorithm for determining such coordinates is via the mutation algorithm described in chapter 2, but we note here an empirical rule for selecting $\mathcal{X}$-coordinates for which we know no counterexample: a conformally invariant ratio x of $\mathcal{A}$-coordinates is an $\mathcal{X}$-coordinate if $1 + x$ also factors into a ratio of products of $\mathcal{A}$-coordinates and if x is positive-valued everywhere inside the positive domain (this is the subset of $\mathrm{Conf}_n(\mathbb{P}^3)$ for which $\langle abcd\rangle > 0$ whenever $a < b < c < d$)[3]. This algorithm reveals for example that between

$$\frac{\langle 1235\rangle\langle 1278\rangle\langle 2456\rangle\langle 5678\rangle}{\langle 1256\rangle\langle 2578\rangle\langle 78(123)\cap(456)\rangle} \quad \text{and} \quad -\frac{\langle 2(13)(56)(78)\rangle\langle 5(12)(46)(78)\rangle}{\langle 1256\rangle\langle 2578\rangle\langle 78(123)\cap(456)\rangle} \tag{4.2}$$

(whose difference is 1) only the first is an $\mathcal{X}$-coordinate.

4.1.1 Cluster polylogarithm functions

Now we turn to the heart of this chapter: providing a definition of *cluster polylogarithm functions*. Good definitions in mathematics must lie in a Goldilocks zone: they must be sufficiently constraining so as to select out only certain objects with interesting behavior, yet they must not be so constraining as to preclude the existence of any examples. In defining cluster polylogarithm functions we are guided by the physics of two-loop MHV amplitudes in SYM theory: these functions certainly exist, yet have properties which render them very special amongst the class of all weight-four polylogarithm functions on $\mathrm{Conf}_n(\mathbb{P}^3)$.

We first define a cluster $\mathcal{A}$-function of weight k to to be a conformally invariant function of transcendentality weight k whose symbol can be written with only the $\mathcal{A}$-coordinates of some cluster algebra appearing in its entries. Functions of this type for the $\mathrm{Gr}(4,6)$ cluster algebra (and satisfying various other physical constraints) were extensively classified and studied in the papers [67, 68, 107].

[3] It is a logical possibility that there could exist some x which satisfies this criterion yet which is not an $\mathcal{X}$-coordinate, though we have never encountered such an object in various explorations through $n = 9$.

Our goal here is to impose additional mathematical constraints to focus on a different (and at least for larger n, much smaller) collection of functions: those which "depend on" only the cluster $\mathcal{X}$-coordinates of some cluster algebra. At weight $k < 4$, where we know that the classical polylogarithm functions generate all of $\mathcal{L}_k$, we can make this statement immediately precise: a cluster $\mathcal{X}$-function of weight $k < 4$ is a linear combination of the functions $-\operatorname{Li}_k(-x)$ for x drawn from the set of $\mathcal{X}$-coordinates of some cluster algebra.

At weight 1 there is no distinction between cluster $\mathcal{A}$- and $\mathcal{X}$-functions because any conformally invariant cross-ratio can be expressed as a ratio of products of $\mathcal{X}$-coordinates. Hence any conformally invariant linear combination of logarithms of $\mathcal{A}$-coordinates can be reexpressed as a linear combination of logarithms of $\mathcal{X}$-coordinates.

At weight 2 there is still no distinction; cluster $\mathcal{A}$-functions consist of all functions $-\operatorname{Li}_2(-y)$ for which both y and $1+y$ factor into ratios of products of $\mathcal{A}$-coordinates. But then either y or $-(1+y)$ (whichever is positive throughout the positive domain) is a cluster $\mathcal{X}$-coordinate by the criterion discussed above. If y is not the $\mathcal{X}$-coordinate then we can represent the function $-\operatorname{Li}_2(-y)$ equivalently by $\operatorname{Li}_2(1+y)$ (modulo π^2 and products of logs), establishing that it is a cluster $\mathcal{X}$-function.

At weight 3 there is a third term in the polylogarithm identity

$$-\operatorname{Li}_3(-y) - \operatorname{Li}_3(1+y) - \operatorname{Li}_3(1+1/y) = 0 \text{ (modulo products of logs)}, \qquad (4.3)$$

which implies that "only half" of weight-3 cluster $\mathcal{A}$-functions are $\mathcal{X}$-functions. More precisely: if m is the dimension of the space spanned by the functions $-\operatorname{Li}_3(-x)$ for all cluster $\mathcal{X}$-coordinates x, then the space of weight-3 cluster $\mathcal{A}$-functions is $2m$ dimensional, containing in addition all functions of the form $-\operatorname{Li}_3(1+x)$.

Weight 4 is the first place where things become nontrivial. We first need a more precise definition of cluster $\mathcal{X}$-functions, since not every weight-four polylogarithm can be expressed in terms of the classical function Li_4 only. Motivated by the results of chapter 2 we define a weight-four cluster $\mathcal{X}$-function (henceforth referred to simply as a *cluster polylogarithm function* or just *cluster function*) to be a cluster $\mathcal{A}$-function whose coproduct components can be written as a linear combination of $\{x_i\}_2 \wedge \{x_j\}_2$ or $\{x_i\}_3 \otimes x_j$ for cluster $\mathcal{X}$-coordinates x_i, x_j. Of course the classical function $-\text{Li}_4(-x)$ is trivially such a cluster $\mathcal{X}$-function whenever x is an $\mathcal{X}$-coordinate, so we will often use the word "nontrivial" to denote those cluster $\mathcal{X}$-functions with nonzero $\Lambda^2 \, \text{B}_2$ content.

We do not yet propose a definition of cluster functions for weight greater than 4. As mentioned above, an appropriate definition would be as restrictive as possible without ruling out the existence of non-trivial examples, and should include interesting examples of functions from SYM theory. We believe that the identification of a suitable definition requires first a better understanding of the structure of MHV amplitudes at higher loop order, of which the only example currently in the literature is the tour de force calculation of the three-loop MHV amplitude for $n = 6$ in [107].

In the next two sections we classify and study the properties of the cluster functions for the simplest nontrivial cluster algebras.

4.2 The A_2 function

Let us begin with the simplest nontrivial cluster algebra, the $\text{Gr}(3,5)$ (or A_2) algebra. This algebra has five cluster $\mathcal{X}$-coordinates which may be generated from an initial pair x_1, x_2 via the relation

$$x_{i+1} = \frac{1 + x_i}{x_{i-1}}. \tag{4.4}$$

Several relevant pieces of information about this algebra are encoded graphically in the pentagon shown in fig. 4.1. To each oriented edge is associated a cluster $\mathcal{X}$-variable x; in each case $1/x$ would be associated to the same edge with opposite

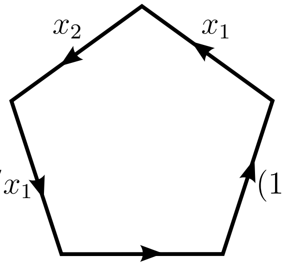

Figure 4.1: The A_2 cluster algebra: to each oriented edge is associated a cluster $\mathcal{X}$-variable (reversing an arrow requires inverting the associated variable), and to each vertex is associated the pair of variables (called the cluster) associated to the edges emanating from that vertex. Moving from one cluster to an adjacent one along some edge is accomplished by mutating on the variable associated to that edge.

orientation. To each vertex is associated the pair of variables (the *cluster*) given by the edge variables emanating away from that vertex—so, for example, the cluster associated with the top vertex in the figure contains the variables $(x_2, 1/x_1)$.

We seek nontrivial cluster polylogarithm functions of weight 4—that is, solutions of eq. (2.36) for which b_{22} and b_{31} can be written simply in terms of the five available cluster $\mathcal{X}$-coordinates. Since A_2 is a finite cluster algebra, this is a simple problem in linear algebra. The dimension of B_1 is 5—spanned by the five multiplicatively independent $\mathcal{X}$-coordinates, the dimension of B_2 is 4—spanned by the five $\{x_i\}_2$ subject to the Abel identity

$$\sum_{i=1}^{5} \{x_i\}_2 = 0, \tag{4.5}$$

and the dimension of B_3 is again 5—spanned by the five $\{x_i\}_3$, which are independent.

It is simple to check that in the 10-dimensional space $\Lambda^2 \mathrm{B}_2$, there is a unique element b_{22} for which there exists a b_{31} in the 25-dimensional $\mathrm{B}_3 \otimes \mathbb{C}^*$ satisfying eq. (2.36). We call this solution the A_2 *function* (or the pentagon function). The $\mathrm{B}_3 \otimes \mathbb{C}^*$ component of the A_2 function is not uniquely fixed by eq. (2.36) since one always has the freedom to add any linear combination of the five $-\operatorname{Li}_4(-x_i)$. We fix this freedom by choosing to define the A_2 function to have the coproduct components

$$\begin{aligned} \delta f_{A_2}(x_1,x_2)|_{\Lambda^2 \mathrm{B}_2} &= \sum_{i,j=1}^{5} j\{x_i\}_2 \wedge \{x_{i+j}\}_2, \\ \delta f_{A_2}(x_1,x_2)|_{\mathrm{B}_3 \otimes \mathbb{C}^*} &= 5\sum_{i=1}^{5} \left(\{x_{i+1}\}_3 \otimes x_i - \{x_i\}_3 \otimes x_{i+1}\right). \end{aligned} \tag{4.6}$$

This is the unique choice which is skew-dihedral invariant—that means it is (1) cyclically invariant under $x_i \to x_{i+1}$ and (2) changes sign under $x_i \to x_{6-i}$. A very important facet of this definition is the antisymmetry of $\delta f_{A_2}(x_1,x_2)|_{\mathrm{B}_3 \otimes \mathbb{C}^*}$ under $\{x\}_3 \otimes y \to \{y\}_3 \otimes x$. In some sense we can therefore consider f_{A_2} to be a "purely non-classical" cluster function (although this notion is not precisely defined), since any linear combination of the classical functions $-\operatorname{Li}_4(-x_i)$ functions has a naturally symmetric $\mathrm{B}_3 \otimes \mathbb{C}^*$ component. This antisymmetry property of the A_2 function makes them useful building blocks for expressing scattering amplitudes, as discussed below in sec. 4.4.

It is also interesting to note that the $\mathrm{B}_3 \otimes \mathbb{C}^*$ content of f_{A_2} can be expressed in an evidently "local" manner—by this we mean that the two $\mathcal{X}$-coordinates in each term $\{x_i\}_3 \otimes x_j$ always have $j = i \pm 1$ and therefore appear together inside some cluster and moreover have Poisson bracket $\{x_i, x_{i\pm1}\} = \pm 1$. In contrast, the $\Lambda^2 \mathrm{B}_2$ component is *non*-local: the two variables appearing in each term $\{x_i\}_2 \wedge \{x_j\}_2$ do not in general appear together in a common cluster and do not have any particularly simple Poisson bracket with each other.

Let us pause to clarify one point of notation which will allow us to avoid confusion later. All five $\mathcal{X}$-coordinates appear on the right-hand sides of (4.6), but we appropriately write $f_{A_2}(x_1,x_2)$ as a function of only two variables since the others may be expressed in terms of these via the relation (4.4). Below we will frequently need to discuss A_2 subalgebras of larger cluster algebras. Any such subalgebra is generated by a pair of $\mathcal{X}$-coordinates which appear together inside some cluster and which have

Poisson bracket $\{x, y\} = 1$. When this happens the corresponding A_2 function is simply $f_{A_2}(x, y)$. To summarize using the quiver notation reviewed in [52]: $f_{A_2}(x, y)$ is a function of any two $\mathcal{X}$-coordinates appearing inside a quiver as $x \to y$.

We emphasize that the equations (4.6) completely and unambiguously define the A_2 function as an element of $\mathcal{L}_4$—i.e., modulo products of functions of lower weight. Nevertheless, the reader with an appetite for seeing an *actual function* with these coproduct components may turn to appendix A for satisfaction, and we can write here a relatively simple expression for the symbol of a representative of f_{A_2}:

$$\text{symbol}(f_{A_2}(x_1, x_2)) \sim \frac{5}{4} \sum_{\text{skew-dihedral}} x_1 \otimes x_2 \otimes x_1 \otimes \frac{x_2}{x_5} + x_1 \otimes x_2 \otimes x_2 \otimes \frac{x_1}{x_3}. \quad (4.7)$$

We write $\sim$ instead of $=$ because as long as we consider f_{A_2} only as an element of $\mathcal{L}_4$ its symbol is not even well-defined—eq. (4.7) represents one particular way of fixing the ambiguity associated to products of lower-weight functions (it is the choice which makes the symbol an eigenvector of ρ), but we are not yet ready to commit to any choice.

Although we believe this function to be new (and hopefully interesting) to the mathematics community, it may seem that this example is too trivial to be relevant to SYM theory, where the relevant algebras are $\mathrm{Gr}(4, n)$. For sure, $\mathrm{Gr}(4, n)$ contains many A_2 subalgebras, and we may evaluate f_{A_2} on each of these, but are there any other solutions of (2.36) for these algebras? Surprisingly, we have checked in addition to A_2 the finite algebras A_3, A_4 and D_4, and in each case we have found that there are no other solutions—for these cluster algebras, *all non-trivial weight-four cluster functions are linear combinations of A_2 functions*[4]!

It remains an interesting mathematical problem to determine, for general cluster algebras (even for infinite ones), the set of non-trivial cluster polylogarithm functions;

[4]This statement has also been verified for the E_6 ($= \mathrm{Gr}(4, 7)$) cluster algebra by D. Parker and A. Scherlis.

that is, the subspace of $\Lambda^2 \mathrm{B}_2$ on which (2.36) can be solved in terms of an element b_{31} expressible purely in terms of cluster $\mathcal{X}$-coordinates. However, even if more exotic solutions exist in general, for the limited purpose of studying two-loop n-point MHV amplitudes it seems clear that the A_2 functions are completely sufficient, in part because these amplitudes only live in a finite (and small) piece of the relevant cluster algebras, as discussed in sec. 4.4.

4.3 The A_3 function

We now turn our attention to cluster polylogarithms for the A_3 cluster algebra, beginning with the seed quiver $x_1 \to x_2 \to x_3$[5]. This quiver generates the following 15 cluster $\mathcal{X}$-coordinates:

$$\begin{aligned}
&x_{1,1} = x_1 && x_{1,2} = 1/x_3 && v_1 = \frac{(x_2+1)(x_1x_2x_3+x_2x_3+x_3+1)}{x_1x_2} \\
&x_{2,1} = (x_1x_2+x_2+1)\,x_3 && x_{2,2} = \frac{x_1x_2+x_2+1}{x_1} && v_2 = \frac{x_3+1}{x_2x_3} \\
&x_{3,1} = \frac{x_2x_3+x_3+1}{x_2} && x_{3,2} = \frac{x_2x_3+x_3+1}{x_1x_2x_3} && v_3 = (x_1+1)\,x_2 \\
&e_1 = \frac{x_1x_2x_3+x_2x_3+x_3+1}{(x_1+1)\,x_2} && e_2 = \frac{1}{(x_2+1)\,x_3} && e_3 = \frac{(x_1+1)\,x_2x_3}{x_3+1} \\
&e_4 = \frac{x_2+1}{x_1x_2} && e_5 = \frac{x_1(x_3+1)}{x_1x_2x_3+x_2x_3+x_3+1} && e_6 = x_2.
\end{aligned} \tag{4.8}$$

The structure of the algebra is summarized in the Stasheff polytope shown in fig. (4.2). The polytope has 9 faces (comprising six pentagons and three quadrilaterals), 14 vertices, and 21 edges, each of which is labeled by an $\mathcal{X}$-coordinate.

We now review a few facts about the natural Poisson structure [33] on $\mathrm{Conf}_n(\mathbb{P}^3)$. A pair of cluster $\mathcal{X}$-coordinates has a simple Poisson bracket ("simple" means ± 1 or 0) only if they appear together inside some cluster. The coordinates in eq. (4.8) have

[5]Note that this is really shorthand for "a triplet of $\mathcal{X}$-coordinates $\{x_1, x_2, x_3\}$ that are all in the same cluster (this distinguishes between x_i and $1/x_i$) and have the Poisson structure $\{x_1, x_2\} = \{x_2, x_3\} = 1,\ \{x_1, x_3\} = 0$."

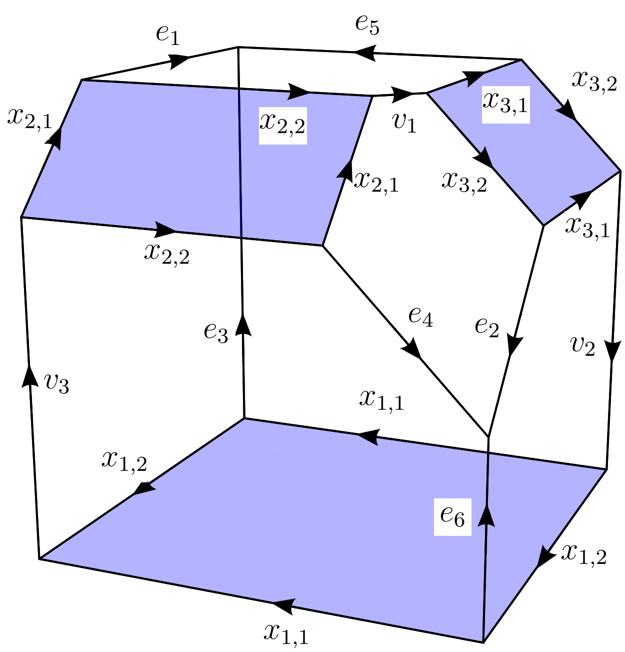

Figure 4.2: The Stasheff polytope for the A_3 cluster algebra. The caption of fig. (4.1) applies, except that here a cluster of three $\mathcal{X}$-coordinates is associated to each vertex. The three quadrilateral faces are shaded blue to distinguish them visually from the six pentagonal faces. The interior of this polytope can be identified with the blow-up of the positive domain in $\mathrm{Conf}_6(\mathbb{P}^3)$, see for example [108].

the following Poisson structure:

$$\{x_{i,1}, x_{i,2}\} = 0, \quad \{e_i, e_{i+4}\} = 1, \quad \{v_i, x_{i\pm 1,a}\} = \mp 1, \quad \{e_i, x_{i+1,a}\} = -1, \tag{4.9}$$

where v and x have indices mod 3 and e has indices mod 6. This means that there are 3 pairs of $\mathcal{X}$-coordinates that Poisson commute and 30 pairs with Poisson bracket ± 1.

Quadrilateral faces of a Stasheff polytope are in correspondence with pairs of cluster $\mathcal{X}$-coordinates which Poisson commute, thereby generating $A_1 \times A_1$ subalgebras. Pentagonal faces of a Stasheff polytope correspond to A_2 subalgebras, generated by pairs of cluster $\mathcal{X}$-coordinates which have Poisson bracket ± 1. For the A_3 algebra there are 30 such pairs—5 (one at each vertex) each for the six pentagonal faces evident in fig. (4.2). The sign of the Poisson bracket is unfortunately not manifest in the figure, so we record here explicitly the five $\mathcal{X}$-coordinates $(x_1, \ldots, x_5)$ (following the notation of sec. 4.2) for each of the six A_2 subalgebras:

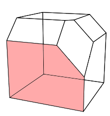 $(e_4, 1/e_6, x_{1,1}, v_3, x_{2,2})$, 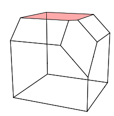 $(e_5, 1/e_1, x_{2,2}, v_1, x_{3,1})$,

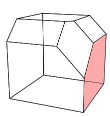 $(e_6, 1/e_2, x_{3,1}, v_2, x_{1,2})$, 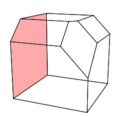 $(e_1, 1/e_3, x_{1,2}, v_3, x_{2,1})$, (4.10)

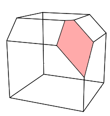 $(e_2, 1/e_4, x_{2,1}, v_1, x_{3,2})$, 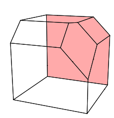 $(e_3, 1/e_5, x_{3,2}, v_2, x_{1,1})$.

Each cyclically adjacent pair of variables appearing here, for example $\{e_6, 1/e_4\}$ or $\{x_{2,1}, e_1\}$, has Poisson bracket $+1$. The three entries in the left column can be read off from fig. (4.2) by going around the pentagons clockwise (as seen from outside the Stasheff polytope), while the three entries in the right column must be read off counterclockwise.

Finally we come to the question of cluster functions for the A_3 algebra. As revealed already at the end of the previous section, it is a simple problem in linear algebra to verify that the equation (2.36) admits solutions only when b_{22} lies in the 6-dimensional subspace of $\Lambda^2 \mathrm{B}_2$ spanned by the six A_2 functions associated to (4.10). We may represent these six functions as $f_{A_2}(e_i, 1/e_{i+2})$ for $i = 1, \ldots, 6$ thanks to the cyclic invariance of the A_2 function.

It is now time, in our quest to cook up a fine selection of special functions for the two-loop MHV amplitudes, to toss in one more very special ingredient. Beyond the fact that they are cluster polylogarithm functions, an even more amazing property of these amplitudes is that they have $\Lambda^2 \mathrm{B}_2$ content which can be expressed entirely in terms of pairs of cluster $\mathcal{X}$-coordinates $\{x_i\}_2 \wedge \{x_j\}_2$ which Poisson commute: $\{x_i, x_j\} = 0$! This was shown to be true for $n = 7$ in chapter 2, and is in fact known to be true for all n (see chapter 6).

For the A_3 algebra it is simple to check that there is a unique linear combination of the six A_2 functions with this property, which we naturally call the A_3 function:

$$f_{A_3} = \frac{1}{10} \sum_{i=1}^{6} (-1)^i f_{A_2}(e_i, 1/e_{i+2}). \tag{4.11}$$

The coproduct of the A_3 function has the spectacularly simple, "local" $\Lambda^2 \mathrm{B}_2$ content

$$\delta f_{A_3}|_{\Lambda^2 B_2} = \sum_{i=1}^{3} \{x_{i,1}\}_2 \wedge \{x_{i,2}\}_2. \tag{4.12}$$

We do not write the $\mathrm{B}_3 \otimes \mathbb{C}^*$ component since it does not simplify beyond the alternating sum of six copies of the corresponding component from the A_2 function.

We observed beneath eq. (4.6) that the $\mathrm{B}_3 \otimes \mathbb{C}^*$ content of the A_2 function is "local" (involving only pairs of variables which appear in a common cluster), and the A_3 function obviously inherits this property. However the A_2 function has a non-local $\Lambda^2 \mathrm{B}_2$ component, so it is rather amazing that the particular linear combination of A_2's appearing inside A_3 give rise to the completely local eq. (4.12). Moreover, the two coproduct components see distinct aspects of the geometry of the Stasheff polytope—the $\Lambda^2\,\mathrm{B}_2$ component involves the three quadrilateral faces (i.e., the $A_1\times A_1$ subalgebras) while the $\mathrm{B}_3\otimes\mathbb{C}^*$ component involves the six pentagonal faces (the A_2 subalgebras). It is tempting to anticipate the possibility that this notion of locality within the Stasheff polytope might underlie the structure of SYM theory scattering amplitudes in a very deep way. If this proves to be so, we cannot help but wonder (following somewhat the motivation espoused by [40]) whether there exists an alternative formulation of SYM theory scattering amplitudes which makes this "locality in the Stasheff polytope" manifest.

A conjecture central to our approach is that the set of f_{A_3} for all possible A_3 subalgebras of $\mathrm{Gr}(4,n)$ spans the space of all weight-four cluster polylogarithm functions whose coproduct components are completely "local" (involving only quadrilaterals in $\Lambda^2\,\mathrm{B}_2$ and only pentagons in $\mathrm{B}_3\otimes\mathbb{C}^*$).

We now display a simple realization of the A_3 function in a familiar setting: the $\mathrm{Gr}(4,6)$ algebra, relevant to 6-particle scattering, which is in fact isomorphic to A_3. In order to align with the notation in chapter 2, we consider $(x_1,x_2,x_3)=(x_1^-,e_6,1/x_1^+)$ and relate $x_{i,1}=x_i^-$ and $x_{i,2}=x_i^+$. The 15 $\mathcal{X}$-coordinates can then be written as

$$\begin{aligned}
v_1 &= \frac{\langle 1246\rangle\langle 1345\rangle}{\langle 1234\rangle\langle 1456\rangle}, & v_2 &= \frac{\langle 1235\rangle\langle 2456\rangle}{\langle 1256\rangle\langle 2345\rangle}, & v_3 &= \frac{\langle 1356\rangle\langle 2346\rangle}{\langle 1236\rangle\langle 3456\rangle},\\
x_1^+ &= \frac{\langle 1456\rangle\langle 2356\rangle}{\langle 1256\rangle\langle 3456\rangle}, & x_2^+ &= \frac{\langle 1346\rangle\langle 2345\rangle}{\langle 1234\rangle\langle 3456\rangle}, & x_3^+ &= \frac{\langle 1236\rangle\langle 1245\rangle}{\langle 1234\rangle\langle 1256\rangle},\\
x_1^- &= \frac{\langle 1234\rangle\langle 2356\rangle}{\langle 1236\rangle\langle 2345\rangle}, & x_2^- &= \frac{\langle 1256\rangle\langle 1346\rangle}{\langle 1236\rangle\langle 1456\rangle}, & x_3^- &= \frac{\langle 1245\rangle\langle 3456\rangle}{\langle 1456\rangle\langle 2345\rangle},\\
e_1 &= \frac{\langle 1246\rangle\langle 3456\rangle}{\langle 1456\rangle\langle 2346\rangle}, & e_2 &= \frac{\langle 1235\rangle\langle 1456\rangle}{\langle 1256\rangle\langle 1345\rangle}, & e_3 &= \frac{\langle 1256\rangle\langle 2346\rangle}{\langle 1236\rangle\langle 2456\rangle},\\
e_4 &= \frac{\langle 1236\rangle\langle 1345\rangle}{\langle 1234\rangle\langle 1356\rangle}, & e_5 &= \frac{\langle 1234\rangle\langle 2456\rangle}{\langle 1246\rangle\langle 2345\rangle}, & e_6 &= \frac{\langle 1356\rangle\langle 2345\rangle}{\langle 1235\rangle\langle 3456\rangle}.
\end{aligned} \tag{4.13}$$

Notably absent from this list are the three cross-ratios u_1,u_2,u_3 often used in the physics literature; these are related to the v_i's by $u_i = 1/(1+v_i)$. Evaluating eq. (4.11) on the variables in (4.13) generates what we will call "the $\mathrm{Gr}(4,6)$ function".

It is interesting to note that the transformation of the $\mathrm{Gr}(4,6)$ function with respect to the dihedral group acting on the 6 particles is opposite to that of the 5-particle dihedral group acting on the A_2 function. Specifically, the $\mathrm{Gr}(4,6)$ function is invariant under flipping particle i to particle $7-i$, but it is antisymmetric under a cyclic rotation $i \to i+1$. This antisymmetry is manifest for example in eq. (4.12) upon noting that the $x_i^{\pm}$ transform under a cyclic rotation according to

$$x_i^{\pm} \to x_{i+1}^{\mp}. \tag{4.14}$$

The $\mathrm{Gr}(4,6)$ algebra has an additional involution of order 2, called parity in [52] (it corresponds to complex conjugation in Minkowski space kinematics), under which the $\mathcal{X}$-coordinates transform according to

$$v_i \mapsto v_i, \qquad x_i^{\pm} \mapsto x_i^{\mp}, \qquad e_i \mapsto e_{i+3}. \tag{4.15}$$

The $\mathrm{Gr}(4,6)$ function is antisymmetric under this parity operation.

The fact that MHV amplitudes are required to be fully invariant under both parity and cyclic symmetry, yet the unique non-classical weight four function with the right cluster properties is antisymmetric under these symmetries, "explains why" the two-loop 6-particle MHV amplitude [19] must be expressible in terms of classical polylogarithms[6].

[6] An explanation with the same flavor, but based on more physical constraints (rather than our more mathematical constraints) was given in [67].

4.4 Cluster polylogarithms for $\mathrm{Gr}(4,7)$ and the amplitude $R_7^{(2)}$

We now demonstrate the utility of the A_3 function for two-loop MHV scattering amplitudes by providing, as an illustrative example, an explicit representation of the two-loop 7-particle MHV amplitude (modulo products of functions of lower weight, as always). We have carried out this exercise for $n > 7$ (where the cluster algebras $\mathrm{Gr}(4,n)$ are of infinite type) with no difficulty, but we relegate a detailed analysis of these more complicated results to chapter 6

First let us take a look at the A_2 subalgebras. The $\mathrm{Gr}(4,7) = E_6$ cluster algebra has 1071 A_2 subalgebras (i.e., 1071 pentagonal faces on its generalized Stasheff polytope) on which the A_2 function can be evaluated, but only 504 of these give distinct results. We can tabulate here the 504 "distinct A_2 subalgebras" by providing their quivers, in terms of cluster $\mathcal{X}$-coordinates for $\mathrm{Gr}(4,7)$. First we have

$$\frac{\langle 1245\rangle\langle 1567\rangle}{\langle 1257\rangle\langle 1456\rangle} \to \frac{\langle 1247\rangle\langle 1256\rangle\langle 1345\rangle}{\langle 1234\rangle\langle 1257\rangle\langle 1456\rangle}, \qquad \frac{\langle 1237\rangle\langle 1245\rangle\langle 4567\rangle}{\langle 2457\rangle\langle 1(23)(45)(67)\rangle} \to \frac{\langle 1267\rangle\langle 1457\rangle\langle 2345\rangle}{\langle 2457\rangle\langle 1(23)(45)(67)\rangle}, \tag{4.16}$$

and their cyclic images ($2 \times 7 = 14$ total quivers). It suffices to take just the cyclic images because both parity and $i \to 8-i$ map this set back to itself. Next we have

$$\begin{aligned}
&\frac{\langle 1236\rangle\langle 1245\rangle}{\langle 1234\rangle\langle 1256\rangle} \to \frac{\langle 1237\rangle\langle 1246\rangle}{\langle 1234\rangle\langle 1267\rangle}, \frac{\langle 1237\rangle\langle 1246\rangle}{\langle 1234\rangle\langle 1267\rangle} \to \frac{\langle 1247\rangle\langle 1456\rangle\langle 2346\rangle}{\langle 1234\rangle\langle 1467\rangle\langle 2456\rangle},\\
&\frac{\langle 1237\rangle\langle 1246\rangle}{\langle 1234\rangle\langle 1267\rangle} \to -\frac{\langle 1247\rangle\langle 3456\rangle}{\langle 4(12)(35)(67)\rangle}, \frac{\langle 1236\rangle\langle 1345\rangle}{\langle 1234\rangle\langle 1356\rangle} \to \frac{\langle 1237\rangle\langle 1346\rangle}{\langle 1234\rangle\langle 1367\rangle},\\
&\frac{\langle 1236\rangle\langle 1567\rangle}{\langle 1267\rangle\langle 1356\rangle} \to \frac{\langle 1237\rangle\langle 1256\rangle\langle 1346\rangle}{\langle 1234\rangle\langle 1267\rangle\langle 1356\rangle}, \frac{\langle 1234\rangle\langle 1357\rangle}{\langle 1237\rangle\langle 1345\rangle} \to \frac{\langle 1235\rangle\langle 1367\rangle\langle 3457\rangle}{\langle 1237\rangle\langle 1345\rangle\langle 3567\rangle},\\
&\frac{\langle 1246\rangle\langle 1345\rangle}{\langle 1234\rangle\langle 1456\rangle} \to \frac{\langle 1247\rangle\langle 1346\rangle}{\langle 1234\rangle\langle 1467\rangle},
\end{aligned} \tag{4.17}$$

along with their cyclic and parity images ($7 \times 14 = 98$ total quivers). In this case it suffices to take only these images since $i \to 8-i$ maps this set back to itself. And finally,

$$\begin{aligned}
&\frac{\langle 1236\rangle\langle 1245\rangle}{\langle 1234\rangle\langle 1256\rangle} \to \frac{\langle 1246\rangle\langle 1345\rangle}{\langle 1234\rangle\langle 1456\rangle}, \frac{\langle 1234\rangle\langle 1256\rangle}{\langle 1236\rangle\langle 1245\rangle} \to \frac{\langle 1235\rangle\langle 1267\rangle\langle 1456\rangle}{\langle 1236\rangle\langle 1245\rangle\langle 1567\rangle},\\
&\frac{\langle 1236\rangle\langle 1245\rangle}{\langle 1234\rangle\langle 1256\rangle} \to \frac{\langle 1246\rangle\langle 2345\rangle}{\langle 1234\rangle\langle 2456\rangle}, \frac{\langle 1234\rangle\langle 1256\rangle}{\langle 1236\rangle\langle 1245\rangle} \to \frac{\langle 1235\rangle\langle 1267\rangle\langle 2456\rangle}{\langle 1236\rangle\langle 1245\rangle\langle 2567\rangle},\\
&\frac{\langle 1234\rangle\langle 1256\rangle}{\langle 1236\rangle\langle 1245\rangle} \to \frac{\langle 1235\rangle\langle 1267\rangle\langle 3456\rangle}{\langle 1236\rangle\langle 5(12)(34)(67)\rangle}, \frac{\langle 1235\rangle\langle 4567\rangle}{\langle 5(12)(34)(67)\rangle} \to \frac{\langle 1236\rangle\langle 1245\rangle}{\langle 1234\rangle\langle 1256\rangle},\\
&\frac{\langle 1235\rangle\langle 1456\rangle}{\langle 1256\rangle\langle 1345\rangle} \to \frac{\langle 1237\rangle\langle 1245\rangle}{\langle 1234\rangle\langle 1257\rangle}, \frac{\langle 1237\rangle\langle 1245\rangle}{\langle 1234\rangle\langle 1257\rangle} \to \frac{\langle 1247\rangle\langle 2345\rangle}{\langle 1234\rangle\langle 2457\rangle},\\
&\frac{\langle 1234\rangle\langle 1257\rangle}{\langle 1237\rangle\langle 1245\rangle} \to \frac{\langle 1235\rangle\langle 1267\rangle\langle 2457\rangle}{\langle 1237\rangle\langle 1245\rangle\langle 2567\rangle}, \frac{\langle 1236\rangle\langle 1456\rangle}{\langle 1256\rangle\langle 1346\rangle} \to \frac{\langle 1237\rangle\langle 1246\rangle}{\langle 1234\rangle\langle 1267\rangle},\\
&\frac{\langle 1234\rangle\langle 1356\rangle}{\langle 1236\rangle\langle 1345\rangle} \to \frac{\langle 1235\rangle\langle 1367\rangle\langle 3456\rangle}{\langle 1236\rangle\langle 1345\rangle\langle 3567\rangle}, \frac{\langle 1234\rangle\langle 1356\rangle}{\langle 1236\rangle\langle 1345\rangle} \to \frac{\langle 1235\rangle\langle 1567\rangle\langle 3456\rangle}{\langle 1256\rangle\langle 1345\rangle\langle 3567\rangle},\\
&\frac{\langle 1235\rangle\langle 1567\rangle}{\langle 1257\rangle\langle 1356\rangle} \to \frac{\langle 1237\rangle\langle 1256\rangle\langle 1345\rangle}{\langle 1234\rangle\langle 1257\rangle\langle 1356\rangle}, \frac{\langle 1234\rangle\langle 1267\rangle\langle 1356\rangle}{\langle 1237\rangle\langle 1256\rangle\langle 1346\rangle} \to \frac{\langle 1236\rangle\langle 1567\rangle\langle 3456\rangle}{\langle 1256\rangle\langle 1346\rangle\langle 3567\rangle},
\end{aligned} \tag{4.18}$$

along with their dihedral and parity images ($14 \times 28 = 392$ total quivers).

The A_2 function evaluates to 504 distinct results on these 504 algebras, but the 504 resulting quantities are not linearly independent: there are 56 linear relationships amongst these A_2 functions. It would be interesting to clarify the geometric origin of these linear relations. We conjecture, but lack the computer power to prove by explicit computation, that these 504 quantities span the space of nontrivial weight-four cluster functions for the $\mathrm{Gr}(4,7)$ algebra.

The $\mathrm{Gr}(4,7)$ algebras has 476 A_3 subalgebras on which we can evaluate f_{A_3}, but only 364 of these give distinct results. We conjecture that these 364 quantities span the space of non-trivial weight-four cluster functions with completely local coproducts having the desired Poisson structure properties (0 in $\Lambda^2\,\mathrm{B}_2$ and ± 1 in $\mathrm{B}_3 \otimes \mathbb{C}^*$).

We can list the 364 distinct A_3 evaluations by separating them in to three classes, and providing one (out of a possible six) generating quiver for each. First of all there are $14 \times 2 = 28$ A_3's generated by the quivers

$$\begin{aligned}
&\frac{\langle 1236\rangle\langle 1245\rangle}{\langle 1234\rangle\langle 1256\rangle} \to \frac{\langle 1234\rangle\langle 2456\rangle}{\langle 1246\rangle\langle 2345\rangle} \to \frac{\langle 1256\rangle\langle 2345\rangle\langle 4567\rangle}{\langle 1245\rangle\langle 2567\rangle\langle 3456\rangle},\\
&\frac{\langle 1256\rangle\langle 2345\rangle\langle 4567\rangle}{\langle 1245\rangle\langle 2567\rangle\langle 3456\rangle} \to \frac{\langle 1246\rangle\langle 2567\rangle}{\langle 1267\rangle\langle 2456\rangle} \to \frac{\langle 1236\rangle\langle 1245\rangle}{\langle 1234\rangle\langle 1256\rangle},
\end{aligned} \tag{4.19}$$

along with their dihedral images. Next there are $14 \times 6 = 84$ A_3's generated by the quivers

$$
\begin{aligned}
&\frac{\langle 1245\rangle\langle 3456\rangle}{\langle 1456\rangle\langle 2345\rangle} \to \frac{\langle 1235\rangle\langle 1456\rangle}{\langle 1256\rangle\langle 1345\rangle} \to \frac{\langle 1234\rangle\langle 1256\rangle}{\langle 1236\rangle\langle 1245\rangle},\\
&\frac{\langle 1234\rangle\langle 1257\rangle}{\langle 1237\rangle\langle 1245\rangle} \to \frac{\langle 1237\rangle\langle 1256\rangle}{\langle 1235\rangle\langle 1267\rangle} \to \frac{\langle 1245\rangle\langle 1567\rangle}{\langle 1257\rangle\langle 1456\rangle},\\
&\frac{\langle 1267\rangle\langle 1356\rangle}{\langle 1236\rangle\langle 1567\rangle} \to \frac{\langle 1346\rangle\langle 3567\rangle}{\langle 1367\rangle\langle 3456\rangle} \to \frac{\langle 1236\rangle\langle 1345\rangle}{\langle 1234\rangle\langle 1356\rangle},\\
&\frac{\langle 1237\rangle\langle 1245\rangle}{\langle 1234\rangle\langle 1257\rangle} \to \frac{\langle 1234\rangle\langle 2457\rangle}{\langle 1247\rangle\langle 2345\rangle} \to \frac{\langle 1257\rangle\langle 2345\rangle\langle 4567\rangle}{\langle 1245\rangle\langle 2567\rangle\langle 3457\rangle},\\
&\frac{\langle 1237\rangle\langle 1246\rangle}{\langle 1234\rangle\langle 1267\rangle} \to \frac{\langle 1234\rangle\langle 1267\rangle\langle 1456\rangle}{\langle 1247\rangle\langle 1256\rangle\langle 1346\rangle} \to \frac{\langle 1256\rangle\langle 1346\rangle\langle 4567\rangle}{\langle 1246\rangle\langle 1567\rangle\langle 3456\rangle},\\
&\frac{\langle 1257\rangle\langle 2345\rangle\langle 4567\rangle}{\langle 1245\rangle\langle 2567\rangle\langle 3457\rangle} \to \frac{\langle 1247\rangle\langle 2567\rangle}{\langle 1267\rangle\langle 2457\rangle} \to \frac{\langle 1237\rangle\langle 1245\rangle}{\langle 1234\rangle\langle 1257\rangle},
\end{aligned}
\tag{4.20}
$$

along with their cyclic and parity images. Finally we have the $9 \times 28 = 252$ A_3's generated by the quivers

$$
\begin{aligned}
&\frac{\langle 1256\rangle\langle 4567\rangle}{\langle 1567\rangle\langle 2456\rangle} \to \frac{\langle 1246\rangle\langle 1567\rangle}{\langle 1267\rangle\langle 1456\rangle} \to \frac{\langle 1236\rangle\langle 1245\rangle}{\langle 1234\rangle\langle 1256\rangle}, \frac{\langle 1236\rangle\langle 1245\rangle}{\langle 1234\rangle\langle 1256\rangle} \to \frac{\langle 1234\rangle\langle 1456\rangle}{\langle 1246\rangle\langle 1345\rangle} \to \frac{\langle 1256\rangle\langle 1345\rangle\langle 4567\rangle}{\langle 1245\rangle\langle 1567\rangle\langle 3456\rangle},\\
&\frac{\langle 1245\rangle\langle 1567\rangle}{\langle 1257\rangle\langle 1456\rangle} \to \frac{\langle 1235\rangle\langle 1456\rangle}{\langle 1256\rangle\langle 1345\rangle} \to \frac{\langle 1234\rangle\langle 1257\rangle}{\langle 1237\rangle\langle 1245\rangle}, \frac{\langle 1234\rangle\langle 1257\rangle}{\langle 1237\rangle\langle 1245\rangle} \to \frac{\langle 1237\rangle\langle 1256\rangle}{\langle 1235\rangle\langle 1267\rangle} \to \frac{\langle 1245\rangle\langle 2567\rangle}{\langle 1257\rangle\langle 2456\rangle},\\
&\frac{\langle 1245\rangle\langle 2567\rangle}{\langle 1257\rangle\langle 2456\rangle} \to \frac{\langle 1235\rangle\langle 2456\rangle}{\langle 1256\rangle\langle 2345\rangle} \to \frac{\langle 1234\rangle\langle 1257\rangle}{\langle 1237\rangle\langle 1245\rangle}, \frac{\langle 1257\rangle\langle 4567\rangle}{\langle 1567\rangle\langle 2457\rangle} \to \frac{\langle 1247\rangle\langle 1567\rangle}{\langle 1267\rangle\langle 1457\rangle} \to \frac{\langle 1237\rangle\langle 1245\rangle}{\langle 1234\rangle\langle 1257\rangle},\\
&\frac{\langle 1246\rangle\langle 1567\rangle}{\langle 1267\rangle\langle 1456\rangle} \to \frac{\langle 1236\rangle\langle 1456\rangle}{\langle 1256\rangle\langle 1346\rangle} \to \frac{\langle 1234\rangle\langle 1267\rangle}{\langle 1237\rangle\langle 1246\rangle}, \frac{\langle 1246\rangle\langle 1567\rangle}{\langle 1267\rangle\langle 1456\rangle} \to \frac{\langle 1236\rangle\langle 2456\rangle}{\langle 1256\rangle\langle 2346\rangle} \to \frac{\langle 1234\rangle\langle 1267\rangle}{\langle 1237\rangle\langle 1246\rangle},\\
&\frac{\langle 1345\rangle\langle 1567\rangle}{\langle 1357\rangle\langle 1456\rangle} \to \frac{\langle 1235\rangle\langle 3456\rangle}{\langle 1356\rangle\langle 2345\rangle} \to \frac{\langle 1234\rangle\langle 1357\rangle}{\langle 1237\rangle\langle 1345\rangle}
\end{aligned}
\tag{4.21}
$$

along with their dihedral and parity images.

While this collection of functions is dramatically more tame than the vastly over-complete space of completely general non-classical polylogarithms at weight 4, there are still 169 functional identities amongst these 364 f_{A_3}'s. Again, it would be very interesting to understand these relations geometrically.

We now turn our attention to the two-loop 7-point MHV amplitude, whose coproduct was calculated in chapter 2. The $B_3 \otimes \mathbb{C}^*$ portion of the coproduct can be separated into symmetric and antisymmetric parts under $\{x\}_3 \otimes y \to \{y\}_3 \otimes x$. The antisymmetric part, which corresponds to non-classical polylogarithms, can be fit to A_3 functions of the $\mathrm{Gr}(4,7)$ cluster algebra, and the symmetric part can be fit to $\mathrm{Li}_4(-\mathcal{X}\text{-coordinate})$.

The functional identities amongst A_3 functions prevent us from writing down a unique representation of $R_7^{(2)}$ at this point. We settle here for the shortest possible representation[7]:

$$
\begin{aligned}
R_7^{(2)} \sim\ & \frac{1}{2} f_{A_3}\left(\tfrac{\langle 1245\rangle\langle 1567\rangle}{\langle 1257\rangle\langle 1456\rangle}, \tfrac{\langle 1235\rangle\langle 1456\rangle}{\langle 1256\rangle\langle 1345\rangle}, \tfrac{\langle 1234\rangle\langle 1257\rangle}{\langle 1237\rangle\langle 1245\rangle}\right) + \frac{1}{2} f_{A_3}\left(\tfrac{\langle 1345\rangle\langle 1567\rangle}{\langle 1357\rangle\langle 1456\rangle}, \tfrac{\langle 1235\rangle\langle 3456\rangle}{\langle 1356\rangle\langle 2345\rangle}, \tfrac{\langle 1234\rangle\langle 1357\rangle}{\langle 1237\rangle\langle 1345\rangle}\right) \\
& + \mathrm{Li}_4\left(-\tfrac{\langle 1234\rangle\langle 1256\rangle}{\langle 1236\rangle\langle 1245\rangle}\right) + \mathrm{Li}_4\left(-\tfrac{\langle 1234\rangle\langle 1257\rangle}{\langle 1237\rangle\langle 1245\rangle}\right) + \frac{1}{4}\mathrm{Li}_4\left(-\tfrac{\langle 1234\rangle\langle 1357\rangle}{\langle 1237\rangle\langle 1345\rangle}\right) + \frac{1}{4}\mathrm{Li}_4\left(-\tfrac{\langle 1234\rangle\langle 1456\rangle}{\langle 1246\rangle\langle 1345\rangle}\right) \\
& - \frac{1}{4}\mathrm{Li}_4\left(-\tfrac{\langle 1234\rangle\langle 1257\rangle\langle 1356\rangle}{\langle 1237\rangle\langle 1256\rangle\langle 1345\rangle}\right) + \frac{1}{4}\mathrm{Li}_4\left(-\tfrac{\langle 1234\rangle\langle 1267\rangle\langle 1356\rangle}{\langle 1237\rangle\langle 1256\rangle\langle 1346\rangle}\right) + \frac{1}{4}\mathrm{Li}_4\left(-\tfrac{\langle 1235\rangle\langle 1456\rangle}{\langle 1256\rangle\langle 1345\rangle}\right) \\
& - \frac{1}{4}\mathrm{Li}_4\left(-\tfrac{\langle 1234\rangle\langle 1257\rangle\langle 1456\rangle}{\langle 1247\rangle\langle 1256\rangle\langle 1345\rangle}\right) - \frac{1}{4}\mathrm{Li}_4\left(-\tfrac{\langle 1234\rangle\langle 1267\rangle\langle 1456\rangle}{\langle 1247\rangle\langle 1256\rangle\langle 1346\rangle}\right) - \frac{1}{4}\mathrm{Li}_4\left(-\tfrac{\langle 1234\rangle\langle 1457\rangle}{\langle 1247\rangle\langle 1345\rangle}\right) \\
& + \text{ dihedral} + \text{parity conjugate.}
\end{aligned}
\tag{4.22}
$$

As indicated by the $\sim$, this result expresses the "most complicated part" of $R_7^{(2)}$— the difference between the function presented here and the actual amplitude is some weight-four polynomial in the functions $-\mathrm{Li}_k(-x)$ for $k = 1, 2, 3$ (and π^2), with arguments x drawn from the 385 $\mathcal{X}$-coordinates of the $\mathrm{Gr}(4, 7)$ cluster algebra.

We end this section by reiterating some important features of the A_2 and A_3 functions as conveyed in eq. (4.22). Given the known symbol of $R_7^{(2)}$ there is no difficulty in principle to find a representation of the non-classical component of this amplitude in terms of (for example) the collection $\mathrm{Li}_{2,2}$ functions (see the appendix) with simple ratios of $\mathcal{X}$-coordinates as arguments. The problem with fitting the non-classical portion of the amplitude to some general basis of this type is that these functions in general have non-$\mathcal{A}$ coordinates as entries in their symbols. Therefore, the remaining classical Li's needed to express the full amplitude could then have arbitrarily complicated algebraic functions of $\mathcal{X}$-coordinates as arguments, which makes constructing an ansatz exceptionally difficult. The A_2 function solves this problem because it has only $\mathcal{A}$-coordinates in its symbol, therefore providing a basis which is sufficient to capture the non-classical component while ensuring that the remaining

[7]Future developments may reveal that a different, longer representation is "better" by manifesting other properties, either a physical property such as smooth behavior under the collinear limit or possibly even an additional, so far unnoticed mathematical property.

classical Li's can be taken to have only (minus) $\mathcal{X}$-coordinates as arguments. The packaging of A_2 functions into A_3's manifests even more structure of the amplitude $R_7^{(2)}$—namely the complete (i.e., term-by-term) locality and Poisson structure of its coproduct components.

4.5 Conclusion

Motivated by the cluster structure apparently underlying the structure of amplitudes in SYM theory, in this chapter we defined and studied the simplest few examples of *cluster polylogarithm functions* at transcendentality weight four. We found that the A_2 algebra admits a single non-trivial function f_{A_2} of this type, and for several other cluster algebras which we were able to analyze by explicit computation we found that the space of cluster functions is spanned by f_{A_2} evaluated on all available A_2 subalgebras. Interestingly, we found that these functions all have "Stasheff polytope local" $B_3 \otimes \mathbb{C}^*$ content which can be expressed in terms of $\{x\}_3 \otimes y - \{y\}_3 \otimes x$ with pairs x, y having Poisson bracket 1 (and therefore associated to pentagonal faces of the appropriate generalized Stasheff polytope).

We then considered an even more special collection of "Stasheff polytope local" functions which have $\Lambda^2 \, \mathrm{B}_2$ content expressible in terms of $\{x\}_2 \wedge \{y\}_2$ with x, y having Poisson bracket 0 (and therefore associated to quadrilateral faces). For the A_3 algebra we found a unique nontrivial function f_{A_3} with this property, and conjectured that the space of such functions for more general algebras is spanned by the function f_{A_3} evaluated on all available A_3 subalgebras.

Obviously it would be of mathematical interest to further explore these classes of functions, as well as suitable generalizations of them at higher weight and for more general cluster algebras (especially algebras of infinite type).

We used the A_3 function to write an explicit formula for the "most complicated part" of the two-loop 7-particle MHV amplitude in SYM theory. We are confident that the A_3 function suffices to similarly express two-loop MHV amplitudes for all n, both because we have checked some cases explicitly but more importantly because we know that these amplitudes have completely local coproducts in the sense mentioned a moment ago (see chapter 6).

However a number of important questions about the cluster structure of these amplitudes remain. For example, attention was called in chapter 2 to the curious fact that the $\Lambda^2 B_2$ component of the 7-particle amplitude can be written as a 42-term linear combination of $\{x_i\}_2 \wedge \{x_j\}_2$ involving only 42 out of the 1785 distinct pairs of Poisson commuting $\mathcal{X}$-coordinates available in the $\mathrm{Gr}(4,7)$ cluster algebra. It was natural to wonder whether there is any characteristic of these 42 which distinguishes them from the rest, and which might be able to explain "why" the amplitude's coproduct can be expressed in terms of only these 42. Unfortunately we are no closer to answering this question than in chapter 2. The first obstacle is that eq. (2.40) is not manifestly expressible in terms of A_3 functions: there does not exist any A_3 subalgebra of $\mathrm{Gr}(4,7)$ which has a quadrilateral face corresponding to the first term in eq. (2.40) (nor to any of its symmetric images). In contrast, if we evaluate the $\Lambda^2 B_2$ content of the amplitude by starting with eq. (4.22) and associating to each f_{A_3} the corresponding coproduct component shown in eq. (4.12) we obtain a 56-term linear combination which is nontrivially equal to the 42-term expression presented in eq. (2.40)[8]. Also, the results of this chapter unfortunately shed no light on the curiosity noted in chapter 2 that for both $n = 6, 7$, the coproduct of the n-particle two-loop MHV amplitude can be expressed in terms of only 3/5 of the $\mathcal{X}$-coordinates available in the $\mathrm{Gr}(4,n)$ cluster algebra.

Our exploration of the appropriate function space for two-loop MHV amplitudes

[8]It turns out that 14 terms in the former correspond exactly to the 14 terms on the second line of eq. (2.40) of the latter; so perhaps it would be better to say that the nontrivial relation is between a 42-term expression and a 28-term expression in $\Lambda^2 B_2$.

at arbitrary n was strongly motivated by a similar exploration of functions appropriate for non-MHV and higher-loop $n = 6$ amplitudes by Dixon and collaborators [67, 68, 107]. It would be very interesting to explore the (necessarily very close) relationship between their "hexagon functions" and the various cluster functions we have explored, which we leave to future work. Here however we have focused exclusively on purely mathematical constraints: the $\mathcal{A}$-coordinate condition on symbols, the $\mathcal{X}$-coordinate condition on functions, and the locality and Poisson structure constraints on the coproduct. These are listed in order of increasing mathematical power, but also in order of increasing physical obscurity. We confess to having no physical explanation of why SYM theory should select weight-four polylogarithm functions whose coproducts are local in the generalized Stasheff polytope or have any particular relation to the Poisson structure, except to speculate that it might be related to the integrability of SYM theory. Notice also that clusters represent sets of coordinates that are compatible in some way. For instance, it is known [33] that for $\mathrm{Gr}(2, n)$ the cluster structure is isomorphic to that of polygon triangulations, and that in turn to planar tree diagrams. To each tree corresponds a cluster, which can therefore be thought of as a channel for the tree amplitude. Cluster coordinates are then compatible in the sense that they correspond to possible simultaneous poles in planar scattering. Perhaps some more sophisticated version of this argument will hold here. It is natural to wonder if there exists an alternative formulation for SYM theory amplitudes which makes these (and perhaps other, still hidden) cluster algebraic properties manifest.

With our current understanding of how to write down the most complicated part of the two-loop MHV amplitudes it is reasonable to contemplate finding fully analytic expressions for them. To this end the next step is to begin applying various physical constraints to fix ambiguities involving products of functions of lower weight as well as beyond-the-symbol terms. The most obvious such constraints include the first-and last-entry conditions on the symbol, the requirement of smooth behavior under collinear limits, and especially the highly constraining requirement of analyticity inside the Euclidean kinematic region. We believe the last of these, in particular, might be strong enough to fix a unique (or almost unique) "analytic tail" to the A_3 function, perhaps similar in form to the analytic tail which appears in the $L(x^+, x^-)$ building block of the GSVV formula [19]. Adding these terms of lower weight will help us resolve the ambiguities present in eq. (4.22), where we had to arbitrarily choose one out of many possible representations in terms of A_3 functions. Moreover we suspect that "the right" completion of the A_3 function (once it is found) will continue to be the unique non-classical building block for all n-particle two-loop MHV amplitudes.

Based on the surprising fact that the fundamental building block of the two-loop MHV amplitudes seems to be a function involving only $n = 6$ particles, it is natural to hope that the available results on higher-loop and NMHV functions for $n = 6$, when supplemented by suitable "cluster algebraic" constraints of the type we have discussed in this chapter, may serve as a springboard for unlocking the structure of n-particle MHV and NMHV amplitudes at higher loop order.

Chapter 5

Calculating $R_7^{(2)}$

In this chapter we tie together several threads which have run through the earlier chapters but have not yet been fully wrapped up. Our immediate goal will be to construct an explicit analytic formula for the two-loop seven-point MHV amplitude $R_7^{(2)}$ in SYM theory[1]. While it may be interesting in its own right, we do not view the formula itself as the primary result of this chapter. Rather our aim is to first review the various obstacles that arise in the pursuit of writing such analytic formulas, and then to bring together the relevant ideas and results from the previous chapters to argue that the problem of constructing analytic formulas for $R_n^{(2)}$ for any desired n may be considered "solved" (modulo the availability of sufficient computer power, of course). By this we mean that we describe an algorithm which, building on the scaffolding provided by Caron-Huot's computation [20] of the symbol of $R_n^{(2)}$, may be used to construct an analytic formula for any desired n. The result for $n = 6$ appeared in [19], and we present a result for $n = 7$ here as a specific application of our algorithm. Numerical studies of $R_n^{(2)}$ have been carried out for $n = 6$ in [51, 53, 109] and for higher n in [66, 110], and explicit formulas are known for the special case when all particles have momenta lying in a common $\mathbb{R}^{1,1}$ subspace of four-dimensional Minkowski space [70, 71, 82].

We do not address here the question of how the computational complexity of our algorithm scales with n because we hope that this will ultimately be an irrelevant question. As has happened often before in physics, and especially so in the study of SYM theory, we believe that once suitably packaged and digestible results accumulate for various relatively small values of n, the structure might become clear enough that one can extrapolate an all-n formula, which could subsequently be proven to be correct or at least could be checked to be consistent with all known properties of the true

[1]More precisely $R_n^{(L)}$ stands for the n-particle L-loop *remainder function*, after the infrared singularities of the amplitude have been subtracted in a now standard way following [13, 14]. Dual conformal symmetry requires $R_n^{(L)}$ to vanish for $n < 6$ at any loop order [28, 30], but a numerical study [109] established that $R_6^{(2)}$ is nonzero.

amplitudes.

Amplitudeology is a data-driven enterprise where insights gleaned by analyzing the results of a seemingly difficult calculation have often revealed hidden structure which trivialize the original calculation, and help to make the next set of calculations simpler (or even just possible). We very much anticipate that the formula we obtain for $R_7^{(2)}$ will not be the simplest or "best" one possible, but hope that the algorithm described in this chapter will prove useful for generating new data for the amplitude community.

Section 5.1 contains some brief background material and definitions. Section 5.2 comments on the difficulties of integrating symbols in general, and on the tools we employ to overcome these difficulties. We also discuss the relation of our work to a complementary approach to similar problems which has been used by Dixon and collaborators to achieve several impressive results on multi-loop six-point amplitudes [67, 68, 107, 111]. Section 5.3 outlines our general algorithm, while section 5.4 discusses its application to the specific case of $R_7^{(2)}$, culminating in the construction of a complete analytic formula for this amplitude, some properties of which are discussed in section 5.5.

5.1 Background

This section is a brief review of some of the more advanced mathematics that will appear throughout the rest of the chapter, namely the coproduct δ and cluster algebras. For a more thorough introduction to these topics, see chapters 2 and 4.

The space of polylogarithm functions modulo products is a Lie coalgebra with coproduct[2] δ. The coproduct maps a polylogarithm function of weight 4 (the case of relevance to two-loop amplitudes) into two component spaces, $\Lambda^2 B_2$ and $B_3 \otimes \mathbb{C}^*$.

[2]Throughout this chapter, we use the word "coproduct" to denote δ, which satisfies $\delta^2 = 0$, rather than Δ which operates by simply deconcatenating the symbol. We refer the reader to [55] for additional details.

Here, B_k refers to the Bloch group, which roughly speaking represents the space of classical weight k polylogarithm functions modulo functional relationships amongst Li_k and modulo products of functions of lower weight. Elements of B_k are linear combinations of objects denoted by $\{x\}_k$, which stands for the equivalence class containing the function $-\mathrm{Li}_k(-x)$. The $\Lambda^2 B_2$ component of the coproduct captures the obstruction to writing a function in terms of the classical polylogarithm functions Li_k [32, 112]. The $B_3 \otimes \mathbb{C}^*$ component of the coproduct encapsulates all of the intrinsically weight 4 terms in a function.

Cluster algebras are generated by a preferred set of variables ("cluster coordinates") grouped in disjoint sets called clusters related to each other by a transformation called mutation. The cluster algebra relevant for two-loop MHV scattering amplitudes in SYM theory is the $\mathrm{Gr}(4,n)$ Grassmannian cluster algebra, which is related to the kinematic configuration space for n particles, $\mathrm{Conf}_n(\mathbb{P}^3)$. These coordinates come in two flavors, $\mathcal{A}$- and $\mathcal{X}$- coordinates. An example of $\mathcal{A}$-coordinates are the standard Plücker coordinates $\langle ijkl\rangle = \det(Z_i Z_j Z_k Z_l)$ (in terms of momentum-twistor variables [46]). Slightly more complicated examples that will appear later in this chapter are of the type

$$\langle a(bc)(de)(fg)\rangle \equiv \langle abde\rangle\langle acfg\rangle - \langle abfg\rangle\langle acde\rangle, \tag{5.1}$$

$$\langle ab(cde)\cap(fgh)\rangle \equiv \langle acde\rangle\langle bfgh\rangle - \langle bcde\rangle\langle afgh\rangle. \tag{5.2}$$

Cluster $\mathcal{X}$-coordinates are a special class of cross-ratios built from $\mathcal{A}$-coordinates.

These two topics, polylogarithms and cluster algebras, merge beautifuly in the arena of SYM theory. Firstly, only cluster $\mathcal{A}$-coordinates for $\mathrm{Gr}(4,n)$ appear in the symbol for $R_n^{(2)}$. Moreover, the coproduct of $R_7^{(2)}$ was calculated in chapter 2 and it was noted that the elements $\{x\}_2$ and $\{x\}_3$ appearing in the coproduct were cluster $\mathcal{X}$-coordinates of the $\mathrm{Gr}(4,7)$ Grassmannian cluster algebra. Furthermore, it was noted that the function for $R_6^{(2)}$ obtained in [19] can be written purely in terms of classical polylogarithms Li_k with (negative) $\mathcal{X}$-coordinates as arguments. In this chapter we extend these connections to a general algorithm for constructing the function $R_n^{(2)}$.

Let us note that the $\mathrm{Gr}(4,n)$ cluster algebra has infinitely many $\mathcal{A}$- and $\mathcal{X}$-coordinates when $n > 7$, but we believe that this presents no obstruction to our algorithm since it is evident from the result of [20] that only finitely many (in fact, precisely $\frac{3}{2}n(n-5)^2$) of the $\mathcal{A}$-coordinates actually appear in the two-loop MHV amplitude $R_n^{(2)}$, and our experience has shown that the "most complicated part" of these amplitudes (see chapter 4 for details) can be expressed in terms of the $\mathcal{X}$-coordinates belonging to finitely many A_3 subalgebras of $\mathrm{Gr}(4,n)$. For the special cases $n = 6, 7$, we expect that the two-loop symbol alphabet (which contains already all available $\mathcal{A}$-coordinates) will be sufficient to express all amplitudes (whether MHV or not) to all loop order, but for $n > 7$ we know of no reason to exclude the possibility that the symbol alphabet could grow larger at higher loops (indeed we expect it to become infinite for ten-point N^3MHV amplitudes starting already at only two loops).

A salient feature of cluster $\mathcal{X}$-coordinates is that they are positive when evaluated inside the positive Grasmmannian, defined as the subset of the Euclidean domain where $\langle ijkl\rangle > 0$ whenever $i < j < k < l$. This is incredibly important because it allows us to impose analyticity inside the positive domain with relative ease (since $\mathrm{Li}_k(x)$ is smooth for $x < 0$), in particular without having to worry about branch cuts. It would be interesting to check the extension of our final formula to more general Euclidean kinematics, for which it would be necessary to specify where to take the branch cut of each $\mathrm{Li}_k(x)$ (as was done for example in [19] for $n = 6$). It would also be interesting to explore the analytic continuation to other regions outside the Euclidean domain, for example to make contact with work on the seven-point amplitude in the multi-Regge regime [77, 102, 113].

Before we describe our algorithm we would first like to clarify the difficulties that our cluster algebraic approach allows us to overcome.

5.2 The Problem of Integrating Symbols

The problem of finding an explicit polylogarithm function whose symbol matches a given random (but integrable) symbol is hopeless; no algorithm exists in general. Fortunately, amplitudes in SYM theory do not have random symbols, nor do we expect them to be expressed in terms of completely random functions.

In such happier cases the problem can be tractable if the desired function may be expressed in terms of some class of generalized polylogarithm functions whose arguments are all drawn from some particular finite collection of well-behaved variables. Then the problem of integrating the symbol becomes simply one of linear algebra: one writes a general linear combination of the functions in the ansatz, and chooses the coefficients to match the desired symbol. Ideally, the ansatz should be just big enough to contain the answer, and not too big. If the ansatz is too overcomplete[3] there can be considerable ambiguity in choosing a functional representative for the integrated symbol.

If one were merely interested in being able to obtain numerical values for SYM amplitudes, then such ambiguity would be of little concern. If the goal however is to unlock their mathematical structure, then it is desirable to have functional representations which manifest, to the extent possible, all of their known properties. From this point of view, any ambiguity in how to write an amplitude is seen as an inefficiency, a wasted opportunity.

In a series of papers [67, 68, 107, 111], Dixon and collaborators have pursued one approach to this problem by studying "hexagon functions", defined as polylogarithm

[3]Some overcompleteness is inevitable in our approach due to Li_k identities involving configurations of points in projective space (see for example [32, 112, 114]), but such identities are rare when the arguments are restricted to be (negative) cluster $\mathcal{X}$-coordinates. The only currently known non-trivial identities of this type are the 5-term A_2 identity (Abel's identity) for Li_2 and the 40-term D_4 identity for Li_3 described in [52].

functions whose symbol can be expressed in terms of a certain 9-letter alphabet (in our terminology, the alphabet of $\mathcal{A}$-coordinates for the $\mathrm{Gr}(4,6)$ Grassmannian cluster algebra) and which have the appropriate analytic structure for scattering amplitudes (specifically, that they must be analytic everywhere inside the Euclidean domain, with branch points on the boundary of the Euclidean domain when $\langle i\, i{+}1\, j\, j{+}1\rangle = 0$ for some i, j). By systematically classifying such hexagon functions through weight eight, and by using physical input about the near-collinear limit derived from the Wilson loop OPE approach [84, 103, 104, 115, 116] and from the multi-Regge limit [68, 79, 117–123], they have determined analytic expressions for the six-point NMHV amplitude at two loops, and the six-point MHV amplitude at three and four loops.

It would be extremely interesting to pursue a similar approach for $n > 6$, by exploring for example the space of "heptagon functions". Our trepidation to take this route stems from the fact that the required symbol alphabet grows rapidly with n: as mentioned above, the symbol alphabet for $R_n^{(2)}$ has $\frac{3}{2}n(n-5)^2$ entries [20], so the space of weight-four symbols has dimension[4] $\mathcal{O}(n^{12})$.

We have pursued instead the somewhat orthogonal approach of organizing our calculations not from left-to-right in the symbol, but rather in order of decreasing mathematical complexity of the functional constituents. At weight four, this means that we first focus our attention on the "non-classical" part of the amplitude: the $\Lambda^2 B_2$ component of its coproduct. The remaining purely classical pieces of an amplitude can be systematically computed in order from most to least complicated by following the procedure outlined in [19]. This approach has the disadvantage of leaving the analytic properties of amplitudes obscure, while it has the advantage of making some remarkable mathematical properties—the relation to the cluster structure on the kinematic domain—manifest.

The very first step in this approach is the one most fraught with peril, as we now

[4]This is rather too pessimistic; the analyticity condition cuts this down by one power of n and the integrability condition no doubt cuts down by some more powers of n.

explain. The $\Lambda^2 B_2$ component of the coproduct of $R_n^{(2)}$ can be expressed as a linear combination of various $\{x_i\}_2 \wedge \{x_j\}_2$ where the x's are drawn from the $\mathcal{X}$-coordinates of the $\mathrm{Gr}(4,n)$ cluster algebra. Moreover, the x's always appear together in pairs satisfying $\{x_i, x_j\} = 0$ with respect to the natural Poisson structure on the kinematic domain $\mathrm{Conf}_n(\mathbb{P}^3)$; this implies that each pair of variables generates an $A_1 \times A_1$ subalgebra of the $\mathrm{Gr}(4,n)$ cluster algebra.

For several years a guiding aim of this research program, strongly advocated by Goncharov, has been that it should be possible to write each amplitude under consideration as a linear combination of special functions associated with smaller building blocks ("atoms"). For example, it is well-known that the function[5]

$$L_{2,2}(x,y) = \frac{1}{2}\int_0^1 \frac{dt}{t}\,\mathrm{Li}_2(-tx)\,\mathrm{Li}_1(-ty) - (x \leftrightarrow y) \tag{5.3}$$

has the simple $\Lambda^2 B_2$ coproduct component $\{x\}_2 \wedge \{y\}_2$. Therefore one might be tempted to construct the non-classical part of a desired $R_n^{(2)}$ by writing down an appropriate linear combination of $L_{2,2}(x_i, x_j)$ functions; the difference between this object and $R_n^{(2)}$ must then be expressible in terms of the classical functions Li_k only.

The fatal flaw in this approach is that while $L_{2,2}(x_i, x_j)$ indeed has a simple coproduct, it is poorly adapted to applications where one wants to manifest cluster structure because its symbol has some entries of the form $x_i - x_j$, which is never expressible as a product of cluster $\mathcal{A}$-coordinates (and thus can never be an $\mathcal{X}$-coordinate). Therefore one would have to considerably enlarge the symbol alphabet under consideration in order to fit all of the classical pieces of the amplitude left over by subtracting a linear combination of $L_{2,2}$'s. Just as bad, one would almost inevitably generate Li_k functions whose arguments range over the entire real line, greatly complicating the

[5] We caution the reader that several variants of this function exist in the literature, beginning with [60], all of which differ from each other by the addition of terms proportional to Li_4, or products of lower-weight Li_k's. In fact even in this short chapter we will use a second variant $K_{2,2}$ momentarily. All of these variants have the same $\Lambda^2 B_2$ coproduct component. The particular $L_{2,2}(x,y)$ used here may also be expressed as $L_{2,2}(x,y) = \frac{1}{2}\,\mathrm{Li}_{2,2}(x/y, -y) - (x \leftrightarrow y)$ in terms of the $\mathrm{Li}_{2,2}$ function.

problem of arranging all of the branch cuts of the individual terms to conspire to cancel out everywhere in the positive domain.

So if we want to maintain a connection to the cluster structure (and, more practically, to avoid enormously complicating the calculation by being forced to clean up unwanted mess in the symbol), we should abandon the idea that each individual term $\{x_i\}_2 \wedge \{x_j\}_2$ may be thought of as an atom[6]. The problem of identifying the smallest building block manifesting all of the known cluster properties of $R_n^{(2)}$ was solved (at least, for a few of the simplest cluster algebras, and more generally conjectured) in chapter 4. The solution is a function associated to the A_3 cluster algebra which we can write in the form

$$f_{A_3}(x_1, x_2, x_3) = \sum_{i=1}^{3} K_{2,2}(x_{i,1}, x_{i,2}), \tag{5.4}$$

where

$$\begin{aligned} x_{1,1} &= x_1, & x_{1,2} &= 1/x_3, \\ x_{2,1} &= (x_1 x_2 + x_2 + 1)\, x_3, & x_{2,2} &= \frac{x_1 x_2 + x_2 + 1}{x_1}, \\ x_{3,1} &= \frac{x_2 x_3 + x_3 + 1}{x_2}, & x_{3,2} &= \frac{x_2 x_3 + x_3 + 1}{x_1 x_2 x_3} \end{aligned} \tag{5.5}$$

and

$$K_{2,2}(x,y) = L_{2,2}(x,y) - \left[\mathrm{Li}_4(x/y) - \frac{1}{3}\mathrm{Li}_3(x/y)\log(x/y) - (x \leftrightarrow y)\right] - \frac{1}{2}\mathrm{Li}_2(-x)\,\mathrm{Li}_2(-y). \tag{5.6}$$

The expression for $K_{2,2}$ given here differs from the one presented in appendix A by the addition of terms proportional to products of logarithms as well as the final $\mathrm{Li}_2\,\mathrm{Li}_2$ term, none of which affect the coproduct of $K_{2,2}$.

[6]Instead they are perhaps quarks: never allowed to appear alone, but always bound safely together in A_2 functions or perhaps other, not yet discovered, more exotic baryons.

As long as the three x_i generate an A_3 algebra $x_1 \to x_2 \to x_3$ (which could be a subalgebra of a larger algebra), the A_3 function accomplishes a remarkable feat:

- the $\Lambda^2 B_2$ component of its coproduct, $\sum_{i=1}^{3} \{x_{i,1}\}_2 \wedge \{x_{i,2}\}_2$, involves only pairs of Poisson commuting $\mathcal{X}$-coordinates;
- the $B_3 \otimes \mathbb{C}^*$ component of its coproduct can be written in terms of $\mathcal{X}$-coordinates (the Li_4 term in $K_{2,2}$ is crucial here);
- its symbol can be written entirely in terms of $\mathcal{A}$-coordinates (here the $\mathrm{Li}_3 \log$ term is crucial);
- and it is smooth and real-valued everywhere inside the positive domain (i.e., as long as $x_1, x_2, x_3 > 0$), thanks to the terms which were added compared to eq. (A.4).

The $\mathrm{Li}_2 \mathrm{Li}_2$ term in (5.4) is completely innocuous and was chosen for inclusion because it was observed to nicely package together most of the $\mathrm{Li}_2 \mathrm{Li}_2$ terms in the amplitude $R_7^{(2)}$. It would be very interesting to see if a more optimal packaging of subleading terms could be obtained, whether for $n = 7$ or even for all n.

Working with A_3 functions, rather than the underlying individual $L_{2,2}$'s, therefore allows us to avoid having to enlarge the symbol alphabet beyond the set of cluster $\mathcal{A}$-coordinates. Moreover, when expressing the classical contributions to an amplitude we are able to restrict our attention to the functions $\mathrm{Li}_k(-x)$, which are smooth and real-valued throughout the positive domain as long as the arguments x are always taken from the set of cluster $\mathcal{X}$-coordinates.

5.3 The Algorithm for $R_n^{(2)}$

The algorithm is naturally broken into four steps. (1) As discussed in the previous section, we start by writing down a linear combination of A_3 cluster functions with the same $\Lambda^2 B_2$ content as the desired $R_n^{(2)}$. After subtracting this linear combination from the amplitude we are left with a function which (2) we express in terms of the classical polylogarithms Li_k following the algorithm described in [19]. One minor difference with respect to [19] is that we prioritize the Li_4 terms over those which can be written as products of lower-weight Li_k's, since only the former contribute to the $B_3 \otimes \mathbb{C}^*$ component of the coproduct. So, to be explicit, we proceed in the following order: f_{A_3}, Li_4, $\mathrm{Li}_2\,\mathrm{Li}_2$, $\mathrm{Li}_2 \log\log$, $\mathrm{Li}_3 \log$, $\log\log\log\log$.

At this stage we have a function with the same symbol as the amplitude, so the difference is expected to be equal to π^2 times polylogarithm functions of weight two. We ought not find any terms proportional to $i\pi$ times a function of weight three since at each step we work with functions that are manifestly free of branch cuts in the positive domain. (3) The $\mathcal{O}(\pi^2)$ terms can be found by comparison to the all-n formula for the differential $dR_n^{(2)}$ of the amplitude calculated in chapter 3. (4) Finally, the overall additive constant in the amplitude can be determined by enforcing smoothness of the collinear limit $R_n^{(2)} \to R_{n-1}^{(2)}$, a property which is built into the definition of the remainder function [14].

5.4 The Construction of $R_7^{(2)}$

We present here some details about the expression for $R_7^{(2)}$ generated by our algorithm. Some of the contributions, in particular the terms of the form $\mathrm{Li}_2 \log\log$ or $\log\log\log\log$, are too numerous to reasonably display in the text, so we refer the reader to the Mathematica file associated to [124] for the full symbolic result[7].

We begin by recalling the representation of the non-classical pieces of $R_7^{(2)}$ in terms

[7]In case of any discrepancy between formulas in the text and the Mathematica file, the latter is authoritative.

of A_3 functions, presented in chapter 4 as

$$\frac{1}{2} f_{A_3}\left(\frac{\langle 1245\rangle\langle 1567\rangle}{\langle 1257\rangle\langle 1456\rangle}, \frac{\langle 1235\rangle\langle 1456\rangle}{\langle 1256\rangle\langle 1345\rangle}, \frac{\langle 1234\rangle\langle 1257\rangle}{\langle 1237\rangle\langle 1245\rangle}\right) + \frac{1}{2} f_{A_3}\left(\frac{\langle 1345\rangle\langle 1567\rangle}{\langle 1357\rangle\langle 1456\rangle}, \frac{\langle 1235\rangle\langle 3456\rangle}{\langle 1356\rangle\langle 2345\rangle}, \frac{\langle 1234\rangle\langle 1357\rangle}{\langle 1237\rangle\langle 1345\rangle}\right)$$
$$+ \text{ dihedral} + \text{parity conjugate.} \quad (5.7)$$

As we emphasized in chapter 4, the difference between $R_7^{(2)}$ and (5.7) is a weight-four polynomial in the functions $\mathrm{Li}_k(-x)$ for $k = 1, 2, 3$ (and π^2), with arguments x drawn from the 385 $\mathcal{X}$-coordinates of the $\mathrm{Gr}(4, 7)$ cluster algebra.

The $B_3 \otimes \mathbb{C}^*$ component of the coproduct of $R_7^{(2)}$ was computed in chapter 2. We find that the Li_4 terms

$$-\mathrm{Li}_4\left(-\frac{\langle 1234\rangle\langle 1256\rangle}{\langle 1236\rangle\langle 1245\rangle}\right) - \mathrm{Li}_4\left(-\frac{\langle 1234\rangle\langle 1257\rangle}{\langle 1237\rangle\langle 1245\rangle}\right) - \frac{1}{2}\mathrm{Li}_4\left(-\frac{\langle 1234\rangle\langle 1357\rangle}{\langle 1237\rangle\langle 1345\rangle}\right) - \frac{1}{2}\mathrm{Li}_4\left(-\frac{\langle 1234\rangle\langle 1456\rangle}{\langle 1246\rangle\langle 1345\rangle}\right)$$
$$+ \text{ dihedral} + \text{parity conjugate,} \quad (5.8)$$

must be added to eq. (5.7) in order to correctly reproduce the full coproduct of the amplitude.

At this stage we know that the difference between $R_7^{(2)}$ and eqs. (5.7) plus (5.8) is a product of Li_k functions of weight strictly less than four. Following the procedure outlined in [19] we find that the missing $\mathrm{Li}_2\,\mathrm{Li}_2$ terms (beyond the ones that we have already snuck in via eq. (5.4)) are

$$\begin{aligned}
&\mathrm{Li}_2\left(\frac{\langle 3(17)(24)(56)\rangle}{\langle 1237\rangle\langle 3456\rangle}\right)\mathrm{Li}_2\left(\frac{\langle 1456\rangle\langle 3(17)(24)(56)\rangle}{\langle 1234\rangle\langle 1567\rangle\langle 3456\rangle}\right) + \mathrm{Li}_2\left(-\frac{\langle 1234\rangle\langle 1257\rangle}{\langle 1237\rangle\langle 1245\rangle}\right)\mathrm{Li}_2\left(-\frac{\langle 1234\rangle\langle 1457\rangle}{\langle 1247\rangle\langle 1345\rangle}\right)\\
&-\frac{1}{2}\mathrm{Li}_2\left(-\frac{\langle 1234\rangle\langle 1257\rangle}{\langle 1237\rangle\langle 1245\rangle}\right)\mathrm{Li}_2\left(-\frac{\langle 1245\rangle\langle 1567\rangle}{\langle 1257\rangle\langle 1456\rangle}\right) - \mathrm{Li}_2\left(-\frac{\langle 1234\rangle\langle 1357\rangle}{\langle 1237\rangle\langle 1345\rangle}\right)\mathrm{Li}_2\left(-\frac{\langle 1345\rangle\langle 1567\rangle}{\langle 1357\rangle\langle 1456\rangle}\right)\\
&-\mathrm{Li}_2\left(-\frac{\langle 1237\rangle\langle 1467\rangle}{\langle 1267\rangle\langle 1347\rangle}\right)\mathrm{Li}_2\left(-\frac{\langle 1236\rangle\langle 2567\rangle}{\langle 1267\rangle\langle 2356\rangle}\right) + \mathrm{Li}_2\left(-\frac{\langle 1236\rangle\langle 2567\rangle}{\langle 1267\rangle\langle 2356\rangle}\right)\mathrm{Li}_2\left(-\frac{\langle 2345\rangle\langle 3467\rangle}{\langle 2347\rangle\langle 3456\rangle}\right)
\end{aligned}$$
$$+ \text{ dihedral} + \text{parity conjugate.} \quad (5.9)$$

We also find the $\mathrm{Li}_3 \log$ terms to be

$$\begin{aligned}
&\left(\frac{1}{2}\mathrm{Li}_3\left(-\tfrac{\langle 1267\rangle\langle 1456\rangle}{\langle 1246\rangle\langle 1567\rangle}\right) - \frac{1}{2}\mathrm{Li}_3\left(-\tfrac{\langle 1246\rangle\langle 1345\rangle}{\langle 1234\rangle\langle 1456\rangle}\right)\right)\log\left(\tfrac{\langle 1237\rangle\langle 1246\rangle}{\langle 1234\rangle\langle 1267\rangle}\right)\\
&+\Bigg(-\frac{1}{2}\mathrm{Li}_3\left(-\tfrac{\langle 1237\rangle\langle 1345\rangle}{\langle 1234\rangle\langle 1357\rangle}\right)-\frac{1}{2}\mathrm{Li}_3\left(-\tfrac{\langle 1247\rangle\langle 1345\rangle}{\langle 1234\rangle\langle 1457\rangle}\right)+\mathrm{Li}_3\left(-\tfrac{\langle 1257\rangle\langle 1347\rangle}{\langle 1237\rangle\langle 1457\rangle}\right)+\mathrm{Li}_3\left(-\tfrac{\langle 1257\rangle\langle 1456\rangle}{\langle 1245\rangle\langle 1567\rangle}\right)\\
&+\frac{1}{2}\mathrm{Li}_3\left(-\tfrac{\langle 1267\rangle\langle 1456\rangle}{\langle 1246\rangle\langle 1567\rangle}\right)+\frac{1}{2}\mathrm{Li}_3\left(-\tfrac{\langle 1357\rangle\langle 1456\rangle}{\langle 1345\rangle\langle 1567\rangle}\right)-\mathrm{Li}_3\left(-\tfrac{\langle 1235\rangle\langle 1267\rangle\langle 1457\rangle}{\langle 1237\rangle\langle 1245\rangle\langle 1567\rangle}\right)\Bigg)\log\left(\tfrac{\langle 1247\rangle\langle 1345\rangle}{\langle 1234\rangle\langle 1457\rangle}\right)\\
&+\Bigg(-\mathrm{Li}_3\left(-\tfrac{\langle 1236\rangle\langle 1245\rangle}{\langle 1234\rangle\langle 1256\rangle}\right)-\frac{1}{2}\mathrm{Li}_3\left(-\tfrac{\langle 1237\rangle\langle 1245\rangle}{\langle 1234\rangle\langle 1257\rangle}\right)+\mathrm{Li}_3\left(-\tfrac{\langle 1247\rangle\langle 1256\rangle}{\langle 1245\rangle\langle 1267\rangle}\right)+\frac{1}{2}\mathrm{Li}_3\left(-\tfrac{\langle 1237\rangle\langle 1345\rangle}{\langle 1234\rangle\langle 1357\rangle}\right)\\
&+\frac{1}{2}\mathrm{Li}_3\left(-\tfrac{\langle 1246\rangle\langle 1345\rangle}{\langle 1234\rangle\langle 1456\rangle}\right)+\mathrm{Li}_3\left(-\tfrac{\langle 1247\rangle\langle 1345\rangle}{\langle 1234\rangle\langle 1457\rangle}\right)-\frac{1}{2}\mathrm{Li}_3\left(-\tfrac{\langle 1257\rangle\langle 1456\rangle}{\langle 1245\rangle\langle 1567\rangle}\right)-\frac{1}{2}\mathrm{Li}_3\left(-\tfrac{\langle 1267\rangle\langle 1456\rangle}{\langle 1246\rangle\langle 1567\rangle}\right)\\
&-\frac{1}{2}\mathrm{Li}_3\left(-\tfrac{\langle 1456\rangle\langle 2345\rangle}{\langle 1245\rangle\langle 3456\rangle}\right)-\mathrm{Li}_3\left(-\tfrac{\langle 1457\rangle\langle 2345\rangle}{\langle 1245\rangle\langle 3457\rangle}\right)+\mathrm{Li}_3\left(-\tfrac{\langle 1457\rangle\langle 2456\rangle}{\langle 1245\rangle\langle 4567\rangle}\right)\Bigg)\log\left(\tfrac{\langle 1237\rangle\langle 1245\rangle}{\langle 1234\rangle\langle 1257\rangle}\right)\\
&\qquad+\ \text{dihedral}+\text{parity conjugate.} \qquad (5.10)
\end{aligned}$$

The remaining $\mathrm{Li}_2 \log\log$ and $\log\log\log\log$ terms which must be added to eqs. (5.7), (5.8), (5.9) and (5.10) in order to fully match the known symbol of $R_7^{(2)}$ are too numerous to display here and are recorded in the attached Mathematica file [124].

Next we turn to the problem of fixing "beyond-the-symbol" terms, given by numerical constants (in this application, rational numbers times π^k) times functions of weight $4-k$. The terms proportional to π^2 may be deduced by computing the full differential of all of the terms we have accumulated so far, and subtracting the result from the known analytic formula for $dR_7^{(2)}$ [20, 100]. The result is a linear combination (with rational coefficients) of terms like $\pi^2\log(a_1)d\log a_2$ for various $\mathcal{A}$-coordinates a_1, a_2. This can be integrated analytically to a linear combination of terms like $\pi^2\,\mathrm{Li}_2(-x_i)$ and $\pi^2\log(x_j)\log(x_k)$ with all arguments being $\mathcal{X}$-coordinates. In this manner we find that the $\pi^2\,\mathrm{Li}_2$ terms in our representation of $R_7^{(2)}$ are given by

$$\frac{7\pi^2}{48}\,\mathrm{Li}_2\left(-\tfrac{\langle 1247\rangle\langle 1345\rangle}{\langle 1234\rangle\langle 1457\rangle}\right)-\frac{\pi^2}{8}\,\mathrm{Li}_2\left(-\tfrac{\langle 1(23)(45)(67)\rangle}{\langle 1234\rangle\langle 1567\rangle}\right)+\text{dihedral}+\text{parity conjugate}, \quad (5.11)$$

while the $\pi^2 \log\log$ terms are again somewhat too numerous to efficiently display here.

At this point we have constructed a function which agrees with $R_7^{(2)}$ up to a single overall additive constant[8]. This constant, expected to be a rational number times π^4, can be determined by the requirement that $R_7^{(2)} \to R_6^{(2)}$ smoothly in the collinear limit. We choose to parameterize the $6 \parallel 7$ collinear limit following [20] by replacing

$$Z_7 \to Z_7(t) = Z_6 - t(\alpha Z_1 + \beta Z_5) + t^2 Z_2, \tag{5.12}$$

with α and β being arbitrary parameters, and then taking the limit $t \to 0$. As long as the starting point $(Z_1, \ldots, Z_7)$ is inside the positive domain and α and β are chosen to be positive, then there exists a finite $t_0 > 0$ such that $(Z_1, \ldots, Z_6, Z_7(t))$ lies in the positive domain for all $0 < t < t_0$. Then the collinear limit[9]

$$\lim_{t\to 0^+} R_7^{(2)}(Z_1, \ldots, Z_6, Z_7(t)) = R_6^{(2)}(Z_1, \ldots, Z_6), \tag{5.13}$$

together with the known formula [19] for $R_6^{(2)}$, determines the overall additive constant in $R_7^{(2)}$.

Each cross-ratio appearing our formula for $R_7^{(2)}$ approaches either 0, ∞, or a finite value in the limit $t \to 0^+$, so it is a simple matter to compute the limit of the formula

[8]There are no $\zeta(3)\log$ terms since $dR_n^{(2)}$ is known [20] to not contain any terms proportional to $\zeta(3)$.

[9]We caution the reader that our normalization convention for $R_7^{(2)}$ agrees with that of [20], which differs by a factor of four from that of [19], so the $R_6^{(2)}$ appearing on the right-hand side of eq. (5.13) should be four times the function $R_6^{(2)}$ given in the latter reference.

using the asymptotic behavior of the polylogarithm functions

$$\mathrm{Li}_2(-1/t) \sim -\frac{1}{2}\log^2 t - \frac{\pi^2}{2}, \tag{5.14}$$

$$\mathrm{Li}_3(-1/t) \sim +\frac{1}{6}\log^3 t + \frac{\pi^2}{6}\log t, \tag{5.15}$$

$$\mathrm{Li}_4(-1/t) \sim -\frac{1}{24}\log^4 t - \frac{\pi^2}{12}\log^2 t - \frac{7\pi^4}{360} \tag{5.16}$$

together with the asymptotic expansions (when x, t and a are positive)

$$L_{2,2}(x,t) \sim 0, \tag{5.17}$$

$$L_{2,2}(x,1/t) \sim \frac{1}{4}\mathrm{Li}_2(-x)\log^2 t + \mathrm{Li}_3(-x)\log t + \mathrm{Li}_4(-x) + \frac{\pi^2}{12}\mathrm{Li}_2(-x), \tag{5.18}$$

$$\begin{aligned} L_{2,2}(1/t, a/t^2) \sim -\frac{5}{24}\log^4 t + \frac{1}{3}\log a \log^3 t - \frac{1}{8}\log^2 a \log^2 t \\ + \frac{\pi^4}{24}\log^2 t - \frac{\pi^2}{24}\log^2 a - \frac{\pi^4}{30}, \end{aligned} \tag{5.19}$$

where $\sim$ signifies the omission of terms which vanish as powers of t (or powers of t times powers of $\log t$). We have taken the limit of $R_7^{(2)}$ by choosing various random initial kinematic points in the positive domain with all momentum twistors having integer entries. Then, after taking the limit $t \to 0^+$, the two sides of eq. (5.13) can be evaluated numerically with arbitrary precision. In this manner we find that that we have to add $-\frac{13}{36}\pi^4$ to our formula for $R_7^{(2)}$ in order for eq. (5.13) to be satisfied.

5.5 The Function $R_7^{(2)}$

Several very different ingredients have gone into the construction of our formula for $R_7^{(2)}$, from Caron-Huot's calculation of symbols via an extension of superspace to the mathematical structure of cluster algebras. As an independent test that all of these ingredients have been put together correctly it is reassuring to compare our result to numerical values for $R_7^{(2)}$ obtained in [66] via the Wilson loop approach to scattering amplitudes in SYM theory.

To get an intuition for a function it is often useful to see a plot of it, such as fig. 11 of [66] which shows $R_7^{(2)}$ evaluated on the "symmetric line", the locus where

$$(u_{14}, u_{25}, u_{36}, u_{47}, u_{15}, u_{26}, u_{37}) = (u, u, u, u, u, u, u) \tag{5.20}$$

in terms of

$$u_{ij} = \frac{\langle i\, i{+}1\, j{+}1\, j{+}2\rangle \langle i{+}1\, i{+}2\, j\, j{+}1\rangle}{\langle i\, i{+}1\, j\, j{+}1\rangle \langle i{+}1\, i{+}2\, j{+}1\, j{+}2\rangle}. \tag{5.21}$$

When the seven momentum vectors of the scattering particles are required to lie in four spacetime dimensions, the u_{ij} are not free (indeed they cannot be, since the dimension of $\mathrm{Conf}_7(\mathbb{P}^3)$ is only six) but are constrained to satisfy a particular seventh-order polynomial equation called the Gram determinant constraint. The symmetric line intersects the Gram locus only at isolated points (specifically, at the roots of $(1+u)(1-4u+3u^2+u^3)^2$). The authors of [66] evaded this constraint by allowing the momenta to lie in arbitrary dimension. By making use of momentum twistor machinery our result for $R_7^{(2)}$ is solidly tied to four-dimensional kinematics, although we anticipate that it should not be very difficult to relax this constraint.

Until that is done we are therefore unable to provide a plot of our $R_7^{(2)}$ formula along the symmetric line. Instead we display in fig. 5.1 a plot of this function along the line segment

$$(u_{14}, u_{25}, u_{36}, u_{47}, u_{15}, u_{26}, u_{37}) = (u, u, u, u, u, u, \tfrac{(1-u-u^2)^2}{1-2u^2}) \tag{5.22}$$

which satisfies the Gram constraint for all u and which lies in the positive domain for $0 < u < u_0 = 0.35689586789\ldots$, this number being the smallest positive root of $1 - 4u + 3u^2 + u^3 = 0$.

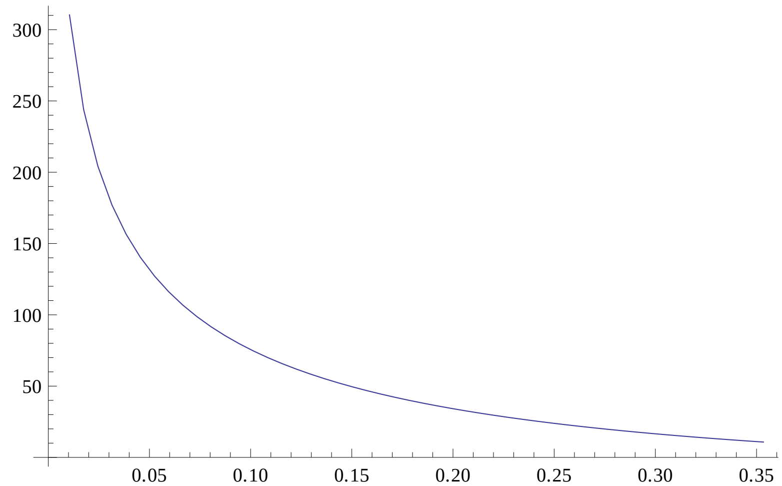

Figure 5.1: The two-loop seven-point MHV remainder function $R_7^{(2)}$ evaluated along the line segment parameterized by eq. (5.22) between $u = 0$ and the boundary of the positive domain at $u \approx 0.3569$.

The endpoint of this line segment at $u = u_0$ is rather special[10]: it touches the symmetric line at the tip of the positive domain. At this special point we find

$$R_7^{(2)}(u_0, u_0, u_0, u_0, u_0, u_0, u_0) = 10.4368451968\ldots. \tag{5.23}$$

At a conveniently chosen non-symmetric point point satisfying the Gram constraint we find for example

$$R_7^{(2)}(\tfrac{1}{4}, \tfrac{1}{4}, \tfrac{1}{4}, \tfrac{1}{4}, \tfrac{1}{4}, \tfrac{1}{4}, \tfrac{121}{224}) = 23.8717248322\ldots. \tag{5.24}$$

Both of these values are consistent with numerical results obtained using the Wilson loop computation of [66][11]. At all points in the positive domain where we have evaluated $R_7^{(2)}$, we have always found it take positive values, supporting the conjecture of [125].

[10]This point is a close analog to the special point $(u_{14}, u_{25}, u_{36}) = (\frac{1}{4}, \frac{1}{4}, \frac{1}{4})$ in six-particle kinematics.

[11]We thank A. Brandhuber, P. Heslop and G. Travaglini for correspondence and for providing us with their results at these kinematic points, which match eqs. (5.23) and (5.24) to 0.003%, within the estimated margin of error of their numerical calculation.

5.6 Conclusion

We have described an algorithm for bootstrapping explicit analytic formulas for the two-loop n-point MHV remainder functions $R_n^{(2)}$ in SYM theory from the differential of $R_n^{(2)}$ calculated in chapter 3. The algorithm expresses these amplitudes as linear combination of A_3 cluster polylogarithm functions and (products of) classical polylogarithm functions $\mathrm{Li}_k(-x)$ with arguments x drawn from the set of $\mathcal{X}$-coordinates [33] for the $\mathrm{Gr}(4,n)$ cluster algebra. Each building block utilized in the construction is manifestly real-valued and singularity-free inside the positive domain, ensuring that the generated formula for $R_n^{(2)}$ manifests this property as well.

As a sample application of this algorithm we have constructed an explicit analytic representation for $R_7^{(2)}$. We would like to emphasize that we have put almost no effort into optimizing our result, instead opting to see what we get by treating this as nothing more than a "shift-enter" computation. Although we were somewhat surprised that the answer came out as compact as it did, we anticipate that our result for $R_7^{(2)}$ will not be the "best" representation possible but hope that it may provide a useful starting point for further exploration of the structure of this amplitude. In that sense we suspect our representation for $R_7^{(2)}$ may be more similar to the DDS formula [17, 18] than to the GSVV formula [19] for $R_6^{(2)}$.

Let us end by speculating about some possible ways in which our representation for $R_7^{(2)}$ (and $R_n^{(2)}$ more generally) ought to be improved. As a general statement, it is our hope that amplitudes should admit natural functional representations which are as canonical as possible[12] and that any unexplained ambiguity in how to write an amplitude should be a cause for disappointment. This is because our ultimate dream is that it should be possible to formulate a list of physical and mathematical constraints which determine SYM theory amplitudes uniquely, and any free parameter

[12] Given the various known, but classifiable, polylogarithm identities—the 5-term A_2 identity for Li_2, the 40-term D_4 identity for Li_3, and other possibly existent identities not yet discovered.

appearing in the representation of some amplitude represents a lost opportunity to manifest some otherwise hidden property it satisfies.

For example, we find it suboptimal that (as mentioned in chapter 4) the non-classical part of $R_7^{(2)}$ may be expressed in many different ways in terms of A_3 functions. It would be fantastic if one could identify some particular A_3 subalgebras inside the $\mathrm{Gr}(4,7)$ cluster algebra (or $\mathrm{Gr}(4,n)$ more generally) which are for some reason preferred for expressing two-loop MHV amplitudes. Moreover it would be nice if all of the classical terms tabulated in section 4 could be absorbed into an appropriate redefinition of the A_3 function given in eq. (5.4) so that the complete formula for $R_7^{(2)}$, or even all $R_n^{(2)}$, could be written as a simple linear combination of suitably defined A_3 functions and nothing else. If this magic A_3 function were positive-valued inside the positive domain, it would furthermore manifest the conjectured [125] positivity of $R_n^{(2)}$ itself. It would be ideal if this could be done for all n in a way which manifests collinear limits, with the various A_3 functions appearing in $R_n^{(2)}$ tending either to zero or to $n-1$-point A_3 functions in the collinear limit. Finally, perhaps it is not the A_3 function but something else which is the right building block for realizing all of these dreams.

Chapter 6

Calculating $\delta\left(R_n^{(2)}\right)|_{\Lambda^2 B_2}$

The scattering amplitudes of planar $\mathcal{N}=4$ supersymmetric Yang-Mills (SYM) theory [126] comprise a collection of functions with remarkable mathematical properties, tightly restricted by the physical constraints they must satisfy. Indeed the mathematical and physical properties of these amplitudes are, collectively, so restrictive that one marvels that the functions can even exist at all. The program of using known (or supposed) general properties of amplitudes to assemble concrete new results, which can then be verified by applying consistency checks, is generally known as the amplitude bootstrap. One of the ultimate goals of this program is to formulate a concise list of simple physical and mathematical constraints which might uniquely determine the precise functional form of all amplitudes in SYM theory.

The simplest incarnation of the bootstrap program applies to those L-loop n-particle $\mathrm{N}^k\mathrm{MHV}$ amplitudes which belong to the class of generalized polylogarithm functions [21]. All amplitudes with $L < 2$ or $n < 10$ or $k < 3$ are believed [40] to belong to this class. Tools for dealing with the classes of functions which might appear in more general amplitudes are currently lacking, but there is every reason to suspect that a bootstrap program will forge ahead once the appropriate techniques are developed.

The essential tool for dealing with amplitudes of the generalized polylogarithm type is the symbol map (see [127]). The symbol of an amplitude of weight w $(= 2L)$ is an element of the w-fold tensor product of the multiplicative group generated by certain rational functions on the kinematic configuration space $\mathrm{Conf}_n(\mathbb{P}^3) = \mathrm{Gr}(4,n)/(\mathbb{C}^*)^{n-1}$ for n-particle scattering in SYM theory. A fundamental working hypothesis of the bootstrap is that the set of rational functions allowed to appear in the symbol of any amplitude (i.e., the "symbol alphabet") is the set of $\mathcal{A}$-coordinates on the $\mathrm{Gr}(4,n)$ cluster algebra. Starting with the special collection of functions (or symbols) of this type, one bootstraps an amplitude by applying constraints and comparing with independent data from the literature (for example, from the amplitude

OPE expansion [81, 83, 84, 128], or from multi-Regge limits [78, 117, 118, 123]), until one arrives at a unique putative result. The cluster $\mathcal{A}$-coordinate hypothesis is supported by all explicit results for amplitudes available in the literature to date, including two-loop MHV for all n [20], two-loop NMHV for $n = 6, 7$ [67, 69], three-loop MHV and NMHV for $n = 6$ [107, 129], and four-loop MHV for $n = 6$ [111].

Previous chapters have revealed that the connection between the cluster structure [33] on $\mathrm{Conf}_n(\mathbb{P}^3)$ and the mathematical structure of amplitudes in SYM theory runs much deeper than merely specifying the appropriate symbol alphabet. We use the term "cluster bootstrap" to emphasize that our focus will be on understanding the implications of these "more clustery" properties, and in particular on how to harness their power via bootstrap. In this chapter our attention is focused specifically on the planar n-particle two-loop MHV amplitudes $R_n^{(2)}$. We argue that these amplitudes are completely determined (modulo classical polylogarithm functions Li_k) by a straightforward cluster property together with a few simple physical constraints. Consideration of these constraints leads us to the concise explicit formula (6.13) which specifies $R_n^{(2)}$ modulo Li_k's.

6.1 Cluster Coordinates and Coproducts

Let us begin by recalling a few relevant facts about the $\mathrm{Gr}(4, n)$ Grassmannian cluster algebra. Cluster $\mathcal{X}$-coordinates are a preferred set of cross-ratios (dual conformally invariant [31] ratios of products of homogeneous polynomials in the $\mathcal{A}$-coordinates) on the kinematic domain $\mathrm{Conf}_n(\mathbb{P}^3)$. A "cluster" is a collection $\{x_i\}$ of $3(n-5)$ such coordinates with the property that the Poisson bracket matrix $B_{ij} = \{\log x_i, \log x_j\}$ has integer entries and maximal (if n is odd) or nearly maximal (if n is even) rank. Cluster $\mathcal{X}$-coordinates may be systematically constructed via a process called mutation, and a given $\mathcal{X}$-coordinate may appear in one or more clusters. For $n = 6, 7$ iterated application of mutations close on a finite set of clusters (14 and 833, respectively) containing a finite number of distinct $\mathcal{X}$-coordinates (15, 385).

For $n > 7$ one can mutate indefinitely to produce an infinite number of $\mathcal{A}$- and $\mathcal{X}$-coordinates, but this poses no conceptual obstacle to the bootstrap program since only finitely many can appear in any individual generalized polylogarithm function (i.e., at any finite loop order). For example, the symbol of $R_n^{(2)}$ contains $\frac{n}{2}(3n^2 - 30n + 77)$ $\mathcal{A}$-coordinates. These can easily be enumerated by inspecting the all-n result of [20]: in the notation of that paper, there are $n(n-6)$ symbol letters of the form $\langle 1(23)(n{-}1\,n)(i\,i{+}1)\rangle$ (plus all cyclic partners), $\frac{n}{2}(n-6)(n-7)$ of the form $\langle 12\,\bar{i} \cap \bar{j}\rangle$ (plus cyclic), and $\frac{n}{2}(n-5)(n-6)$ of the form $\langle 1(n2)(i\,i{+}1)(j\,j{+}1)\rangle$ (plus cyclic). Finally, there are of course the simple Plücker coordinates $\langle ijkl\rangle$, which number $\binom{n}{4}$; however it is evident from [20] that the only ones which appear in the two-loop MHV amplitudes are those in which at least one pair among ij, jk, kl or li are cyclically adjacent (for example, $\langle 1357\rangle$ does not appear for $n > 7$), so we must subtract $\frac{n}{24}(n-5)(n-6)(n-7)$ from $\binom{n}{4}$. Adding up all of these types we find a total of $\frac{n}{2}(3n^2 - 30n + 77)$ symbol letters.

To determine whether a dual conformal cross-ratio R formed from these letters is an $\mathcal{X}$-coordinate, we apply a simple heuristic, originally described in sec. 2.6.6: R is an $\mathcal{X}$-coordinate if $1 + R$ can also be expressed as a ratio of products of letters and if R is positive everywhere inside the positive domain (i.e., the domain in which $\langle ijkl\rangle > 0$ for all $i < j < k < l$). We know of no example where this heuristic fails.

Although the symbol of $R_n^{(2)}$ is known for all n [20], explicit analytic results for the function $R_n^{(2)}$ are available only for $n = 6, 7$ [19, 124]. While obtaining more general fully analytic results is certainly a worthwhile goal, in order to cut to the core of the mathematical structure of these functions it is natural to focus on the coproduct

$$\delta(R_n^{(2)}) \in \Lambda^2\,\mathrm{B}_2 \bigoplus \mathrm{B}_3 \otimes \mathbb{C}^*. \tag{6.1}$$

We remind the reader that the Bloch group B_n is generated by elements denoted $\{x\}_n$. Concretely, $\{x\}_n$ denotes the equivalence class of weight-n functions, modulo products, containing $-\mathrm{Li}_n(-x)$. Any generalized polylogarithm of weight 4 is determined, modulo products of functions of lower weight, by the two coproduct components shown above. Moreover the $\Lambda^2 \mathrm{B}_2$ component captures the "most nontrivial" part of a function and determines the $\mathrm{B}_3 \otimes \mathbb{C}^*$ component modulo terms involving the quadrilogarithm function Li_4 [32, 112].

In principle one could compute the coproduct $\delta(R_n^{(2)})$ directly from the known symbol of $R_n^{(2)}$. However, the representation of the symbol given in [20] does not have the appropriate cluster structure manifest, making such a calculation infeasible. Instead we put aside our knowledge of the symbol for a moment while we bootstrap our way towards an explicit formula for $\delta(R_n^{(2)})|_{\Lambda^2 \mathrm{B}_2}$, shown in eq. (6.13). While this formula is strictly speaking conjectural, being based on some presumed cluster algebra structure of the amplitude, we have checked it by explicit comparison to the results of [20] through $n = 13$.

6.2 Elements of the Cluster Bootstrap

The structure of MHV scattering amplitudes is heavily constrained at the level of the symbol, a fact which Dixon and collaborators have exploited to great effect (see [130] for a recent review on the $n = 6$ bootstrap). We wish to adopt a similar approach at the level of the coproduct, specifically the $\Lambda^2 \mathrm{B}_2$ component. To this end we start by formulating a hypothesis for what kinds of variables x, y the cluster bootstrap should allow to appear in $\{x\}_2 \wedge \{y\}_2$. In chapter 2 it was observed "experimentally", for small values of n, that the two-loop MHV amplitudes have the very special feature that their $\Lambda^2 \mathrm{B}_2$ coproduct components are always expressible in terms of linear combinations of terms $\{v\}_2 \wedge \{z\}_2$ where

1. each v is drawn from a set of cluster $\mathcal{X}$-coordinates specially adapted to the analytic structure of the amplitude (related to what is called the "first-entry condition"),

2. each z is drawn from a set of cluster $\mathcal{X}$-coordinates specially adapted to the supersymmetry properties of MHV amplitudes (related to what is called the "last-entry condition"),

3. and the two variables v, z appearing in each term always belong to at least one cluster in common (this means, in particular, that $\{\log v, \log z\} \in \{-1, 0, +1\}$ with respect to the natural Poisson bracket on the kinematic manifold $\mathrm{Conf}_n(\mathbb{P}^3)$).

Let us explain these points in a little more detail.

First we recall that the analytic structure of color-ordered scattering amplitudes is highly constrained: they may only have branch points on the boundary of the Euclidean region at points where some sum of cyclically adjacent momenta becomes null. Requiring that amplitudes have only physical singularities implies that the first entries of the symbol of any amplitude must be drawn from the set of cross-ratios given by

$$u_{ij} = \frac{\langle i\, i{+}1\, j{+}1\, j{+}2\rangle\langle i{+}1\, i{+}2\, j\, j{+}1\rangle}{\langle i\, i{+}1\, j\, j{+}1\rangle\langle i{+}1\, i{+}2\, j{+}1\, j{+}2\rangle}. \tag{6.2}$$

Unfortunately, none of the u_{ij} are cluster $\mathcal{X}$-coordinates. Instead we consider the closely related quantities

$$v_{ijk} = \frac{1}{\prod_{a=j}^{k-1} u_{ia}} - 1 = -\frac{\langle i{+}1(i\, i{+}2)(j\, j{+}1)(k\, k{+}1)\rangle}{\langle i\, i{+}1\, k\, k{+}1\rangle\langle i{+}1\, i{+}2\, j\, j{+}1\rangle}, \tag{6.3}$$

where

$$\langle a(bc)(de)(fg)\rangle \equiv \langle abde\rangle\langle acfg\rangle - \langle abfg\rangle\langle acde\rangle. \tag{6.4}$$

v_{ijk} is a $\mathcal{X}$-coordinates as long as $i < j < k \pmod n$. We can phrase the familiar first-entry condition in terms of these unfamiliar variables by saying that only the quantities $1 + v_{ijk}$ are allowed in the first entry of the symbol of any function with physical branch cuts.

Secondly we recall the MHV last-entry condition [69], which states that the last entry of the symbol of any MHV amplitude must, as a consequence of extended supersymmetry, be drawn from the set of Plučker coordinates of the form $\langle \bar{i}\, j\rangle \equiv \langle i{-}1\, i\, i{+}1\, j\rangle$. We therefore might like to include ratios built purely out of these objects in our ansatz. Unfortunately, no $\mathcal{X}$-coordinates of this type exist. Instead we consider the cross-ratios

$$z^+_{ijk} = \frac{\langle i\, i{+}1\, \bar{j} \cap \bar{k}\rangle}{\langle i\, \bar{k}\rangle \langle i{+}1\, \bar{j}\rangle}, \qquad z^-_{ijk} = \frac{\langle i\, i{+}1\, j\, k\rangle \langle \bar{i}\, i{+}2\rangle}{\langle \bar{i}\, k\rangle \langle \overline{i{+}1}\, j\rangle}, \tag{6.5}$$

where

$$\langle ab\bar{c} \cap \bar{d}\rangle \equiv \langle a\bar{c}\rangle \langle b\bar{d}\rangle - \langle b\bar{c}\rangle \langle a\bar{d}\rangle. \tag{6.6}$$

The $z^{\pm}_{ijk}$ are all cluster $\mathcal{X}$-coordinates for $\mathrm{Gr}(4, n)$ as long as $i < j < k \pmod n$, and as suggested by the notation, $z^{\pm}_{ijk}$ are parity conjugates of each other (see sec. 2.2 for a discussion of parity on $\mathrm{Conf}_n(\mathbb{P}^3)$). Despite appearances these are in fact intimately tied to the last-entry condition since

$$1 + z^+_{ijk} = \frac{\langle i\, \bar{j}\rangle \langle i{+}1\, \bar{k}\rangle}{\langle i\, \bar{k}\rangle \langle i{+}1\, \bar{j}\rangle}, \qquad 1 + z^-_{ijk} = \frac{\langle \bar{i}\, j\rangle \langle \overline{i{+}1}\, k\rangle}{\langle \bar{i}\, k\rangle \langle \overline{i{+}1}\, j\rangle}. \tag{6.7}$$

It is useful to define certain boundary cases of the above cross-ratios with overlapping indices:

$$v_{ij} = v_{i\,j\,j+1}, \qquad z_{ij} = z^-_{i\,j\,j+1}, \tag{6.8}$$

where parity takes $z_{ij} \to z_{ji}$. Similar to what was done in the previous paragraph, we may express the familiar last-entry condition in terms of these unfamiliar variables by saying that only the quantities $1 + z^{\pm}_{ijk}$ are allowed in the final entry of the symbol of any MHV amplitude.

Third, it is worth commenting on how the Poisson bracket $\{\log x, \log y\}$ between two $\mathcal{X}$-coordinates may be computed in practice. If one could enumerate all possible clusters (and the Poisson bracket matrix in each cluster), by repeated application of the mutation algorithm starting with the initial cluster reviewed in [124], then one could scan that list to determine whether or not a given pair x, y appears together inside any cluster (and, if so, then one could read off their Poisson bracket). For the infinite algebras we encounter when $n > 7$ it is obviously not feasible to enumerate all clusters. An alternative approach would be to express x and y as algebraic functions of the $\mathcal{X}$-coordinates $(u_1, u_2, \ldots)$ in the initial cluster and then to compute

$$\{\log x, \log y\} = \sum_{i,j} \frac{\partial \log x}{\partial \log u_i} \frac{\partial \log y}{\partial \log u_j} \{\log u_i, \log u_j\}. \tag{6.9}$$

If for a given pair x, y the right-hand side comes out to be 0 or ± 1, then it is guaranteed that there exists a cluster containing both x and y, even if it would be computationally infeasible to find a specific path of mutations connecting that cluster to the initial cluster. However, we have found that the simplest way to compute $\{\log x, \log y\}$ for general x, y is to use the fact that the Poisson bracket on $\mathrm{Gr}(k, n)$ is induced from the easily computible Sklyanin bracket on SL_n, as described for example in [63][1].

The collection of all $\frac{1}{2}n(n-5)^2$ of the v's and $n(n-5)^2$ of the z's constitutes what we call the $\{v, z\}$ basis. Noting that $\{1+x\}_2 = -\{x\}_2$, the discussion in the previous two paragraphs suggests that it is natural to seek a representation for $\delta(R_n^{(2)})|_{\Lambda^2 \mathrm{B}_2}$ as a linear combination of objects of the form $\{v\}_2 \wedge \{z\}_2$ which capture, at the level of the coproduct, the spirit of both the first- and last-entry constraints satisfied by the symbol. Of course, the $\wedge$-product obscures any precise notion of first or last entries for the coproduct, so our argument for restricting to $\{v\}_2 \wedge \{z\}_2$ is meant to be suggestive rather than rigorous. The suitability of this ansatz is justified *a posteriori*

[1]We are very grateful to C. Vergu for pointing out this method to us.

because it leads to a successful bootstrap.

Based on these considerations, as well as explicit calculations at small n, we are motivated to hypothesize that properties 1–3 listed above are true for general n, so we adopt these as core elements of the cluster bootstrap for $R_n^{(2)}$. In addition we impose that $R_n^{(2)}$ should be

4. invariant under the dihedral group acting on the n particle labels, as well as under parity, and

5. well-defined under collinear limits.

We have found that these five simple physical and mathematical conditions uniquely fix $\delta(R_n^{(2)})|_{\Lambda^2 \mathrm{B}_2}$ (up to a single overall multiplicative constant common to all n) to take the value shown explicitly in eq. (6.13). Let us emphasize that in step 5 it is not actually necessary to know the $n-1$-particle result in order to construct the answer for n particles; it is sufficient merely to make an appropriate ansatz for the latter and impose only that the $n \parallel n-1$ collinear limit is well-defined. This determines both the n- and $n-1$-particle results at the same time, and in particular ties together their overall normalizations.

6.3 Applying the bootstrap

Let us explain in some detail how the procedure works beginning with $n = 7$. In this case there are are 14 v's and 28 z's, so we start with the ansatz that $\delta(R_7^{(2)})|_{\Lambda^2 \mathrm{B}_2}$ should be a linear combination of the $14 \times 28 = 392$ possible $\{v\}_2 \wedge \{z\}_2$'s. Only 70 of these pairs have Poisson brackets in the set $\{-1, 0, +1\}$ (i.e., appear together in a cluster), and after imposing dihedral and parity symmetries we are left with the three-parameter ansatz

$$\Big(c_1 \{v_{14}\}_2 \wedge \{z_{14}\}_2 + c_2 \{v_{14}\}_2 \wedge \{z_{15}\}_2 + c_3 \{v_{146}\}_2 \wedge \left\{z_{\bar{6}24}\right\}_2\Big) + \text{ dihedral } + \text{conjugate}. \tag{6.10}$$

We then take the collinear limit parameterized by $Z_n \to Z_{n-1} + \alpha(Z_{n-2} + \beta Z_1) + \gamma Z_2$ with $\gamma \to 0$, then $\alpha \to 0$, leaving β free. This leads to

$$\begin{aligned} c_2\Big(&(\{v_{25}v_{2\beta}/(1+v_{2\beta})\}_2 + \{v_{25}/(1+v_{3\beta})\}_2) \wedge \{z_{36}\}_2 \\ &+ \{v_{14}\}_2 \wedge (\{z_{14}\}_2 + \{z_{25}\}_2) + \{v_{36}\}_2 \wedge (\{z_{14}\}_2 + \{z_{36}\}_2)\Big) \\ &+ (c_1 - c_3)\Big(\{v_{2\beta}\}_2 \wedge \{z_{25}\}_2 - \{v_{3\beta}\}_2 \wedge \{z_{36}\}_2\Big) + \text{conjugate}, \end{aligned} \tag{6.11}$$

where $v_{i\beta} = \beta\langle 1\, i\, i{+}1\, 6\rangle / \langle i\, i{+}1\, 5\, 6\rangle$ and "+ conjugate" applies to the entire expression. For the collinear limit to be well-defined, i.e., independent of β (which specifies the relative length of the collinear momenta 6 and 7), we require $c_1 = c_3$ and $c_2 = 0$. We have therefore determined that $\delta(R_6^{(2)})|_{\Lambda^2 \mathrm{B}_2} = 0$ and also reproduce the result from chapter 2 that

$$\delta(R_7^{(2)})|_{\Lambda^2 \mathrm{B}_2} = \{v_{14}\}_2 \wedge \{z_{14}\}_2 + \{v_{146}\}_2 \wedge \left\{z_{\bar{6}24}\right\}_2 + \text{ dihedral } + \text{conjugate}, \tag{6.12}$$

up to an overall multiplicative constant.

The analogous ansatz for $n = 8$ begins with $36 \times 72 = 2592$ terms of the form $\{v\}_2 \wedge \{z\}_2$. Restricting to pairs that appear together in a cluster reduces this to 400. After imposing the discrete symmetries only 15 free parameters remain, and requiring the $8 \parallel 7$ collinear limit to be well-defined fixes all of them up to an overall normalization, which in turn may be fixed by matching eq. (6.12). The bootstrap may be carried out through sufficiently large n to motivate the all-n conjecture

$$\delta(R_n^{(2)})|_{\Lambda^2 \mathrm{B}_2} = \sum_{1<i<j<n} \Bigg(\{v_{1ij}\}_2 \wedge \Big(-\{z_{ij}\}_2 - \{z_{\bar{j}2i}\}_2 + \{z_{\bar{i}j2}\}_2 + \{z_{\bar{j}\,2\,i+1}\}_2 - \{z_{\bar{i}\,j+1\,2}\}_2 \Big)$$
$$- \{v_{1i}\}_2 \wedge \Big(\{z_{\bar{j}\,2\,i+1}\}_2 + \sum_{j<k\leq 1} \{z_{jk}\}_2 \Big) + \text{cyclic} + \text{conjugate} \Bigg). \quad (6.13)$$

Here "+ cyclic + conjugate" applies to the both lines, and we note that eq. (6.13) does satisfy the full dihedral symmetry even though we have only chosen to manifest + cyclic. The multiple sums contain some boundary terms which evaluate to $\{0\}_2$ or $\{\infty\}_2$; these are understood to be omitted. We have explicitly checked (by comparing its iterated coproduct) that this expression is consistent with the known symbol of $R_n^{(2)}$ through $n = 13$.

6.4 Discussion

A striking and mysterious feature of eq. (6.13) is that all of the pairs $\{v, z\}$ appearing in the formula have Poisson bracket zero. This feature is an output of the bootstrap; the input was much weaker, with the initial ansatz also allowing pairs having Poisson bracket $\{\log v, \log z\} = \pm 1$. Geometrically, this means that the $\Lambda^2 \mathrm{B}_2$ coproduct component wants to be expressed in terms of quadrilateral (rather than pentagonal) dimension-2 faces of the generalized Stasheff polytope associated to the $\mathrm{Gr}(4, n)$ cluster algebra, as noted already in chapter 2.

It would naturally be interesting to formulate a bootstrap for computing the $\mathrm{B}_3 \otimes \mathbb{C}^*$ coproduct components of $R_n^{(2)}$, which contain information about Li_4 terms that $\Lambda^2 \mathrm{B}_2$ does not know about. Unfortunately we have found that the $\{v, z\}$ basis provides an insufficient ansatz for $\mathrm{B}_3 \otimes \mathbb{C}^*$ already at $n = 7$. Of course there is no obstacle to computing this coproduct component on a case by case basis for small n by starting with a larger collection of cluster $\mathcal{X}$-coordinates, but deriving (or even guessing) an all-n formula remains elusive.

It would also be interesting to extend eq. (6.13) to capture more or even all of $R_n^{(2)}$, including terms involving products of Li_k's. Interestingly we have found, using the standard symbol-level (anti-)symmetrization techniques outlined in [19], that all of the $\mathrm{Li}_2\,\mathrm{Li}_2$ terms in $R_n^{(2)}$ are captured by the remarkable formula

$$\text{“eq. (6.13)”} - \left(\sum_{1\le i<j\le n} \mathrm{Li}_2(-v_{ij})\right)^2, \tag{6.14}$$

where the first term refers to eq. (6.13) with the replacement $\{a\}_2 \wedge \{b\}_2 \to \mathrm{Li}_2(-a)\,\mathrm{Li}_2(-b)$. This is a strong indication that there is still more structure to discover in the two-loop n-particle MHV amplitudes.

Surely the most important and interesting open question is whether a suitable “cluster bootstrap” can be formulated for higher-loop MHV or non-MHV amplitudes. The main obstacle is that so few explicit results for such amplitudes are known, even just at the level of symbols, that we do not yet dare to speculate how elements 1–3 of the cluster bootstrap ought to be generalized.

Appendix A

Functional Representatives

We present here functional representations for the A_2 and A_3 functions studied in chapter 4. These functions are completely defined (as always, modulo products of lower-weight functions) by their coproducts, shown in eqs. (4.6) and (4.12), but some readers may be comforted by seeing concrete functional representations for them. However, we relegate these formulas to the appendix because they are provided as is, with no express or implied warranty, and certainly not the implied warranty of suitability for numerically evaluating actual SYM theory amplitudes. For such an application one would first need to append to each of the functions shown below a suitable "analytic tail" comprising a carefully chosen product of lower-weight functions, specially crafted to give the functions the right analytic properties. Nevertheless we do believe that these functions capture the "most complicated part" of all two-loop MHV amplitudes in SYM theory.

There are several different types of generalized polylogarithm functions in terms of which non-classical functions can be expressed. At weight 4 it suffices to use the function $\mathrm{Li}_{2,2}(x,y)$ (see for example [55] for a discussion), whose symbol is

$$\begin{aligned}
&(y-1)\otimes(x-1)\otimes x\otimes y+(y-1)\otimes(x-1)\otimes y\otimes x+(y-1)\otimes y\otimes(x-1)\otimes x\\
&-(xy-1)\otimes(x-1)\otimes x\otimes y-(xy-1)\otimes(x-1)\otimes y\otimes x-(xy-1)\otimes x\otimes(x-1)\otimes x\\
&+(xy-1)\otimes x\otimes x\otimes x+(xy-1)\otimes x\otimes x\otimes y+(xy-1)\otimes x\otimes(y-1)\otimes y\\
&+(xy-1)\otimes x\otimes y\otimes x+(xy-1)\otimes(y-1)\otimes x\otimes y+(xy-1)\otimes(y-1)\otimes y\otimes x\\
&-(xy-1)\otimes y\otimes(x-1)\otimes x+(xy-1)\otimes y\otimes x\otimes x+(xy-1)\otimes y\otimes(y-1)\otimes y.
\end{aligned} \tag{A.1}$$

A.0.1 The A_2 function

The A_2 function may be represented as

$$f_{A_2}\sim\sum_{i,j}^{5} j L_{2,2}(x_i,x_{i+j}) \tag{A.2}$$

in terms of

$$\begin{aligned}
L_{2,2}(x,y)&=\frac{1}{2}\mathrm{Li}_{2,2}\left(\frac{x}{y},-y\right)+\frac{1}{6}\left(\mathrm{Li}_4\left(\frac{1+x}{xy}\right)+\mathrm{Li}_4\left(\frac{x(1+y)}{y(1+x)}\right)\right)\\
&+\frac{1}{5}\left(\mathrm{Li}_4\left(\frac{1+x}{xy}\right)+\frac{1}{2}\mathrm{Li}_4\left(\frac{1+x}{1+y}\right)\right)+\frac{1}{2}\mathrm{Li}_3\left(\frac{x}{y}\right)\log\left(\frac{1+x}{1+y}\right)-(x\leftrightarrow y).
\end{aligned} \tag{A.3}$$

The factor of j in the summand may seem awkward, but when fully expanded out the sum generates a total of 20 $\mathrm{Li}_{2,2}$ terms, each with coefficient $\pm\frac{3}{2}$ or $\pm\frac{1}{2}$ (each possibility occurs five times). Note that the function $L_{2,2}$ has the simple coproduct $\delta L_{2,2}(x,y)|_{\Lambda^2 \mathrm{B}_2}=\{x\}_2\wedge\{y\}_2$ (it is therefore very similar to Goncharov's $\kappa(x,y)$ function [60]). The rather strange looking Li_4 terms in eq. (A.3) of course make no contribution to $\Lambda^2\,\mathrm{B}_2$; they are carefully tuned to ensure that eq. (A.2) has clustery $\mathrm{B}_3\otimes\mathbb{C}^*$ content. The $\mathrm{Li}_3\cdot\log$ terms are of course irrelevant inside $\mathcal{L}_4$, but they are required for f_{A_2} to be a cluster $\mathcal{A}$-function of the A_2 algebra. The symbol of eq. (A.2) is not identical to the one shown in eq. (4.7), but the difference between the two is annihilated by ρ (i.e., they differ by products of functions of lower weight).

A.0.2 The A_3 function

The A_3 function may of course be written as the sum of eq. (A.3)'s for the six pentagons in A_3, but the simple form of $\delta f_{A_3}(x_1, x_2, x_3)|_{\Lambda^2 \mathrm{B}_2}$ suggests that there is a more concise functional representation. Indeed, we find that a representative of the A_3 function can be written as

$$f_{A_3}(x_1, x_2, x_3) \sim \sum_{i=1}^{3} K_{2,2}(x_{i,1}, x_{i,2}) + \frac{1}{2} \sum_{i=1}^{6} (-1)^i \operatorname{Li}_4(-e_i) \tag{A.4}$$

where the $x_{i,j}$ and e_i are defined in (4.8) and we use here the new combination

$$K_{2,2}(x, y) = \frac{1}{2} \operatorname{Li}_{2,2}(x/y, -y) - \operatorname{Li}_4(x/y) - \frac{2}{3} \operatorname{Li}_3(x/y) \log(y) - (x \leftrightarrow y). \tag{A.5}$$

As was the case for the A_2 function, the $\operatorname{Li}_3 \cdot \log$ terms are chosen so that the symbol of (A.4) is expressible entirely in terms of cluster $\mathcal{A}$-coordinates of the A_3 algebra.

Bibliography

[1] S. J. Parke and T. Taylor, *Gluonic Two Goes to Four*, *Nucl.Phys.* **B269** (1986) 410.

[2] S. J. Parke and T. Taylor, *An Amplitude for n Gluon Scattering*, *Phys.Rev.Lett.* **56** (1986) 2459.

[3] R. Britto, F. Cachazo, B. Feng, and E. Witten, *Direct proof of tree-level recursion relation in Yang-Mills theory*, *Phys.Rev.Lett.* **94** (2005) 181602, [hep-th/0501052].

[4] N. Arkani-Hamed, J. L. Bourjaily, F. Cachazo, S. Caron-Huot, and J. Trnka, *The All-Loop Integrand For Scattering Amplitudes in Planar N=4 SYM*, *JHEP* **1101** (2011) 041, [arXiv:1008.2958].

[5] Z. Bern, J. Carrasco, and H. Johansson, *New Relations for Gauge-Theory Amplitudes*, *Phys.Rev.* **D78** (2008) 085011, [arXiv:0805.3993].

[6] L. F. Alday and J. M. Maldacena, *Gluon scattering amplitudes at strong coupling*, *JHEP* **0706** (2007) 064, [arXiv:0705.0303].

[7] J. Drummond, G. Korchemsky, and E. Sokatchev, *Conformal properties of four-gluon planar amplitudes and Wilson loops*, *Nucl.Phys.* **B795** (2008) 385–408, [arXiv:0707.0243].

[8] A. Brandhuber, P. Heslop, and G. Travaglini, *MHV amplitudes in N=4 super Yang-Mills and Wilson loops*, *Nucl.Phys.* **B794** (2008) 231–243, [arXiv:0707.1153].

[9] N. Berkovits and J. Maldacena, *Fermionic T-Duality, Dual Superconformal Symmetry, and the Amplitude/Wilson Loop Connection*, *JHEP* **0809** (2008) 062, [arXiv:0807.3196].

[10] J. M. Drummond, J. M. Henn, and J. Plefka, *Yangian symmetry of scattering amplitudes in N=4 super Yang-Mills theory*, *JHEP* **0905** (2009) 046, [arXiv:0902.2987].

[11] N. Arkani-Hamed and J. Trnka, *The Amplituhedron*, *JHEP* **1410** (2014) 30, [arXiv:1312.2007].

[12] Z. Bern, L. J. Dixon, D. C. Dunbar, and D. A. Kosower, *One loop n point gauge theory amplitudes, unitarity and collinear limits*, *Nucl.Phys.* **B425** (1994) 217–260, [hep-ph/9403226].

[13] C. Anastasiou, Z. Bern, L. J. Dixon, and D. Kosower, *Planar amplitudes in maximally supersymmetric Yang-Mills theory*, *Phys.Rev.Lett.* **91** (2003) 251602, [hep-th/0309040].

[14] Z. Bern, L. J. Dixon, and V. A. Smirnov, *Iteration of planar amplitudes in maximally supersymmetric Yang-Mills theory at three loops and beyond*, *Phys.Rev.* **D72** (2005) 085001, [hep-th/0505205].

[15] Z. Bern, M. Czakon, D. Kosower, R. Roiban, and V. Smirnov, *Two-loop iteration of five-point N=4 super-Yang-Mills amplitudes*, *Phys.Rev.Lett.* **97** (2006) 181601, [hep-th/0604074].

[16] F. Cachazo, M. Spradlin, and A. Volovich, *Iterative structure within the five-particle two-loop amplitude*, *Phys.Rev.* **D74** (2006) 045020, [hep-th/0602228].

[17] V. Del Duca, C. Duhr, and V. A. Smirnov, *An Analytic Result for the Two-Loop Hexagon Wilson Loop in $N = 4$ SYM*, *JHEP* **1003** (2010) 099, [arXiv:0911.5332].

[18] V. Del Duca, C. Duhr, and V. A. Smirnov, *The Two-Loop Hexagon Wilson Loop in $N = 4$ SYM*, *JHEP* **1005** (2010) 084, [arXiv:1003.1702].

[19] A. B. Goncharov, M. Spradlin, C. Vergu, and A. Volovich, *Classical Polylogarithms for Amplitudes and Wilson Loops*, *Phys.Rev.Lett.* **105** (2010) 151605, [arXiv:1006.5703].

[20] S. Caron-Huot, *Superconformal symmetry and two-loop amplitudes in planar N=4 super Yang-Mills*, *JHEP* **1112** (2011) 066, [arXiv:1105.5606].

[21] A. Goncharov, *Galois symmetries of fundamental groupoids and noncommutative geometry*, *Duke Math. J.* **128** (2005), no. 2 209–284, [math/0208144].

[22] O. Schlotterer and S. Stieberger, *Motivic Multiple Zeta Values and Superstring Amplitudes*, arXiv:1205.1516.

[23] J. Drummond and E. Ragoucy, *Superstring amplitudes and the associator*, arXiv:1301.0794.

[24] J. Broedel, O. Schlotterer, and S. Stieberger, *Polylogarithms, Multiple Zeta Values and Superstring Amplitudes*, arXiv:1304.7267.

[25] J. Broedel, O. Schlotterer, S. Stieberger, and T. Terasoma, *All order*

alpha'-expansion of superstring trees from the Drinfeld associator, arXiv:1304.7304.

[26] J. Drummond, J. Henn, V. Smirnov, and E. Sokatchev, *Magic identities for conformal four-point integrals*, *JHEP* **0701** (2007) 064, [hep-th/0607160].

[27] Z. Bern, M. Czakon, L. J. Dixon, D. A. Kosower, and V. A. Smirnov, *The Four-Loop Planar Amplitude and Cusp Anomalous Dimension in Maximally Supersymmetric Yang-Mills Theory*, *Phys.Rev.* **D75** (2007) 085010, [hep-th/0610248].

[28] J. Drummond, J. Henn, G. Korchemsky, and E. Sokatchev, *On planar gluon amplitudes/Wilson loops duality*, *Nucl.Phys.* **B795** (2008) 52–68, [arXiv:0709.2368].

[29] L. F. Alday and J. Maldacena, *Comments on gluon scattering amplitudes via AdS/CFT*, *JHEP* **0711** (2007) 068, [arXiv:0710.1060].

[30] J. Drummond, J. Henn, G. Korchemsky, and E. Sokatchev, *Conformal Ward identities for Wilson loops and a test of the duality with gluon amplitudes*, *Nucl.Phys.* **B826** (2010) 337–364, [arXiv:0712.1223].

[31] J. Drummond, J. Henn, G. Korchemsky, and E. Sokatchev, *Dual superconformal symmetry of scattering amplitudes in N=4 super-Yang-Mills theory*, *Nucl.Phys.* **B828** (2010) 317–374, [arXiv:0807.1095].

[32] A. Goncharov, *Geometry of configurations, polylogarithms, and motivic cohomology*, *Adv. Math.* **114** (1995), no. 2 197–318.

[33] V. V. Fock and A. B. Goncharov, *Cluster ensembles, quantization and the dilogarithm*, *Ann. Sci. Éc. Norm. Supér. (4)* **42** (2009), no. 6 865–930, [math/0311245].

[34] S. Fomin and A. Zelevinsky, *Cluster algebras. I: Foundations*, *J. Am. Math. Soc.* **15** (2002), no. 2 497–529.

[35] S. Fomin and A. Zelevinsky, *Cluster algebras. II: Finite type classification*, *Invent. Math.* **154** (2003), no. 1 63–121.

[36] N. Arkani-Hamed, F. Cachazo, C. Cheung, and J. Kaplan, *A Duality For The S Matrix*, *JHEP* **1003** (2010) 020, [arXiv:0907.5418].

[37] N. Arkani-Hamed, F. Cachazo, and C. Cheung, *The Grassmannian Origin Of Dual Superconformal Invariance*, *JHEP* **1003** (2010) 036, [arXiv:0909.0483].

[38] N. Arkani-Hamed, J. Bourjaily, F. Cachazo, and J. Trnka, *Local Spacetime Physics from the Grassmannian*, *JHEP* **1101** (2011) 108, [arXiv:0912.3249].

[39] N. Arkani-Hamed, J. Bourjaily, F. Cachazo, and J. Trnka, *Unification of Residues and Grassmannian Dualities*, *JHEP* **1101** (2011) 049, [arXiv:0912.4912].

[40] N. Arkani-Hamed, J. L. Bourjaily, F. Cachazo, A. B. Goncharov, A. Postnikov, and J. Trnka, *Scattering Amplitudes and the Positive Grassmannian*, arXiv:1212.5605.

[41] S. Fomin and A. Zelevinsky, *Y-systems and generalized associahedra*, *Ann. Math. (2)* **158** (2003), no. 3 977–1018.

[42] J. D. Stasheff, *Homotopy associativity of H-spaces. I, II*, *Trans. Am. Math. Soc. 108,* **275-292** (1963) 293–312.

[43] R. Penrose, *Twistor algebra*, *J.Math.Phys.* **8** (1967) 345.

[44] R. Penrose and M. A. MacCallum, *Twistor theory: An Approach to the quantization of fields and space-time*, *Phys.Rept.* **6** (1972) 241–316.

[45] E. Witten, *Perturbative gauge theory as a string theory in twistor space*, *Commun.Math.Phys.* **252** (2004) 189–258, [hep-th/0312171].

[46] A. Hodges, *Eliminating spurious poles from gauge-theoretic amplitudes*, arXiv:0905.1473.

[47] L. Mason and D. Skinner, *Dual Superconformal Invariance, Momentum Twistors and Grassmannians*, *JHEP* **0911** (2009) 045, [arXiv:0909.0250].

[48] E. Witten, *An Interpretation of Classical Yang-Mills Theory*, *Phys.Lett.* **B77** (1978) 394.

[49] N. Beisert and C. Vergu, *On the Geometry of Null Polygons in Full N=4 Superspace*, *Phys.Rev.* **D86** (2012) 026006, [arXiv:1203.0525].

[50] N. Beisert, S. He, B. U. Schwab, and C. Vergu, *Null Polygonal Wilson Loops in Full N=4 Superspace*, *J.Phys.* **A45** (2012) 265402, [arXiv:1203.1443].

[51] Z. Bern, L. Dixon, D. Kosower, R. Roiban, M. Spradlin, C. Vergu, and A. Volovich, *The Two-Loop Six-Gluon MHV Amplitude in Maximally Supersymmetric Yang-Mills Theory*, *Phys.Rev.* **D78** (2008) 045007, [arXiv:0803.1465].

[52] J. Golden, A. B. Goncharov, M. Spradlin, C. Vergu, and A. Volovich, *Motivic Amplitudes and Cluster Coordinates*, *JHEP* **1401** (2014) 091, [arXiv:1305.1617].

[53] J. Drummond, J. Henn, G. Korchemsky, and E. Sokatchev, *Hexagon Wilson loop = six-gluon MHV amplitude*, *Nucl.Phys.* **B815** (2009) 142–173, [arXiv:0803.1466].

[54] A. B. Goncharov, *Galois symmetries of fundamental groupoids and noncommutative geometry*, *Duke Math. J.* **128** (2005) 209 – 284.

[55] C. Duhr, H. Gangl, and J. R. Rhodes, *From polygons and symbols to polylogarithmic functions*, *JHEP* **1210** (2012) 075, [`arXiv:1110.0458`].

[56] C. Duhr, *Hopf algebras, coproducts and symbols: an application to Higgs boson amplitudes*, *JHEP* **1208** (2012) 043, [`arXiv:1203.0454`].

[57] C. Vergu, "Lectures at the EPSRC–LMS Durham Symposium on *Polylogarithms as a Bridge between Number Theory and Particle Physics*." `http://www.maths.dur.ac.uk/events/Meetings/LMS/2013/PNTPP13/talks.html`, July, 2013.

[58] S. J. Bloch, *Higher regulators, algebraic K-theory, and zeta functions of elliptic curves.* Providence, RI: American Mathematical Society (AMS), 2000.

[59] A. Suslin, *K_3 of a field and the Bloch group*, *Proc. Steklov Inst. Math.* **183** (1990) 217–239.

[60] A. B. Goncharov, *Polylogarithms and motivic Galois group*, *Proc. Sympos. Pure Math.* **55** (1994) 43 – 96.

[61] S. Fomin and A. Zelevinsky, *The Laurent phenomenon*, *Adv. in Appl. Math.* **28** (2002), no. 2 119–144.

[62] J. S. Scott, *Grassmannians and cluster algebras*, *Proc. Lond. Math. Soc., III. Ser.* **92** (2006), no. 2 345–380.

[63] M. Gekhtman, M. Shapiro, and A. Vainshtein, *Cluster algebras and Poisson geometry*, *Mosc. Math. J.* **3** (2003), no. 3 899–934.

[64] B. Keller, *Cluster algebras, quiver representations and triangulated categories*, in *Triangulated Categories.* Cambridge: Cambridge University Press, 2010.

[65] S. Fomin and N. Reading, *Root systems and generalized associahedra*, in *Geometric combinatorics*, vol. 13 of *IAS/Park City Math. Ser.*, pp. 63–131. Amer. Math. Soc., Providence, RI, 2007.

[66] C. Anastasiou, A. Brandhuber, P. Heslop, V. V. Khoze, B. Spence, and G. Travaglini, *Two-Loop Polygon Wilson Loops in N=4 SYM*, *JHEP* **0905** (2009) 115, [`arXiv:0902.2245`].

[67] L. J. Dixon, J. M. Drummond, and J. M. Henn, *Analytic result for the two-loop six-point NMHV amplitude in N=4 super Yang-Mills theory*, *JHEP* **1201** (2012) 024, [`arXiv:1111.1704`].

[68] L. J. Dixon, J. M. Drummond, and J. M. Henn, *Bootstrapping the three-loop hexagon*, *JHEP* **1111** (2011) 023, [`arXiv:1108.4461`].

[69] S. Caron-Huot and S. He, *Jumpstarting the All-Loop S-Matrix of Planar N=4 Super Yang-Mills*, *JHEP* **1207** (2012) 174, [`arXiv:1112.1060`].

[70] V. Del Duca, C. Duhr, and V. A. Smirnov, *A Two-Loop Octagon Wilson Loop in $N = 4$ SYM*, *JHEP* **1009** (2010) 015, [`arXiv:1006.4127`].

[71] P. Heslop and V. V. Khoze, *Analytic Results for MHV Wilson Loops*, *JHEP* **1011** (2010) 035, [`arXiv:1007.1805`].

[72] P. Heslop and V. V. Khoze, *Wilson Loops @ 3-Loops in Special Kinematics*, *JHEP* **1111** (2011) 152, [`arXiv:1109.0058`].

[73] T. Goddard, P. Heslop, and V. V. Khoze, *Uplifting Amplitudes in Special Kinematics*, *JHEP* **1210** (2012) 041, [`arXiv:1205.3448`].

[74] L. Ferro, *Differential equations for multi-loop integrals and two-dimensional kinematics*, `arXiv:1204.1031`.

[75] J. Bartels, L. Lipatov, and A. Prygarin, *Collinear and Regge behavior of 2 $\to$ 4 MHV amplitude in N = 4 super Yang-Mills theory*, arXiv:1104.4709.

[76] A. Prygarin, M. Spradlin, C. Vergu, and A. Volovich, *All Two-Loop MHV Amplitudes in Multi-Regge Kinematics From Applied Symbology*, *Phys.Rev.* **D85** (2012) 085019, [arXiv:1112.6365].

[77] J. Bartels, A. Kormilitzin, L. Lipatov, and A. Prygarin, *BFKL approach and* $2 \to 5$ *maximally helicity violating amplitude in* $\mathcal{N} = 4$ *super-Yang-Mills theory*, *Phys.Rev.* **D86** (2012) 065026, [arXiv:1112.6366].

[78] L. Lipatov, A. Prygarin, and H. J. Schnitzer, *The Multi-Regge limit of NMHV Amplitudes in N=4 SYM Theory*, *JHEP* **1301** (2013) 068, [arXiv:1205.0186].

[79] L. J. Dixon, C. Duhr, and J. Pennington, *Single-valued harmonic polylogarithms and the multi-Regge limit*, *JHEP* **1210** (2012) 074, [arXiv:1207.0186].

[80] J. Pennington, *The six-point remainder function to all loop orders in the multi-Regge limit*, *JHEP* **1301** (2013) 059, [arXiv:1209.5357].

[81] L. F. Alday, D. Gaiotto, J. Maldacena, A. Sever, and P. Vieira, *An Operator Product Expansion for Polygonal null Wilson Loops*, *JHEP* **1104** (2011) 088, [arXiv:1006.2788].

[82] D. Gaiotto, J. Maldacena, A. Sever, and P. Vieira, *Bootstrapping Null Polygon Wilson Loops*, *JHEP* **1103** (2011) 092, [arXiv:1010.5009].

[83] D. Gaiotto, J. Maldacena, A. Sever, and P. Vieira, *Pulling the straps of polygons*, *JHEP* **1112** (2011) 011, [arXiv:1102.0062].

[84] B. Basso, A. Sever, and P. Vieira, *Space-time S-matrix and Flux-tube S-matrix at Finite Coupling*, arXiv:1303.1396.

[85] N. Beisert, C. Ahn, L. F. Alday, Z. Bajnok, J. M. Drummond, et al., *Review of AdS/CFT Integrability: An Overview*, *Lett.Math.Phys.* **99** (2012) 3–32, [arXiv:1012.3982].

[86] L. F. Alday, D. Gaiotto, and J. Maldacena, *Thermodynamic Bubble Ansatz*, *JHEP* **1109** (2011) 032, [arXiv:0911.4708].

[87] L. F. Alday, J. Maldacena, A. Sever, and P. Vieira, *Y-system for Scattering Amplitudes*, *J.Phys.* **A43** (2010) 485401, [arXiv:1002.2459].

[88] L. Ferro, T. Lukowski, C. Meneghelli, J. Plefka, and M. Staudacher, *Harmonic R-matrices for Scattering Amplitudes and Spectral Regularization*, arXiv:1212.0850.

[89] V. Del Duca, L. J. Dixon, J. M. Drummond, C. Duhr, J. M. Henn, et al., *The one-loop six-dimensional hexagon integral with three massive corners*, *Phys.Rev.* **D84** (2011) 045017, [arXiv:1105.2011].

[90] M. Bullimore and D. Skinner, *Descent Equations for Superamplitudes*, arXiv:1112.1056.

[91] A. Brandhuber, G. Travaglini, and G. Yang, *Analytic two-loop form factors in N=4 SYM*, *JHEP* **1205** (2012) 082, [arXiv:1201.4170].

[92] C. Bogner and F. Brown, *Symbolic integration and multiple polylogarithms*, *PoS* **LL2012** (2012) 053, [arXiv:1209.6524].

[93] A. E. Lipstein and L. Mason, *From the holomorphic Wilson loop to 'd log' loop-integrands for super-Yang-Mills amplitudes*, arXiv:1212.6228.

[94] S. G. Naculich, H. Nastase, and H. J. Schnitzer, *All-loop infrared-divergent behavior of most-subleading-color gauge-theory amplitudes*, arXiv:1301.2234.

[95] J. Drummond, C. Duhr, B. Eden, P. Heslop, J. Pennington, et al., *Leading singularities and off-shell conformal integrals*, arXiv:1303.6909.

[96] A. von Manteuffel and C. Studerus, *Top quark pairs at two loops and Reduze 2*, *PoS* **LL2012** (2012) 059, [arXiv:1210.1436].

[97] T. Gehrmann, L. Tancredi, and E. Weihs, *Two-loop QCD helicity amplitudes for $g\,g \to Z\,g$ and $g\,g \to Z\,\gamma$*, arXiv:1302.2630.

[98] C. Anastasiou, C. Duhr, F. Dulat, and B. Mistlberger, *Soft triple-real radiation for Higgs production at N3LO*, arXiv:1302.4379.

[99] A. Sever and P. Vieira, *Multichannel Conformal Blocks for Polygon Wilson Loops*, *JHEP* **1201** (2012) 070, [arXiv:1105.5748].

[100] J. Golden and M. Spradlin, *The differential of all two-loop MHV amplitudes in $\mathcal{N} = 4$ Yang-Mills theory*, *JHEP* **1309** (2013) 111, [arXiv:1306.1833].

[101] http://www.math.lsa.umich.edu/~fomin/cluster.html.

[102] J. Bartels, A. Kormilitzin, and L. Lipatov, *Analytic structure of the $n = 7$ scattering amplitude in $\mathcal{N} = 4$ SYM theory in the multi-Regge kinematics: Conformal Regge pole contribution*, *Phys.Rev.* **D89** (2014), no. 6 065002, [arXiv:1311.2061].

[103] B. Basso, A. Sever, and P. Vieira, *Space-time S-matrix and Flux tube S-matrix II. Extracting and Matching Data*, *JHEP* **1401** (2014) 008, [arXiv:1306.2058].

[104] G. Papathanasiou, *Hexagon Wilson Loop OPE and Harmonic Polylogarithms*, *JHEP* **1311** (2013) 150, [arXiv:1310.5735].

[105] S. Caron-Huot and S. He, *Three-loop octagons and n-gons in maximally supersymmetric Yang-Mills theory*, *JHEP* **1308** (2013) 101, [arXiv:1305.2781].

[106] M. A. Torres, *Cluster algebras in scattering amplitudes with special 2D kinematics*, *Eur.Phys.J.* **C74** (2014) 2757, [arXiv:1310.6906].

[107] L. J. Dixon, J. M. Drummond, M. von Hippel, and J. Pennington, *Hexagon functions and the three-loop remainder function*, *JHEP* **1312** (2013) 049, [arXiv:1308.2276].

[108] F. C. Brown, *Multiple zeta values and periods of moduli spaces M 0 ,n (R)*, *Annales Sci.Ecole Norm.Sup.* **42** (2009) 371, [math/0606419].

[109] J. Drummond, J. Henn, G. Korchemsky, and E. Sokatchev, *The hexagon Wilson loop and the BDS ansatz for the six-gluon amplitude*, *Phys.Lett.* **B662** (2008) 456–460, [arXiv:0712.4138].

[110] A. Brandhuber, P. Heslop, V. V. Khoze, and G. Travaglini, *Simplicity of Polygon Wilson Loops in N=4 SYM*, *JHEP* **1001** (2010) 050, [arXiv:0910.4898].

[111] L. J. Dixon, J. M. Drummond, C. Duhr, and J. Pennington, *The four-loop remainder function and multi-Regge behavior at NNLLA in planar $N = 4$ super-Yang-Mills theory*, *JHEP* **1406** (2014) 116, [arXiv:1402.3300].

[112] A. B. Goncharov, *Polylogarithms and motivic Galois groups*, in *Motives (Seattle, WA, 1991)*, vol. 55 of *Proc. Sympos. Pure Math.*, pp. 43–96. Amer. Math. Soc., Providence, RI, 1994.

[113] J. Bartels, V. Schomerus, and M. Sprenger, *Heptagon Amplitude in the Multi-Regge Regime*, *JHEP* **1410** (2014) 67, [arXiv:1405.3658].

[114] A. Goncharov, *Deninger's conjecture on L-functions of elliptic curves at $s = 3$*, *J. Math. Sci., New York* **81** (1996), no. 3 2631–2656, [alg-geom/9512016].

[115] B. Basso, *Exciting the GKP string at any coupling*, *Nucl.Phys.* **B857** (2012) 254–334, [arXiv:1010.5237].

[116] B. Basso, A. Sever, and P. Vieira, *Space-time S-matrix and Flux-tube S-matrix III. The two-particle contributions*, *JHEP* **1408** (2014) 085, [arXiv:1402.3307].

[117] J. Bartels, L. Lipatov, and A. Sabio Vera, *BFKL Pomeron, Reggeized gluons and Bern-Dixon-Smirnov amplitudes*, *Phys.Rev.* **D80** (2009) 045002, [arXiv:0802.2065].

[118] J. Bartels, L. Lipatov, and A. Sabio Vera, *N=4 supersymmetric Yang Mills scattering amplitudes at high energies: The Regge cut contribution*, *Eur.Phys.J.* **C65** (2010) 587–605, [arXiv:0807.0894].

[119] R. M. Schabinger, *The Imaginary Part of the $N = 4$ Super-Yang-Mills Two-Loop Six-Point MHV Amplitude in Multi-Regge Kinematics*, *JHEP* **0911** (2009) 108, [arXiv:0910.3933].

[120] L. Lipatov and A. Prygarin, *Mandelstam cuts and light-like Wilson loops in N=4 SUSY*, *Phys.Rev.* **D83** (2011) 045020, [arXiv:1008.1016].

[121] L. Lipatov and A. Prygarin, *BFKL approach and six-particle MHV amplitude in N=4 super Yang-Mills*, *Phys.Rev.* **D83** (2011) 125001, [arXiv:1011.2673].

[122] J. Bartels, L. Lipatov, and A. Prygarin, *MHV Amplitude for 3-¿3 Gluon Scattering in Regge Limit*, *Phys.Lett.* **B705** (2011) 507–512, [arXiv:1012.3178].

[123] V. Fadin and L. Lipatov, *BFKL equation for the adjoint representation of the gauge group in the next-to-leading approximation at N=4 SUSY*, *Phys.Lett.* **B706** (2012) 470–476, [arXiv:1111.0782].

[124] J. Golden and M. Spradlin, *An analytic result for the two-loop seven-point MHV amplitude in $\mathcal{N} = 4$ SYM*, *JHEP* **1408** (2014) 154, [arXiv:1406.2055].

[125] N. Arkani-Hamed, S. Caron-Huot, and J. Trnka. Private communication.

[126] L. Brink, J. H. Schwarz, and J. Scherk, *Supersymmetric Yang-Mills Theories*, *Nucl.Phys.* **B121** (1977) 77.

[127] A. B. Goncharov and V. V. Fock, *Cluster ensembles, quantization, and the dilogarithm*, *Ann. Sci. Ecole. Normale. Sup.* (2009).

[128] A. Sever, P. Vieira, and T. Wang, *OPE for Super Loops*, *JHEP* **1111** (2011) 051, [arXiv:1108.1575].

[129] L. J. Dixon and M. von Hippel, *Bootstrapping an NMHV amplitude through three loops*, *JHEP* **1410** (2014) 65, [arXiv:1408.1505].

[130] L. J. Dixon, J. M. Drummond, C. Duhr, M. von Hippel, and J. Pennington, *Bootstrapping six-gluon scattering in planar N=4 super-Yang-Mills theory*, *PoS* **LL2014** (2014) 077, [arXiv:1407.4724].